Spring 2010

# Synthesis of a Potentially Insulin-Mimetic, Lipid-Linked Inositol Glycan

Meenakshi Goel
*San Jose State University*

# SYNTHESIS OF A POTENTIALLY INSULIN-MIMETIC, LIPID-LINKED INOSITOL GLYCAN

A Thesis

Presented to

The Faculty of the Department of Chemistry

San José State University

In Partial Fulfillment

of the Requirements for the Degree

Master of Science

by

Meenakshi Goel

May 2010

The Designated Thesis Committee Approves the Thesis Titled

Synthesis of a Potentially Insulin-mimetic, Lipid-linked Inositol Glycan

by

Meenakshi Goel

Approved for the Department of Chemistry

San Jose Staté University

May 2010

| | |
|---|---|
| Prof. Marc d'Alarcao | Department of Chemistry |
| Prof. Daryl Eggers | Department of Chemistry |
| Prof. Roy Okuda | Department of Chemistry |

ABSTRACT

SYNTHESIS OF A POTENTIALLY INSULIN-MIMETIC, LIPID-LINKED INOSITOL GLYCAN

by Meenakshi Goel

Inositol glycans (IGs) are naturally occurring oligosaccharides that can stimulate insulin sensitive cells. Several synthetic IG analogues have been shown to activate the insulin-signaling pathway, including the stimulation of the enzyme pyruvate dehydrogenase (PDH) phosphatase that can further stimulate aerobic metabolism in cells. Cancer cells shift to anaerobic metabolism in order to escape intrinsic apoptosis (Warburg Effect). IG's ability to stimulate aerobic metabolism might provide a method to reverse the Warburg Effect and thereby induce apoptosis in the cancer cells. One specific palmitoylated IG analogue has been shown to *selectively* kill cancer cells while having no adverse effect on normal cells. However, this analogue is unstable under physiological conditions due to ester hydrolysis and acyl group migration.

This thesis describes the work on the synthesis of an IG analogue in which the ester linkage has been replaced by ether. Since ethers are comparatively more stable than esters, the resulting IG analogue should be more stable than the parent analogue. Biological activity of this IG analogue will be reported elsewhere.

ACKNOWLEDGEMENTS

I am greatly indebted to my research advisor, Professor Marc d'Alarcao, for giving me an opportunity to work with him on this interesting project. I would like to thank him for his extreme patience and encouragement, especially at times when success seemed so far to me. He is an excellent mentor and a wonderful person to work with. Without his guidance and support this work would never have been accomplished. I would like to thank my thesis committee, Professor Daryl Eggers and Professor Roy Okuda, for their valuable time, comments, and suggestions for the betterment of this work. I would like to thank all my lab-mates especially Leon Castaneda, Jan Bello, and Smita Fulzele for their help, motivation, and useful suggestions from time to time. My special thanks to Douglas Fox for providing the NMR and Spinworks training. I will miss you all very much. Thanks to the Staff working in the Chemistry Department: Rosa Garcia and Maria Segovia, for their help in certain official matters; Steven L. Cappelloni and Khuong Ngo for providing the chemicals and glassware from the stock room. I would like to thank our technicians, Mike Stephens and Craig Wood, for their valuable services including the maintenance of NMR instrument, dry-ice supply, gas cylinders, rotovaps, etc. Finally, I would like to thank my husband, Amit Goel, and my beautiful daughter, Ananya, for their constant support, encouragement, and patience especially during the final stages of writing the thesis. Without their help this work would have never been accomplished.

TABLE OF CONTENTS

Page

LIST OF FIGURES

LIST OF SCHEMES

LIST OF TABLES

LIST OF NMR SPECTRA

# CHAPTER 1

# INTRODUCTION

## 1.1 GLYCOSYLPHOSPHATIDYLINOSITOLS (GPIs) AND INOSITOL-PHOSPHOGLYCANS (IPGs)

### 1.1.1 Glycosylphosphatidylinositols (GPIs)

GPIs are a group of naturally occurring glycolipids that are classified into two categories, GPI-anchors or free-GPIs, depending upon the presence or absence, respectively, of proteins at the terminal end of GPI molecule. GPIs are ubiquitous in eukaryotes, including vertebrates, plants, mollusca, insects, schistosomes, fungi, and protozoa.[1] The main function of GPI-anchors is to anchor certain molecules and proteins to the extracellular surface of the plasma membrane. The biochemistry and functional significance of these structures have been explored in detail since the 1980's.[2-5] Although GPI-anchors serve primarily as an alternative to hydrophobic trans-membrane polypeptide anchors, several other functions have been proposed for these structures. These include roles in intracellular sorting, cell communication, trans-membrane signaling or as soluble mediators of hormone action. Several reviews have been published that describe these functions in detail.[3,6,7] Hydrolysis products of GPIs are known as inositol-phosphoglycans (IPGs), inositol glycans (IGs) or phosphatidylinositolglycans (PIGs). IPGs mimic some of the bioactivities of hormones and cytokines like insulin, nerve growth factor, transforming growth factor-β, interleukin-

2, thyrotropin, follicle stimulating hormone and chorionic gonadotropin. Binding of these hormones to their respective receptors results in the hydrolysis of GPIs and the release of IPGs that serve as second messengers, mediating the signal-transduction pathways of the respective hormones or cytokines.[8] Thus, an understanding of the chemical structures of GPIs and their hydrolysis products might help in understanding several biological events occurring in living systems.

### 1.1.2 Structural relationship between GPIs and IPGs

Much effort has been expended to elucidate the chemical structures of GPI-anchors. The first GPI-anchor to be determined in detail was that of *T. brucei* in 1988 (Figure 1).[1] Since then, the structure of several natural GPI-anchors has been determined including those from *S. cerevisiae*,[9] rat brain Thy-1,[10] and *T. gondii*.[11] All GPIs have similar chemical structures, with minor differences among different species.[12] The common core of a GPI molecule is composed of a sugar moiety, a phosphatidylinositol (PI) moiety, and a terminal hydrophobic moiety that anchors the GPI molecule into the cell membrane. The sugar moiety (or "glycan core") is composed of a glucosamine (GlcN), three mannose residues, and one phospho-ethanolamine residue that can form an amide bond with the C-terminus of a polypeptide. The reducing end of GlcN is glycosidically linked to PI. PI is then linked to the hydrophobic moiety through a phospho-diester linkage. A variety of lipids such as 1,2-diacylglycerol, 1-alkyl-2-acylglycerol, monoacylglycerol, and ceramide can be utilized as the hydrophobic moiety in the GPI molecule.

Thus all GPI-anchors are arranged in a conserved sequence: Protein – Ethanolamine - $PO_4$ - 6 Man α l-2 Man α l-6 Man α l-4 GlcN α l-6 *myo*- inositol – $PO_4$ - lipid (Figure 1). In many GPI-anchors, one or more side chains, like monosaccharides, oligosaccharides or phospho-ethanolamine groups, may further modify the GPI glycan core.[13]

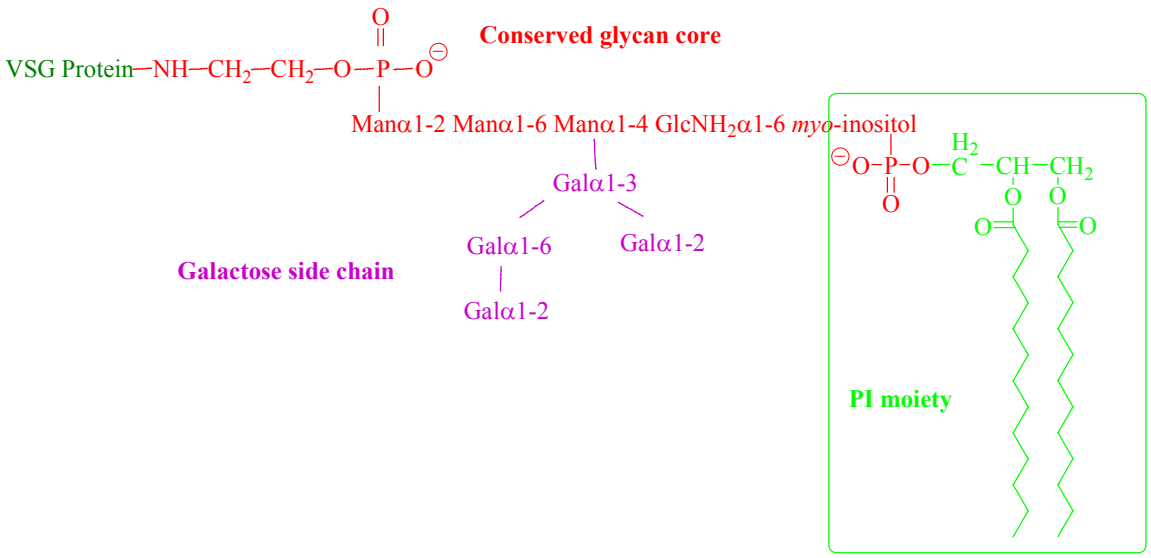


Figure 1. Structure of the GPI anchor of *T. brucei*.

Hydrolysis of GPI-anchors with certain *proteases* or *hydrolases* releases the terminal proteins, giving free-GPIs. Both GPI-anchors and free-GPIs can further undergo lipolytic hydrolysis by the action of enzymes called *phospholipases* to release free IPGs. Phosphatidylinositol-specific phospholipase C (PI-PLC) hydrolyzes the phosphodiester bond of phosphatidylinositol to form 1,2-diacylglycerol and glycopeptide-bound (in GPI-anchor) or glycan-bound (in free-GPI) inositol-1, 2- cyclic- phosphate (Figure 2).[14] Glycan-bound PI molecules, called IPGs, can be internalized into the cytosol *via* certain

IG transporters in the cell membrane and function as "second messengers" of hormone action.[6] Evidence in favor of this behavior comes from the fact that exogenous addition of bacterial PI-PLC has been shown to generate insulin-mimetic compounds.[15]

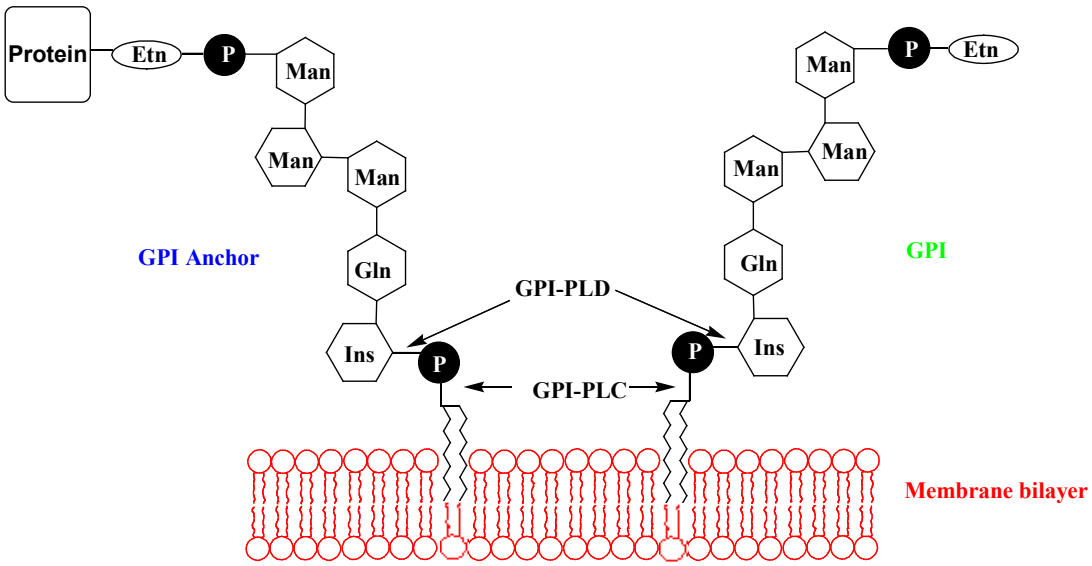


Figure 2. Cleavage of GPI anchor/ GPI with PI-PLC / GPI-PLC or with GPI-PLD. ("Etn" equals ethanolamine).

Some GPI anchors contain an additional fatty acid group (usually palmitoyl) attached to the C-2 position of the inositol moiety.[16] This additional group renders the anchor resistant to the cleavage with PI-PLC.[17] However, extracellular glycosylphosphatidylinositol-specific phospholipase D (GPI-PLD) can hydrolyze GPI-anchors and free-GPIs with acylated inositols.[18] The hydrolysis products of GPI-PLD are phosphatidic acid and IPG lacking a cyclic phosphate.[19] Based on the structural similarity between IPGs and hydrolyzed products of GPIs, it has been speculated that

IPGs are generated by hydrolysis of GPIs. However, the exact source of IPGs is not yet known.

### 1.1.3 Inositol glycans (IGs): Putative second messengers of insulin action

IPGs and IGs are structurally similar to the protein-linked GPI anchors, with the only difference being the absence of the protein fragment and the lipid moiety. A close relationship between IGs and GPIs was confirmed by the observation that treatment of GPI-anchored variant surface glycoprotein (VSG) with PI-PLC (for lipid cleavage) and *pronase* (for protein cleavage) resulted in a fragment with significant insulin-like activity in rat hepatocytes and adipocytes.[20,21] Further studies revealed the presence of two different types of IPGs, IPG-type A (containing a *myo*-inositol and glucosamine)[22] and IPG-type P (containing *chiro*-inositol and galactosamine).[23] Jones and coworkers reviewed comparative studies of two types of IPGs in 1998.[7] Both the IPGs, when added exogenously, were found to mimic certain actions of insulin. Intravenous administration of either IPG type A or P to *streptozotocin* treated diabetic rats reversed hyperglycemia in a manner similar to insulin, thus suggesting a role for IPGs as second messengers of insulin action.[24]

The first natural IG (an IPG-A type) **1** was isolated in 1986 by the treatment of bovine liver with insulin (Figure 3).[15] This natural IG stimulated insulin-sensitive cells even in the absence of insulin, thus suggesting its role as a second messenger in insulin action.[25] Since then, several research groups have been involved in the isolation and purification of natural IGs in order to understand their biological functions in detail.[26-28]

The first natural IPG-P type IG **2** was characterized in 2003 (Figure 3).[29] This pseudo-disaccharide was found to be a putative insulin mediator that activated PDH phosphatase. The presence of a $\beta$-1, 4 linkage between pinitol and galactosamine was noteworthy because all naturally occurring GPI structures previously studied have an α-1, 6 linkage between glucosamine and *myo*-inositol.

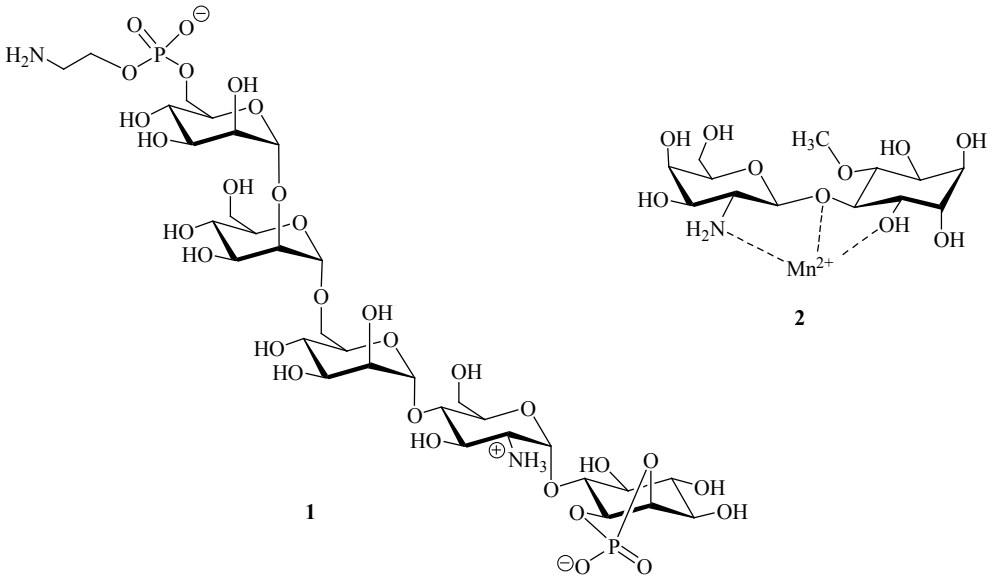


Figure 3. Compound **1**: Structure of VSG anchor fragment (IPG-A type) from *T. bruceii* variant 118; Compound **2**: Structure of natural and fully characterized IPG-P type IG analogue.

Several sub-cellular assays have been done to explore the insulin-mimetic activities of IGs and to discover their role as second messengers of insulin action.[30-32] However, before unraveling the role of IPGs in insulin action, it is first important to understand the role of insulin and its signaling mechanism.

## 1.2 OVERVIEW OF INSULIN SIGNALING

Insulin is a hormone released by pancreatic beta cells in response to elevated levels of nutrients in the blood. Insulin triggers the uptake of glucose, fatty acids and amino acids into adipose tissue, muscle and the liver and promotes the storage of these nutrients in the form of glycogen, lipids, and protein, respectively. Insulin is linked to cellular metabolism via the insulin receptor (IR) located on the surface of certain insulin-sensitive cells like hepatocytes, adipocytes and muscle cells.[33] IR is a heterotetrameric transmembrane glycoprotein, composed of two extracellular α-subunits and two transmembrane β-subunits linked together by disulfide bonds. Activation of IR triggers a cascade of interrelated metabolic pathways regulated by different mechanisms. The interdependency of metabolic events in the insulin-signaling pathway has hindered efforts to understand fully the nature of insulin action. Due to the complexity of the molecular mechanisms by which insulin elicits its numerous metabolic responses, insulin signaling have been the subject of intense research over the past several decades.[33,34]

The intricate pathway of insulin signaling is depicted in Figure 4.[35] Once secreted from the beta cells of pancreas, insulin binds to the insulin receptors (IRs) (1). Binding of insulin to the α-subunit of IR induces a conformational change resulting in the autophosphorylation of a number of tyrosine residues present in the β-subunit (2). Receptor activation leads to the phosphorylation of key tyrosine residues on insulin receptor substrate (IRS) proteins, some of which are recognized by the Src homology 2 (SH2) domain of the p85 regulatory subunit of phosphatidylinositol 3-kinase (PI 3-K), a

lipid kinase (3). The catalytic subunit of PI 3-kinase, p110, then phosphorylates phosphatidylinositol (4,5) bisphosphate ($PIP_2$) (4) and (5) leads to the formation of phosphatidylinositol (3,4,5) trisphosphate ($PIP_3$) (6). A key downstream substrate of elevated concentrations of $PIP_3$ is Akt or protein kinase B (PKB), which is confined to the plasma membrane. Phosphorylation and activation of Akt (7) and (8) requires two different kinases: phosphoinositide-dependent kinase 1 (PDK1), and a recently identified mTOR-RICTOR protein complex called PDK 2.[36] Once active, Akt is responsible for regulation of various metabolic pathways via phosphorylations. Akt catalyzes phosphorylation of glycogen synthase kinase 3 (GSK-3) (9) that leads to inactivation of GSK-3 (10) that in turn prevents phosphorylation and inactivation of glycogen synthase (GS) (11), the major substrate of GSK-3, resulting in increased glycogen synthesis. $PIP_3$ also activates protein phosphatase 1 (PP1), localized on glycogen particles, that in turn dephosphorylates inactive GS (13) and converts it into active GS (12), thus further increasing glycogen synthesis.

In addition to glucose uptake and storage, insulin also promotes the uptake of fatty acids and synthesis of lipids. Lipid biosynthesis is indirectly an outcome of glucose metabolism. Inactivation of GSK-3 inhibits phosphorylation of ATP citrate lyase (ACL) at one site (14). However, phosphorylation of this enzyme at another site by PKB (15) enhances its activity, thus increasing the conversion of citrate to acetyl-CoA in cytosol (16), where it can be utilized in lipid biosynthesis.

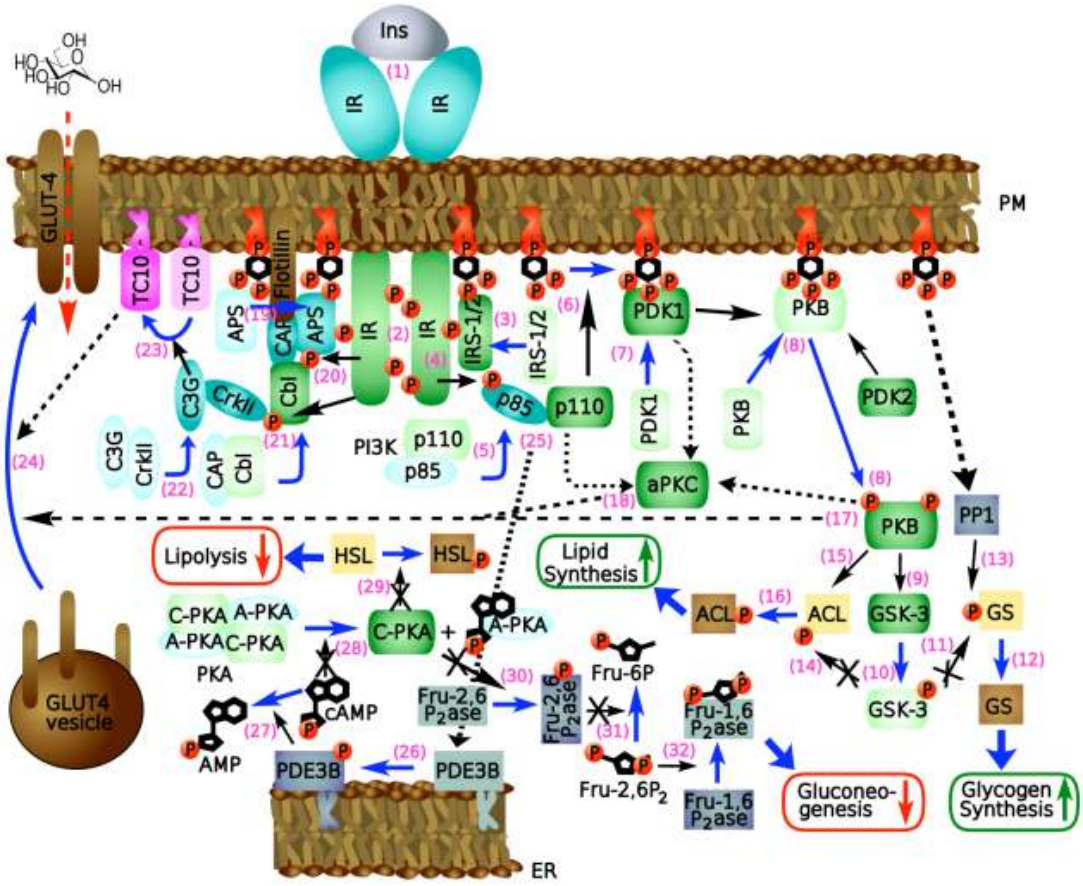


Figure 4. Schematic representation of insulin signaling transduction (Reproduced from Future Medicinal Chemistry (2009), 1(1), 95-118 with permission of Future Science Ltd).

Another key action of insulin is to stimulate glucose uptake into cells by inducing translocation of the glucose transporter, GLUT4, from intracellular storage to the plasma membrane.[37] PI 3-kinase and Akt are known to play a role in GLUT4 translocation, (17) and (18). In addition, a PI 3-kinase-independent pathway provides a second cue for GLUT4 recruitment to the plasma membrane.[34] In this pathway, IR activation (19) leads to the phosphorylation of Cbl (20), which exists as a complex with Cb1 associated protein (CAP). Following phosphorylation (21), the Cbl-CAP complex translocates to

lipid rafts in the plasma membrane. Cbl then interacts with the adaptor protein CrkII (22), which is constitutively associated with the Rho-family guanine nucleotide exchange factor, C3G. C3G in turn activates members of the GTP-binding protein family, TC10 (23), which promote GLUT4 translocation to the plasma membrane *via* an unknown mechanism (24). It is hypothesized that this happens *via* actin cytoskeleton regulation - a function attributed to many of the Rho proteins.[38]

Two other metabolic events controlled by insulin include inhibition of lipolysis and gluconeogenesis. Insulin inhibits lipolysis by decreasing cellular concentrations of cAMP, by activating a cAMP specific phosphodiesterase 3B (PDE3B) in adipocytes [(25) and (26)].[39] Activated PDE3B hydrolyzes cAMP (27). Low cAMP level reduces the activity of protein kinase A (PKA) (28), which in turn is unable to phosphorylate and activate hormone sensitive lipase (HSL) (29), hence decreasing lipolysis. Similarly, gluconeogenesis is also inhibited by inactive PKA. Inactive PKA does not phosphorylate and activate fructose 2,6-bisphosphatase (Fru-2,6$P_2$ase) (30). Inactive Fru-2,6$P_2$ase can not catalyze conversion of fructose-2,6-biphosphate (Fru-2,6$P_2$) into fructose-6-phosphate (Fru-6P) (31). Hence, Fru-2,6$P_2$ accumulates and inhibits fructose 1,6-bisphosphatase (Fru-1,6$P_2$ase) (32) - an enzyme that is involved in gluconeogenesis.[40]

## 1.3 MECHANISM OF ACTION OF INOSITOL GLYCANS

Several natural and synthetic IGs have been shown to mimic some of the actions of insulin. As described above, insulin signaling is an entirely intracellular process. The question arises as to how IGs, which are located on the extracellular face of the plasma

membrane, are able to trigger intracellular signaling events? What kind of endocytosis mechanism is involved?

A study by Alvarez et al in 1991 showed that IGs do get transported through the plasma membrane via an IG transporter.[41] However, there is evidence that internalization is not necessary for the action of IGs. A fluorescent synthetic IG analogue was found to stimulate lipogenesis in rat adipocytes despite the fact that it did *not* enter the cell.[42] On the other hand, the ability of a natural IG to modulate the activity of purified pyruvate dehydrogenase (PDH) phosphatase in a cell free assay suggests an intracellular, as well as an intra-mitochondrial role.[43]

The mystery of the role of IGs as 'second messengers of insulin action' has been resolved, to some extent, through the enormous efforts of Muller and coworkers.[38,44-46] According to their findings, the insulin-signaling pathway is cross-linked downstream to an insulin receptor-independent insulin-mimetic signaling pathway via specialized lipid raft domains like DIGs and caveolae.[47] DIGs and caveolae associate with signaling proteins like non-receptor tyrosine kinases (NRTKs), (dually) acylated small and heterotrimeric G proteins, and GPI-anchored proteins *via* lipid-lipid interactions. Depending upon their cholesterol to caveolin ratio, DIGs may be either hcDIGs (high in cholesterol and other signaling protein content and low buoyant density), or lcDIGs (low in cholesterol content and high buoyant density). Signaling proteins are confined to hcDIGs via binding either to caveolin (for (dually) acylated proteins like NRTKs), or to a trypsin/NaCl/NEM sensitive polypeptide receptor, p115 (for GPI-proteins and phosphatidylinositolglycan peptides [PIG-P]).[46]

A cartoon representation of the mechanism of action of IGs is shown in figure 5.[35] Insulin stimulates a GPI-PLC (1) that lipolytically cleaves GPI-anchored proteins (and, perhaps free GPIs) on the *outer* leaflet of the cell membrane (2). The lipolytically cleaved protein-IG conjugate (and IGs) (3), promotes GPI-anchored protein(s) to dissociate from the receptor and get translocated from hcDIGs to lcDIGs (4). Simultaneously NRTKs like pp59 (Lyn) are dissociated from caveolin and are redistributed between hcDIGs and lcDIGs (5).[48] Activated kinase pp59 (Lyn) further activates another kinase, pp125 (Fak), (6) that is able to recruit IRS proteins (7) for phosphorylation by pp59 (Lyn) (8) at the sites that are recognized by PI-3 kinase. This step triggers the phosphorylation cascade of insulin signaling pathway and acts as a point of convergence between the mechanism of action of IGs and insulin.

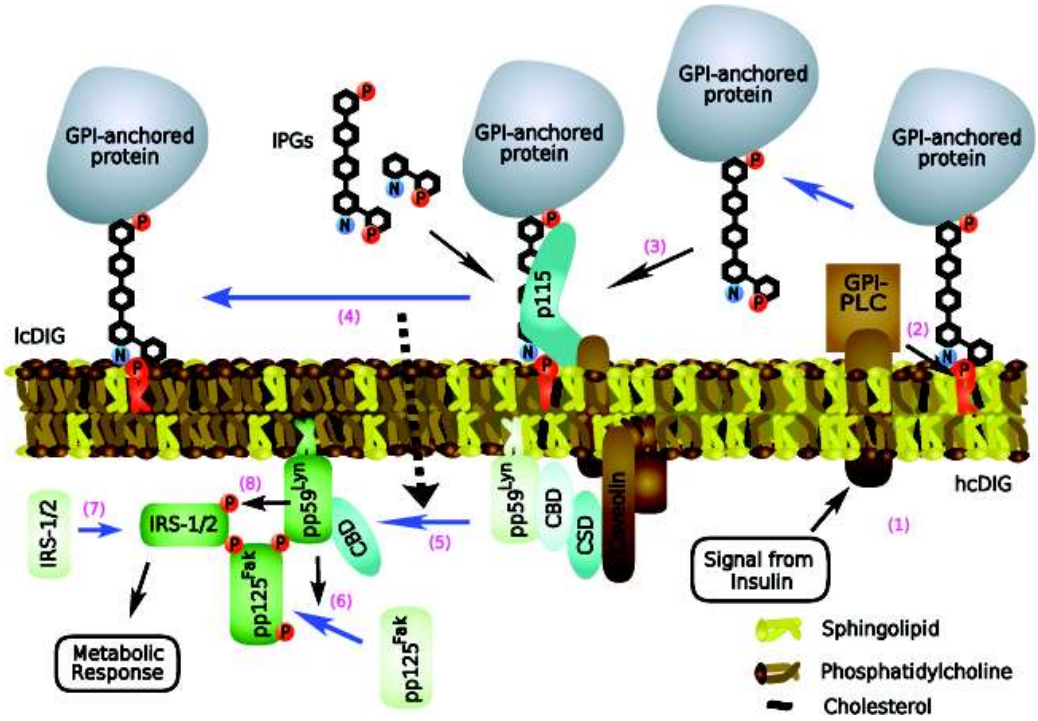


Figure 5. Mechanism of action of IGs on cell surface (Reproduced from Future Medicinal Chemistry (2009), 1(1), 95-118 with permission of Future Science Ltd).

## 1.4 SYNTHETIC IGs: A NEW GENERATION ANTI-DIABETIC AND/OR ANTI-CANCER AGENTS

Although IGs appear to be promising candidates for second messengers of insulin action, the lack of information related to their exact chemical structure, and the difficulty in isolating these compounds in homogeneous forms, make it difficult to study their biological activities in detail. An alternative to purification of natural IGs is to prepare pure IG analogues using organic synthetic chemistry. The design of the first synthetic IG was based on the structure of natural IPG **1** derived from the GPI anchor of the variant surface glycoprotein of *T. brucei* (Figure 3)[1] which was shown to mimic the antigluconeogenic activity of insulin in rat hepatocytes.[20] This synthetic IG analogue was an IPG-A type disaccharide [1D-6-*O*-(2-amino-2-deoxy-α-D-glucopyranosyl)-*myo*-inositol 1,2-(cyclic phosphate)] with moderate insulin-mimetic activity (Figure 6, compound **3**).[49] The absence of charged groups (Figure 6, compound **4** and **5**) or the presence of an acyclic phosphate group on the myo-inositol moiety was found to result in compounds that had no insulin-mimetic activities.[49] This suggested that an insulin-mimetic IG analogue must have at least an amino sugar and a cyclic 1, 2-phosphate group on *myo*-inositol. The glucosamine moiety is also necessary for the insulin-mimetic activity. An IG analogue with an amino group and cyclic 1, 2-phosphate, but lacking a glucosamine moiety, showed no insulin-mimetic activity.[50]

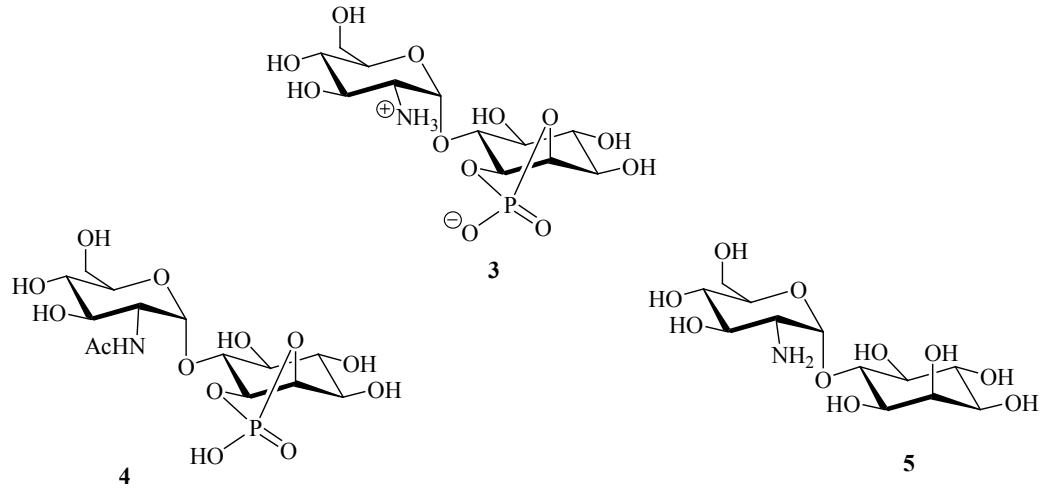


Figure 6. Compound **3** is a synthetic IG disaccharide with modest insulin-mimetic activity; compounds **4** and **5** are IG disaccharides without charged functional groups and having no insulin-mimetic activity.

Based on the above analysis, several research groups have attempted to synthesize different analogues of IG compounds in order to understand their structure-activity relationship.[49,51-57] The most extensive synthetic efforts have been reported from Muller's laboratory.[52] This group synthesized an array of 46 different IPG-A type IG analogues, some of which have potent insulin-mimetic activities. It was concluded that the most important features that should be present in an insulin-mimetic IG are the following: a *myo*-inositol-1, 2-cyclic phosphate; an unacylated glucosamine; and some anionic groups on the distal mannose residues. Some of the IG analogues with potent insulin-mimetic activity are shown in Figure 7. The activity of structurally defined IGs has recently been reviewed.[58]

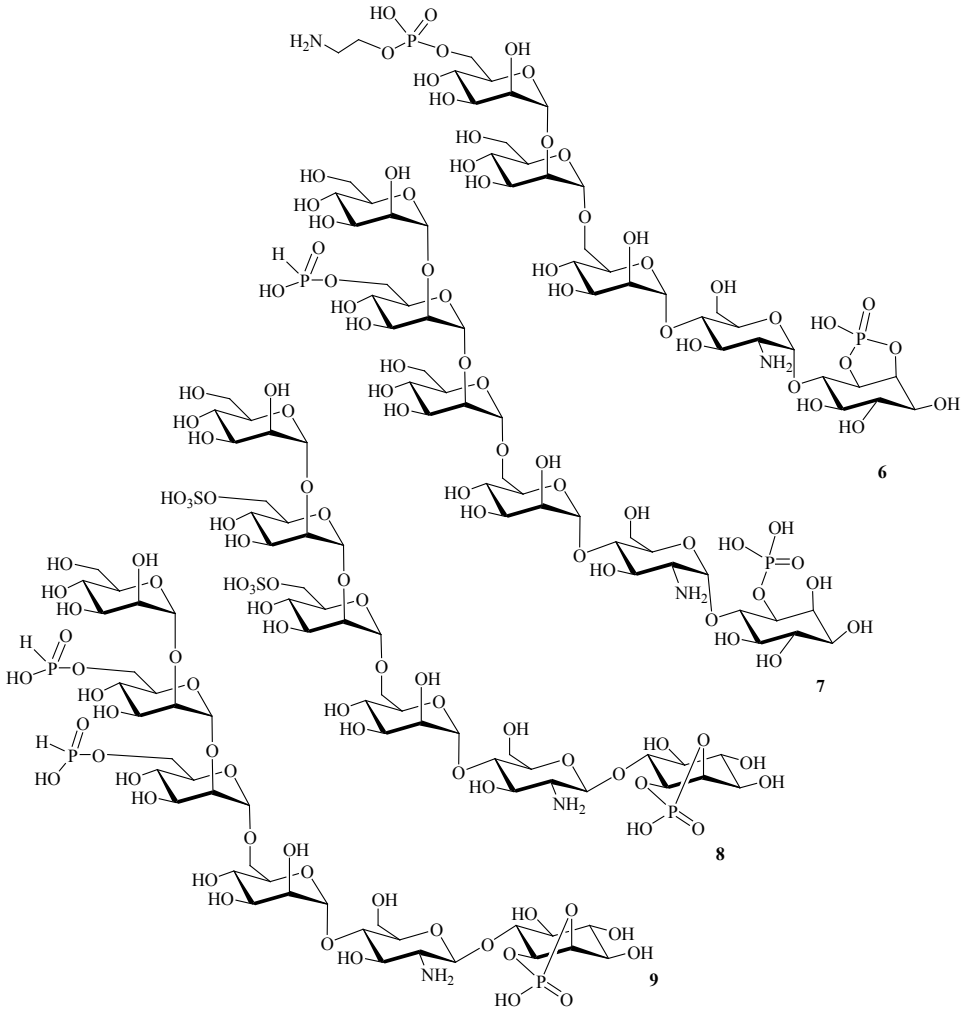

Figure 7. Structures of some potent synthetic IGs.

The structure activity relationship of these IGs also revealed that the number of mannose residues could be reduced, however, without adversely affecting the activity of the compound. Thus compounds **10** and **11** with shorter oligosaccharide chains were found to be as effective as the hexasaccharides shown in Figure 7 (Figure 8).[56]

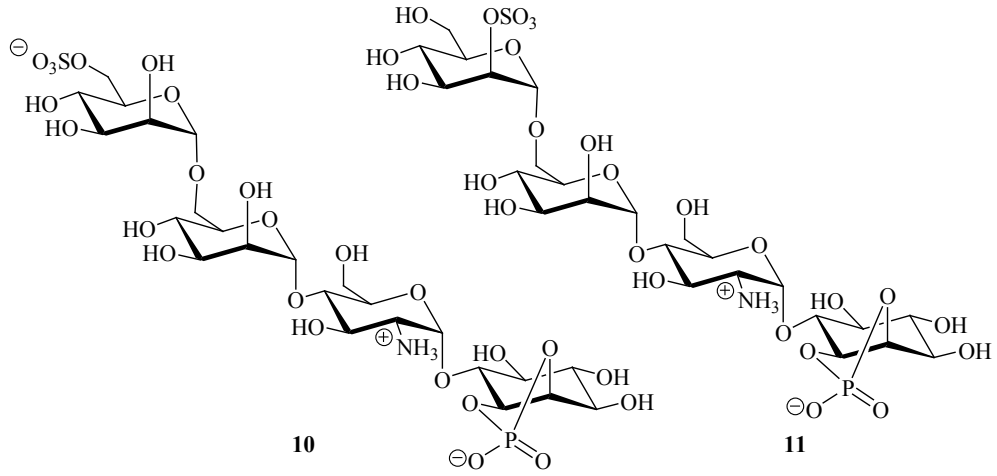


Figure 8. Structures of IG analogues with fewer mannose residues, but with similar insulin-mimetic activity.

Many researchers have also reported syntheses and biological activities of IPG-P type IGs (Figure 9).[57,59] The structure-activity relationship of these synthetic IGs has not yet been completely explored, so it might be possible that the next generation of IGs could be based on such structures.

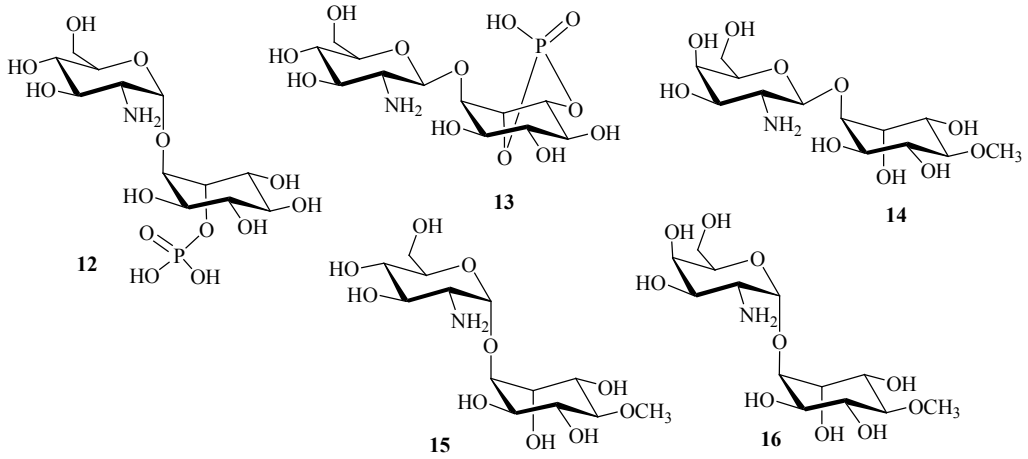


Figure 9. Structures of synthetic IPG-P type IG analogues.

## 1.5 INOSITOL GLYCANS AND DIABETES

As described before, the association of insulin with the IR triggers the insulin-signaling pathway that controls the activity of several metabolic enzymes further downstream. Failure to uptake and store nutrients due to a defect in the action of insulin results in diabetes, a disease associated with excess glucose in blood serum. IGs act downstream of the IR and hence can trigger the insulin signaling pathway even if insulin is absent or if the insulin receptor is defective.[25] Insulin-mimetic activities of IGs include stimulation of anabolic metabolism via increase in glycogen synthesis, glucose transport, and lipogenesis. These activities suggest a possible role for IGs in the treatment of diseases, like type II diabetes, associated with insulin resistance in insulin sensitive cells. So the question arises: what is type II diabetes?

### 1.5.1 Diabetes as a disease

Diabetes mellitus is a disease associated with high glucose concentration in blood and urine, a condition called hyperglycemia. The major cause of diabetes is improper functioning or utilization of the hormone *insulin* by insulin sensitive cells. Insulin regulates transportation of excess glucose into the cells and the overall blood glucose level in the body. Insufficient production of insulin in the pancreas, or the inability of cells to use insulin properly and efficiently, leads to elevated levels of blood glucose or hyperglycemia. Type I diabetes is a condition in which insulin is not produced in sufficient amounts by the pancreas. Type II diabetes is a condition in which insulin is available in the blood stream but it cannot activate the insulin receptor and the insulin

signaling cascade sufficiently. Type I diabetes can be treated by insulin injections and diabetic diet, but in type II diabetes the cells do not respond to the effects of insulin, a condition called "insulin resistance". Hence exogenously supplied insulin is useless for the treatment of type II diabetes. The only resort for a type II diabetic patient is controlled diet, regular exercise, and lifelong medication in order to maintain the normal blood glucose level.

### 1.5.2 Insulin resistance in type II diabetes

Insulin resistance is a condition in which the amount of insulin is insufficient to produce a normal response in insulin sensitive fat, liver and muscle cells.[60] Insulin resistant cells are unable to perform their functions normally resulting in excess hydrolysis of triglycerides into fatty acids, excess production of glucose in liver, and decreased levels of glycogen in muscles. All these factors contribute to the increase in blood glucose levels. In response to the increased blood glucose concentration, the pancreatic beta-cells secrete more insulin. Accumulation of high levels of both insulin and glucose in the blood is characteristic of type II diabetes.

What causes insulin resistance? Negative regulators of insulin signaling are responsible for terminating the insulin signal transduction pathway. Insulin signaling can be terminated by any one of the following: internalization of the insulin-insulin receptor complex into endosomes and degradation of insulin by insulin degrading enzyme (IDE);[61] mutation in Caveolin-1 gene that codes for caveolin, a caveolae localized protein[38] that associates with IR; development of an excess of visceral adipocytes that are

relatively resistant to anti-lipolytic insulin signaling, and as a result, secrete a lot of non-esterified fatty acids (NEFA) into the bloodstream. NEFAs can block insulin signaling in other cells via several possible mechanisms or they can impair glucose metabolism in liver.[62]

### 1.5.3 Treatment of type II diabetes

Type II diabetes has become an area of intense research and development due to the challenges associated with the disease.[34] Therapeutic strategies for the treatment of type II diabetes involve stimulation of pancreatic beta cells (by stimulators like sulfonylureas), inhibition of glucose production in liver (by biguanides, etc.), inhibition of carbohydrate absorption in the intestine, stimulation of insulin sensitive cells to insulin (by insulin sensitizers like thiazolidinediones), and activation of insulin receptor by insulin receptor agonists or insulin mimetics.[63] As described above, agents like IGs, unlike insulin, can trigger the insulin-signaling cascade without interacting with the insulin receptor.[14] This feature makes IGs a possible therapeutic agent for type II diabetes. Some synthetic IGs have been tested for their biological activities and have been shown to have potent insulin-mimetic activities.[58] However, the use of IGs as anti-diabetic drugs is limited by the fact that these compounds are highly complex and involve challenging synthetic strategies.

Synthetic efforts from Prof. Marc d'Alarcao's laboratory have also contributed to the category of biologically active IGs. Recently they have synthesized a simple acylated IPG: GlcN-(α 1-6)-*myo*-Ins-1-phosphate-2-palmitate (Figure 10) that has been tested for

its activity to inhibit lipogenesis.[64] This acylated IPG was shown to inhibit lipogenesis in rat adipocytes to an extent similar to other potent insulin-mimetic IG analogues.

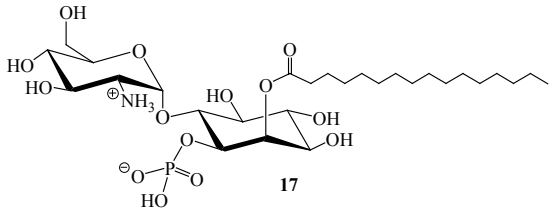


17

Figure 10. Structure of an acylated IPG analogue.

## 1.6 INOSITOL GLYCANS AND CANCER

Cancerous tumor cells switch to an alternate metabolic pathway (called aerobic glycolysis) to escape the natural phenomenon of apoptosis or programmed cell death (PCD) initiated in the mitochondria. Insulin-mimetic IGs can stimulate aerobic metabolism in insulin-sensitive cells *via* stimulation of PDH phosphatase.[65] Before understanding the potential of IGs to treat tumors, it is important to understand the cellular metabolism of cancer.

### 1.6.1 Cancer as a disease

Cancer is a disease characterized by uncontrolled growth of abnormal cells due to certain defects (or mutations) in the process of normal cell division. Normal cells obtain energy by oxidation of glucose and undergo a process of cell proliferation and growth for certain biological functions. After performing their respective roles, cells become worn out and get disposed off *via* the process of apoptosis. Cancer cells proliferate and grow unlimitedly, but in contrast to the normal cells they do not undergo apoptosis. As a

result, these cells develop into a mass of cellular components called a tumor. If a tumor is confined to a tissue or an organ it is generally benign. Such a tumor can be treated by surgery or radiation therapy. However, if a tumor grows without limit, invades and damages the surrounding tissues, enters into the blood vessels, and spreads to other parts of the body (metastasis), it is called a malignant tumor. Malignant tumors cause the major number of cancer deaths.

### 1.6.2 Biochemistry of cancer growth

The major cause of invasive tumors is proposed to be an altered glucose metabolism.[66] Glucose is the main source of energy (in the form of ATP) for all metabolic processes occurring in the body. Under normal conditions glucose enters into the glycolytic pathway that converts glucose into pyruvate. In aerobic metabolism, pyruvate enters the mitochondria where PDH phosphatase converts pyruvate into acetyl CoA, which is further consumed in the tricarboxylic acid (TCA) cycle, producing $CO_2$, $H_2O$ and 36 ATP per glucose molecule. Cancer cells limit the oxidative phosphorylation (though oxygen supply is available) and undergo an alternative metabolic process, aerobic glycolysis, whereby the glycolytic product, pyruvate, is reduced to lactic acid generating two molecules of ATP per glucose molecule (Figure 11).[67,68] Consequently, cancer cells consume far more glucose than normal cells to maintain a sufficient ATP supply for their active metabolism and proliferation.

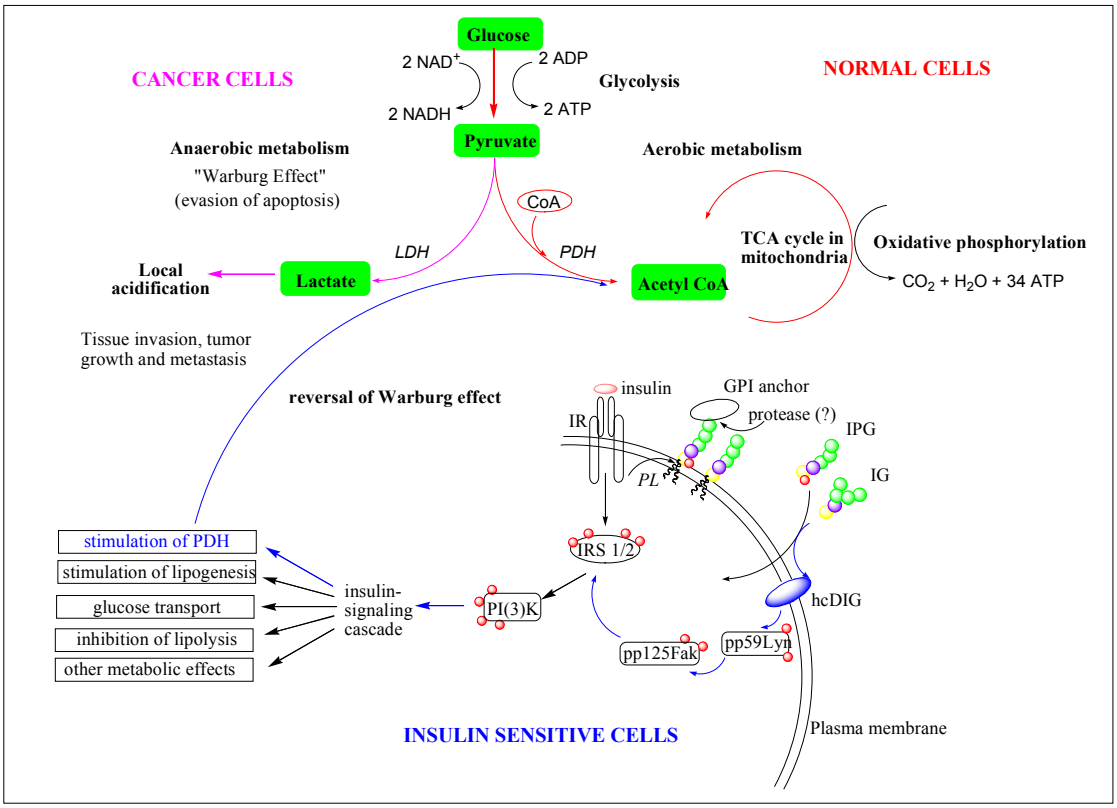


Figure 11. Schematic representation of relationship between IG and the glucose metabolism.

### 1.6.3 Enhanced aerobic glycolysis in cancer cells: The Warburg effect

In 1930 Otto Warburg, a German scientist first observed the phenomenon of increased glycolysis in tumor cells under aerobic conditions. He showed that, compared to normal cells, malignant cells exhibit significantly elevated glycolytic activity even in the presence of sufficient oxygen. Warburg considered this phenomenon the most fundamental metabolic alteration in malignant transformation, or the origin of cancer cells.[69] Later this phenomenon became known as the Warburg effect. Increased uptake of glucose by cancer cells is evident from positron emission tomography (PET) studies

using a glucose analogue tracer $^{18}$fluorodeoxyglucose (FdG).[70] So the question arises: why do cancer cells alter their metabolic pathway? What is the advantage of switching to aerobic glycolysis even in the presence of oxygen? The answer to these questions is evident from understanding the role of mitochondria in glucose metabolism and control of cell growth.

### 1.6.4 Mitochondria, apoptosis, and cancer

Mitochondria are the major source of cellular energy in the form of ATP. Mitochondria also play an important role in the regulation of cellular metabolism and cell death. Old and damaged cells undergo a process of well designed, controlled and regulated programmed cell death (PCD) or apoptosis whereby the damaged cells undergo a "clean" death and excretion from the body.[71] Many pro-apoptotic proteins such as Apoptosis Inducing Factor (AIF), cytochrome c, etc., residing in the mitochondria, control this apoptotic process. Any uncontrolled growth or division of cells is thus regulated in a programmed manner. Due to uncontrolled proliferation, cancer cells should also undergo the process of apoptosis. But cancer cells, due to the aerobic glycolysis, shift the metabolic burden away from mitochondria (Warburg effect). Since cancer cells escape oxidative phosphorylation and switch to anaerobic metabolism, they are able to escape the process of apoptosis that is initiated in the mitochondria.

### 1.6.5 Treatment of cancer via metabolism

Several mechanisms have been suggested to affect energy metabolism of cancer cells that might contribute to the Warburg effect.[71] These metabolic changes may occur due to a number of factors: mitochondrial defects such as mutation in mitochondrial DNA resulting in malfunctioning of oxidative phosphorylation;[72] an adaptation to hypoxic environment in cancer tissues;[67] activation of certain oncogenic signals like Akt, Bcl-2 etc;[73,74] and changes in the function of mitochondrial enzymes, like fumarate and succinate dehydrogenase,[68] or due to abnormal expression of metabolic enzymes like hexokinase II in the voltage dependent anion channel (VDAC) of the outer mitochondrial membrane.[75] Association of hexokinase II with the mitochondrial membrane results in decreased mitochondrial outer membrane permeabilization (or MOMP), a process that mediates intrinsic apoptosis as well as increased aerobic glycolysis.[71] Several compounds target these mitochondrial proteins and membranes in order to induce apoptosis in cancer cells.[73,76]

An alternative strategy is to target aerobic glycolysis in cancer cells.[66,77] Inhibition of the glycolytic pathway would deprive the cancer cells of glucose, the major source of their energy production, and hence prevent them from growing and proliferating. However, normal cells, having functional mitochondria, could still survive inhibition of glycolysis *via* alternative energy sources like fatty acids and amino acids that can produce ATP by alternate pathways in the TCA cycle.[66] Glycolytic inhibitors such as glucose analogues (2-deoxyglucose, mannoheptulose, and 5-thioglucose), hexokinase inhibitors (3-bromopyruvate, and lonidamine), PDH inhibitors (oxythiamine),

and lactate dehydrogenase inhibitors (oxalate, etc) have been shown to selectively kill cancer cells both *in vitro* and *in vivo* suggesting their potential as anticancer drugs.[66] However, use of these glycolytic inhibitors as anticancer drugs is not yet proved to be an absolutely safe treatment for cancer. Certain normal tissues like brain, retinae and testis rely on glucose as the main source of energy (evidence of alternative sources of energy like amino acids, fatty acids, etc, are not known for these tissues). Thus, glycolytic inhibition may deprive these tissues of glucose, and thus result in significant toxicity.[66] Moreover, current glycolytic inhibitors have low potency, stability and safety profiles. Thus, there is a need for more effective and stable anticancer drugs.

### 1.6.6 Inositol glycans and treatment of cancer

Another strategy to control cancerous growth might be to stimulate aerobic metabolism in cancer cells and essentially reverse the Warburg effect. Stimulation of aerobic metabolism in cancer cells would force the cancer cells to undergo normal glycolytic pathway and oxidative phosphorylation in mitochondria, resulting in the induction of intrinsic apoptosis. Compounds like IGs can stimulate aerobic metabolism in insulin-sensitive cells by stimulating the enzyme PDH phosphatase.[65] Similarly, these compounds may also stimulate aerobic metabolism in tumor cells, and consequently, reverse the Warburg effect (Figure 11). Stimulation of aerobic metabolism in tumor cells should reduce the production of lactic acid, the end product of aerobic glycolysis, while maintaining a constant glucose level. Preliminary proof of this hypothesis has been obtained by the fact that one synthetic IG analogue: GlcN-(α 1-6)-*myo*-Ins-2-palmitate,

called **IG-1** (Figure 12), is able to stimulate aerobic metabolism in cultured tumor cells.[35] Currently, the cytotoxic effect of IGs has been demonstrated only in **IG-1**, but the ability of other synthetic IG analogues to exhibit similar anticancer properties cannot be ruled out. Hence, exploration of the efficiency of IGs for the treatment of cancer is still in its initial stages.

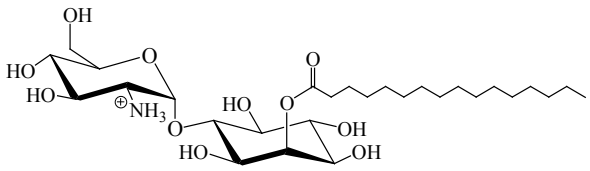


**18**

Figure 12. Structure of **IG-1**.

## 1.7 DESIGN AND METABOLIC ACTIVITY OF SYNTHETIC ANTI-CANCER IG, IG-1

### 1.7.1 Design and chemical structure of IG-1

The chemical structure of **IG-1** was designed on the basis of two factors. First, disaccharides are simpler to synthesize compared to the other complicated structures like those shown in Figures 7 and 8. Secondly, the presence of an acylated fatty acid chain on the C-2 position of the inositol ring was based on the fact that a similarly acylated inositol ring is also present in compound **19**, the chemical structure of an intermediate of the GPI anchor of human erythrocyte acetylcholinesterase (AChE) (Figure 13).[78] Acylation of inositol renders it resistant to the cleavage by PI-PLC, however, the action of GPI-PLD is known to hydrolyze such acylated GPI anchors, generating the "second messengers" or

IPGs.[19] The similarity between structures of **IG-1** and **19** suggests that **IG-1**, like **19**, may not be immunogenic.

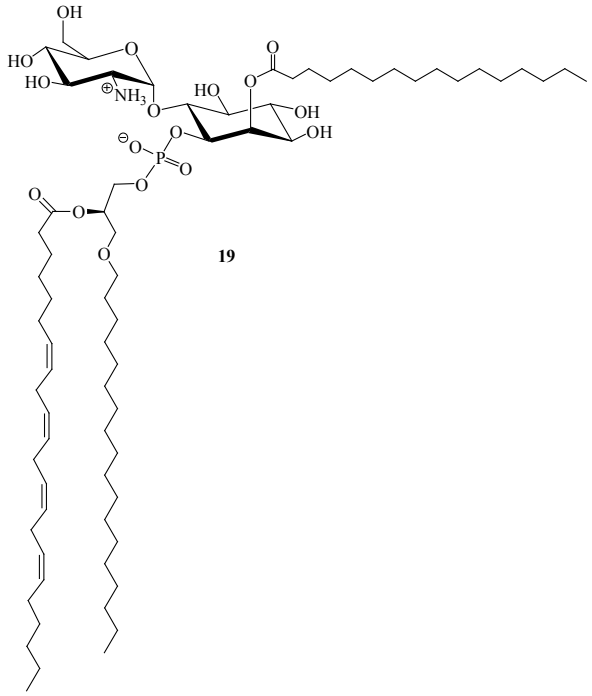


Figure 13. Glycolipid intermediate formed during biosynthesis of GPI anchor of human erythrocyte AchE.

### 1.7.2 Biological activity of IG-1

Synthesis of compound **IG-1** was successfully accomplished in Marc d'Alarcao's laboratory in 2007.[35] The insulin-mimetic activity of **IG-1** was confirmed by its ability to inhibit lipogenesis to an extent comparable to that of the simple disaccharide **3** (Figure 6). The reported activity of **IG-1** was 24% MIR (maximal insulin response) with an $EC_{50}$ value of 14 μM. In addition to being an insulin-mimetic, **IG-1** was also reported to have cytotoxic effects on several human cultured cancer cell lines including cells from mammary cancer (MCF-7), pancreatic cancer (Panc-1, MiaPaca 2, and BXPC3), and gastric cancer (MKN4S). At 100 μM concentration, the cytotoxic effects of **IG-1** were

found to be comparable to compounds like resveratrol and butyrate, both known to induce apoptosis in cancer cells (Figure 14a).[79] Furthermore, the cytotoxicity of **IG-1** was highly *selective*, in the sense that only cancer cells were killed, while the normal cells were completely unaffected by **IG-1** (Figure 14b).

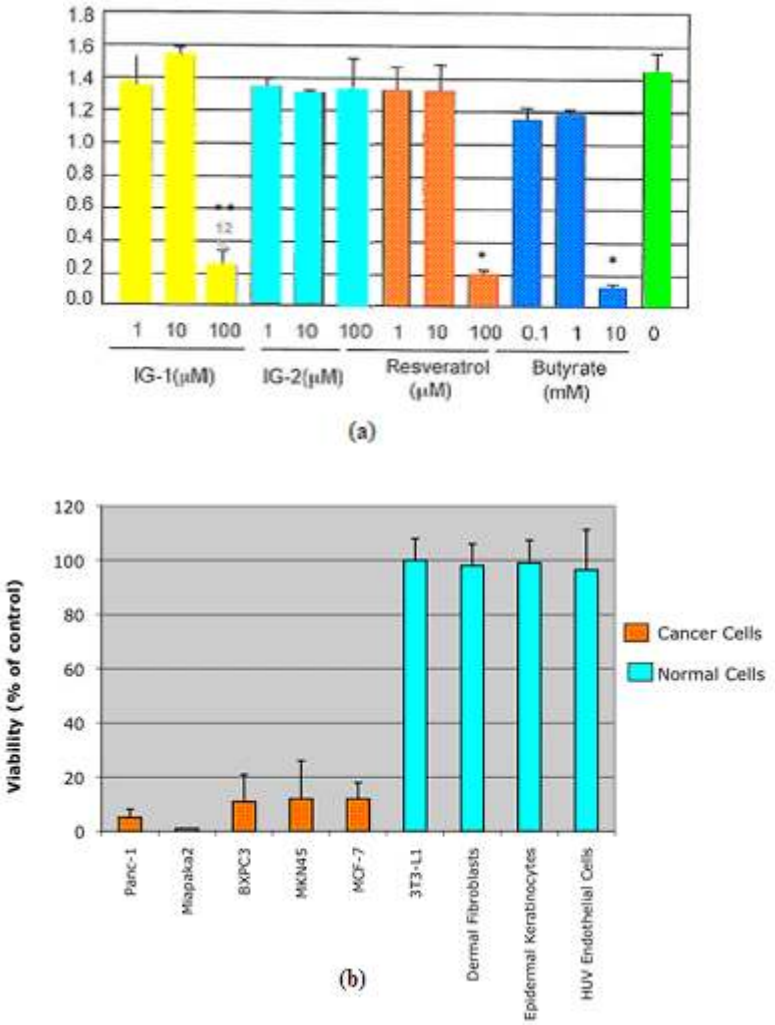


Figure 14. (a) Effect of **IG-1** on MCF-7 cancer cell line compared to another IG analogue, **IG-2**, resveratrol and butyrate (b) Cytotoxic effect of 100 μM **IG-1** on normal (blue) and cancer cells (orange) (Data reproduced with permission of Prof. Marc d'Alarcao, San Jose State University).

These data suggest that **IG-1** has the potential to be used as an anti-cancer drug, acting *via* an unknown mechanism that involves the stimulation of aerobic metabolism, and thus induction of apoptosis in cancer cells. However, the utility of **IG-1** as an anticancer agent is limited due to the instability of the acyl group under physiological conditions as described below.

### 1.7.3 Limitations of IG-1

Compound **IG-1** (Figure 12) is a disaccharide with a palmitoyl group attached at the C-2 position of the inositol ring. The ester linkage, in general, is labile and readily hydrolysable. Compounds with ester linkages can easily be hydrolyzed under acidic or basic conditions. *Esterases* in the blood are also capable of hydrolyzing ester linkages under physiological conditions. **IG-1**, with an ester linkage, is therefore susceptible to such hydrolysis in blood (Figure 15). The hydrolyzed product **20** is reported to have no cytotoxic effects.

Another major issue related to the stability of **IG-1** is the migration of the palmitoyl chain to other hydroxyl groups. **IG-1**, with a palmitoyl chain in the axial position, has the desired cytotoxicity but relatively low stability. Migration of this palmitoyl chain to the more energetically preferable equatorial position (*via* a trans-esterification reaction), results in stable compound **21**, but is also accompanied by complete loss of activity (Figure 15). Thus, either hydrolysis of the ester linkage or migration of the palmitoyl chain to other hydroxyl groups can result in loss of activity of **IG-1**.

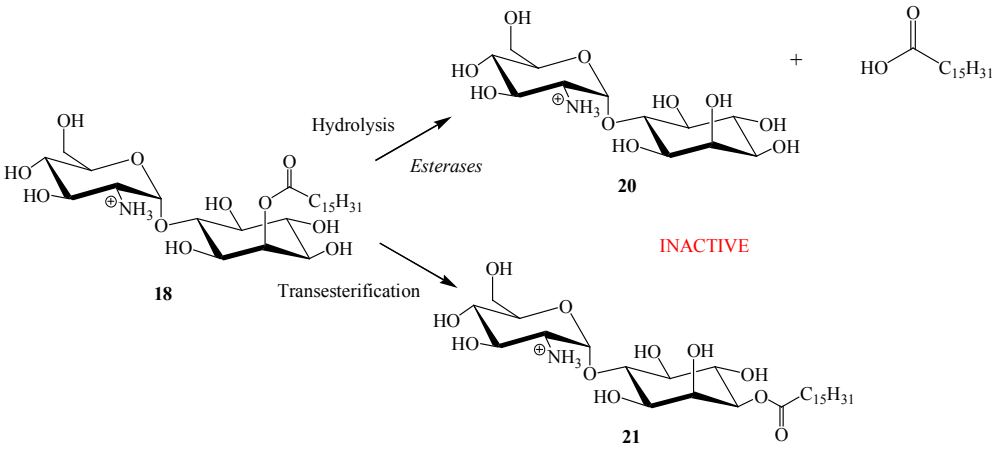


Figure 15. Limitations of **IG-1**.

Any strategy that can prevent these drawbacks of **IG-1** would be effective in synthesizing a potential anticancer IG. One such strategy has been proposed by Prof. Marc d'Alarcao, and it forms the basis of my research project.

# CHAPTER 2

# RESEARCH GOAL AND SYNTHETIC PLAN

## 2.1 RESEARCH GOAL

As discussed in Section 1.7.3 of Chapter 1, the major problem hypothesized with **IG-1** that might restrict its use as an anticancer agent is related to its stability and migration of the palmitoyl chain to other hydroxyl groups under physiological conditions. Thus the current research goal is to synthesize an analogue of **IG-1** that would have either an ether or thioether linkage between the fatty-acid chain and the *myo*-inositol. The hypothesis is that since ethers and thioethers are comparatively more resistant to hydrolysis than esters, replacement of the functional groups might induce extra stability in the compound, thus resulting in a greater half-life of the compound in the body. Consequently, two possible IG analogues, **22** and **23**, have been designed that might be able to mimic the activities of **IG-1**, while maintaining their structural arrangement under physiological conditions (Figure 16).

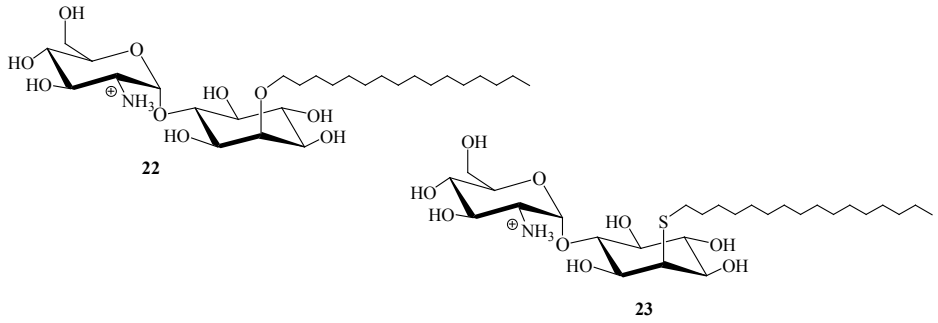


Figure 16. Analogues of **IG-1** with an ether (**22**) or thioether linkage (**23**) at C-2 position of inositol ring.

## 2.2 SYNTHETIC STRATEGY

### 2.2.1 Retrosynthetic analysis of analogues of IG-1, 22 and 23

A retrosynthetic analysis for preparation of the desired analogues **22** and **23** is shown in Scheme 1.

**Scheme 1.** Retrosynthetic analysis of compounds **22** and **23**.

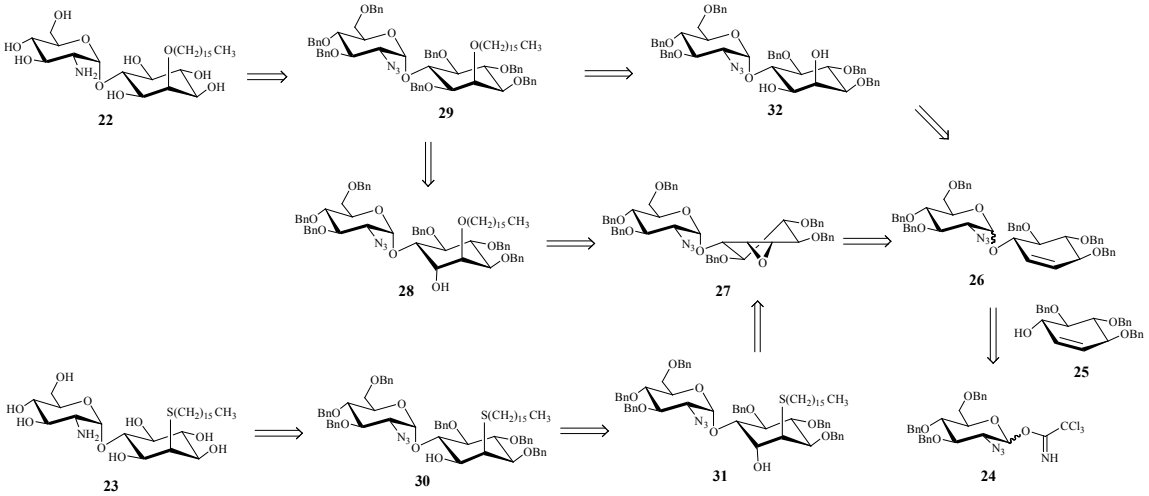

Compounds **22** and **23** could be obtained by reduction of fully protected **29** and **30**, respectively. The protective groups employed for these compounds are benzyl ether and azide groups for the protection of alcohol and amine functional groups, respectively. The advantage of using these protective groups is their easy deprotection. Compound **29** could in turn be obtained from **28** by Mitsunobu inversion at C-1 position of *myo*-inositol ring. Mitsunobu inversion has been widely used for inversion of stereochemistry of alcohols since 1967,[80] particularly due to its advantage of mild reaction conditions and compatibility with a wide array of functional groups. Compound **28** could be obtained regioselectively from **27** by nucleophilic trans-diaxial ring opening of epoxide. Both

acid-catalyzed and base-catalyzed ring opening of the epoxide is possible. However, the acid-catalyzed ring opening reaction is more efficient due to the reversible formation of more reactive conjugate acid of the epoxide and also due to the solvation of the oxonium form of the epoxide in acidic solutions.[81] The acid-catalyzed ring opening of **27** could however, be problematic due to the possibility of hydrolysis of the glycosidic linkage under acidic conditions. Thus optimum conditions for acid catalyzed ring opening of **27** need to be determined. A diastereomeric mixture of two possible epoxides of **27** could in turn be obtained by epoxidation of olefin pseudodisaccharide **26** using either m-chloroperoxybenzoic (mCPBA) or dimethyldioxirane (DMDO) solution in acetone. Olefin pseudodisaccharide **26** can be synthesized by α-selective glycosylation reaction of *myo*-inositol derivative **25** with fully protected 2-azido-2-deoxy-glycosyl bond donor **24** under controlled conditions.[35] Conduritol **25** could be synthesized from commercially available D-xylose **33** in 9 steps as shown in Scheme 2.[53,82] The overall yield for these step reactions is about 16-20%. However, the advantage of following this scheme is that the reactions could be performed on larger scales.

Scheme 2. Synthesis of conduritol **25** from D-xylose.

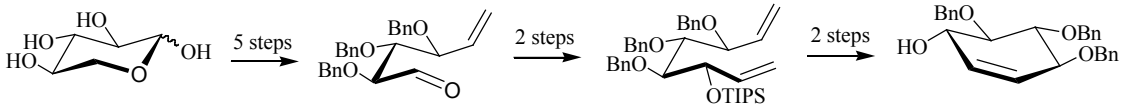


**33** **34** **35** **25**

Alternatively, **29** could also be obtained from diol intermediate **32** by selective alkylation at the axial hydroxyl group (Scheme 1).[35] In alkylation reactions of an axial-

equatorial pair of cis-diols, the equatorial oxygen would react preferentially.[83,84] However, benzylation of the equatorial hydroxyl group of **32** followed by an alkylation reaction with palmityl halide might yield **29** regioselectively. Diol intermediate **32** is a known compound that could be prepared from olefin pseudodisaccharide **26** by the well-known Sharpless asymmetric dihydroxylation reaction using catalytic amounts of osmium tetroxide and triethylenediamine (DABCO).[35] The disadvantage of this pathway would be the difficulty in asymmetric dihydroxylation of cis-alkenes.[85] However, the advantage would be a much shorter synthetic route to the target compound **22** as compared to the epoxidation pathway.

The trichloroacetimidate donor **24** is also a known compound that could be synthesized from commercially available D-glucosamine **36** as shown in Scheme 3b.[86,87] An alternate strategy for synthesis of **24** was also proposed in Scheme 3a. The advantage of scheme 3a would have been a novel synthetic route to **24**. Unfortunately, the proposed scheme did not work.

Scheme 3. Synthesis of trichloroacetimidate donor **24** from D-glucosamine.

**Scheme 3a**

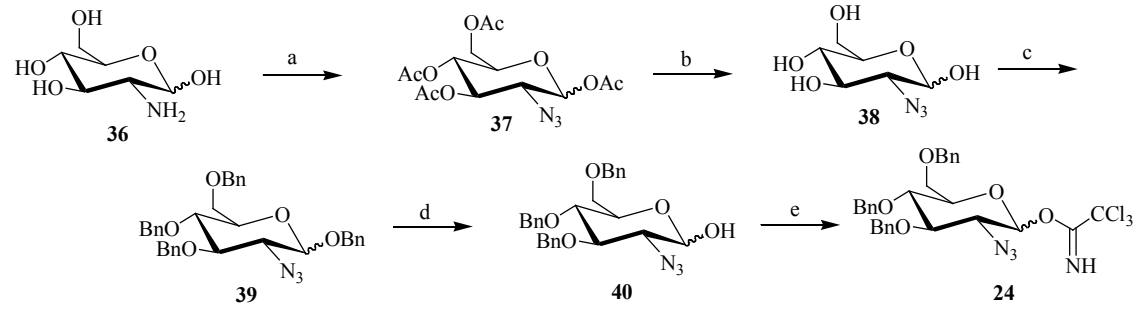

Reagents: a) 1. $TfN_3$, $H_2O$, $K_2CO_3$, $CH_2Cl_2$, MeOH, $CuSO_4$ ; 2. $Ac_2O$, pyridine, DMAP ; b) MeOH, $CH_3ONa$; c) BnBr, NaH, THF ; d) AcOH, $CH_3SO_3H$, dioxane e) $CCl_3CN$, $K_2CO_3$, $CH_2Cl_2$.

**Scheme 3b**

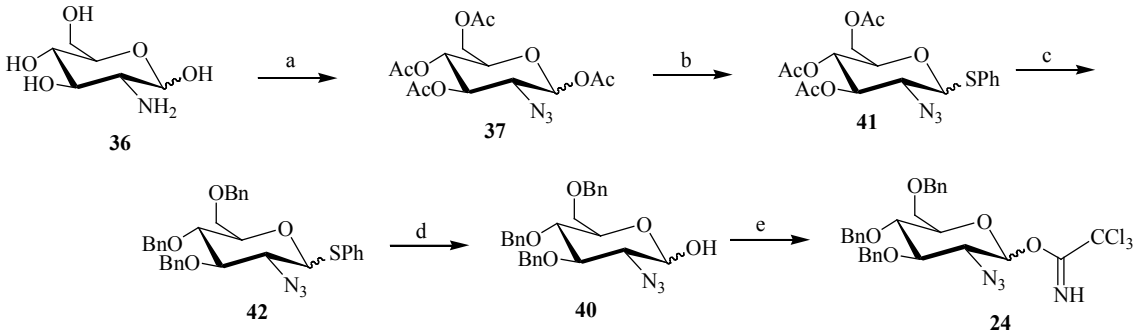

Reagents: a) 1. $TfN_3$, $H_2O$, $K_2CO_3$, $CH_2Cl_2$, MeOH, $CuSO_4$ ; 2. $Ac_2O$, pyridine, DMAP ; b) $BF_3.Et_2O$, PhSH, $CH_2Cl_2$; c) 1. aq. NaOH, $nBu_4NHSO_4$, benzene; 2. BnBr; d) NBS, aq. acetone; e) $CCl_3CN$, $K_2CO_3$, $CH_2Cl_2$.

The synthetic scheme to **23** was based on the trans-diaxial ring opening of the epoxide **27** using the corresponding thiolate anion of commercially available hexadecanethiol (instead of the alkoxide anion of haxadecanol) as a nucleophile (Scheme 1). Thiolate anion would be a better nucleophile than alcohol owing to the larger size and lower electronegativity of sulfur as compared to oxygen. So, there could be a better chance of successful nucleophilic substitution with the thiolate anion as opposed to the

alkoxide anion. Also the thioethers are amenable to further oxidation resulting in the corresponding sulfoxides and sulfones. A sulfoxide analogue of **23** would be structurally more analogous to **IG-1** (similarity with the carbonyl group), and thus there could be a better chance for synthesizing a more stable compound than **IG-1** with similar biological activities. However, there are two possible diastereomers of the sulfoxide, complicating the synthesis.

### 2.2.2 Regioselective monoalkylation of vicinal diols

Monoalkylation of vicinal diols with alkyl halides typically results in the corresponding ethers. The most general method for such *O*-alkylation of alcohols is the Williamson's ether reaction that involves the treatment of an alkyl halide with alkoxide ion prepared from the corresponding alcohol in presence of a suitable base. However, in carbohydrate polyols, attempts at selective alkylation of secondary hydroxyl groups (bearing similar reactivity) by a Williamson-type procedure would result in a mixture of ethers. Thus selective protection of hydroxyl groups in carbohydrate diols or polyols is required.

Use of organotin derivatives for regioselective acylation, alkylation and oxidation of alcohols has been extensively reviewed in the past.[83] Treatment of vicinal diols (c*is* or *trans*) with dibutyltin oxide provides a cyclic "stannylene acetal" derivative (Scheme 4). The electropositive character of tin metal causes an increase in the reactivity (nucleophilicity) of an attached oxygen atom so that subsequent acylations or alkylations may be performed under mild conditions. Moreover, due to a high degree of selectivity

for reaction at equatorial positions, this method is particularly useful for monoalkylation of equatorial hydroxy group in an equatorial-axial pair.[88] Besides, the dibutyltin oxide method is able to selectively afford *O*-monosubstituted diol moieties even in the presence of other unprotected hydroxyl groups.[89]

Scheme 4. Selective monoalkylation of vicinal diols.

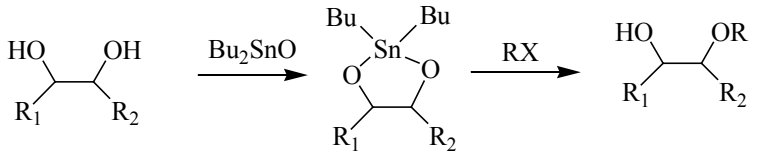


Thus, based on the easy preparation of stannylene intermediates, their simple usage, and good yields and selectivity obtained, this method was chosen for the selective palmitylation of the *cis*-dihydroxylated compound **32**.

### 2.2.3 Epoxidation of olefin pseudodisaccharide 26 using mCPBA and (salen)-Mn complexes

A literature search on epoxidation procedures revealed the use of catalytic amounts of chiral salen-based complexes for enantioselective epoxidation of olefins.[90] Oxidizing agents like mCPBA or bleach (NaOCl) are reported to be effective reagents for epoxidation, but they do not provide the desired selectivity.[91] However, in the presence of co-oxidants such as N-methylmorpholine N-oxide (NMO) and Jacobsen's catalyst (N, N'-bis(3,5-di-ter-butylsalicylaldehyde)-1,2 cyclohexanediaminomanganese(III) chloride) (Figure 17), highly selective epoxidation products could be obtained.

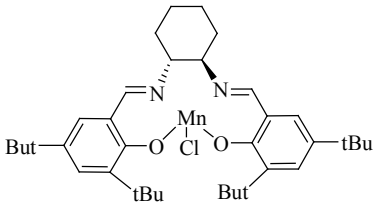


Figure 17. Structure of R,R-Jacobsen's catalyst.

Jacobsen's catalyst is the most common salen-based complex used for stereoselective epoxidation of olefins.[92] The likely mechanism of this catalytic reaction is illustrated in Scheme 5. Initial transfer of the oxygen atom from the oxidant to (salen) Mn (III) results in a reactive (salen)-Mn (V) oxo intermediate that acts as an epoxidizing agent for the olefin. Epoxidation proceeds via radical intermediate that can either form a C-O bond directly, or it may undergo rotation followed by C-O bond formation to give the two possible isomers of the epoxide. However, in the case of cyclohexenes (as in our case) only the cis isomer is possible because of the high strain in a trans cyclohexene like structure.

Scheme 5. Mechanism of (salen)-Mn complex catalyzed epoxidation.

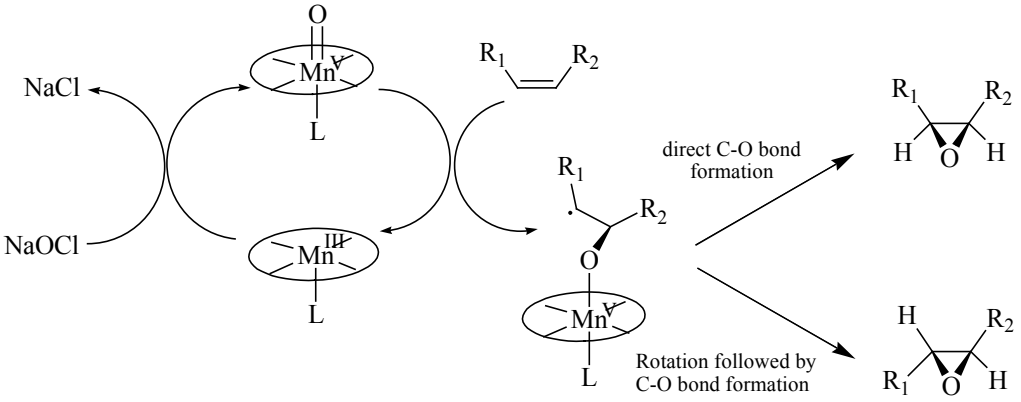

The salen-based catalysts have chiral centers in the diamine bridge and chiral groups near the metal center, and, therefore, high catalytic activity and enantioselectivity could be obtained for a wide variety of olefins. Enantioselection in the epoxidation of olefin is based on a side-on perpendicular approach of olefin to the Mn-oxo bond in the Mn (V) intermediate.[90] Use of either of the commercially available isomers (R, R or S, S) may yield the desired epoxide in high enantiomeric excesses.[91]

### 2.2.4 Alternative approach to synthesis of epoxide 27 using dimethyl dioxirane (DMDO solution)

Use of DMDO solution in acetone can also be employed for stereospecific epoxidation of alkenes. DMDO is a powerful oxidizing agent that can be prepared as a solution in acetone from distillation of a buffered aqueous solution of potassium peroxomonosulfate or oxone ($2KHSO_5.KHSO_4.K_2SO_4$) in acetone.[93,94] DMDO is a volatile peroxide, and hence it is usually prepared as dilute solutions (0.4 to 0.15M) in acetone. Being a strained cyclic peroxide, DMDO can readily transfer its peroxide oxygen to the alkene, thereby forming stable acetone as the only biproduct (Scheme 6). Thus advantages of using DMDO for epoxidation reaction are mild reaction conditions and easy work up. Various computational models of the transition state show that the reaction occurs by a concerted mechanism similar to that with other peroxy acids.[95]

Scheme 6. Epoxidation of olefin pseudodisaccharide **26** using DMDO solution.

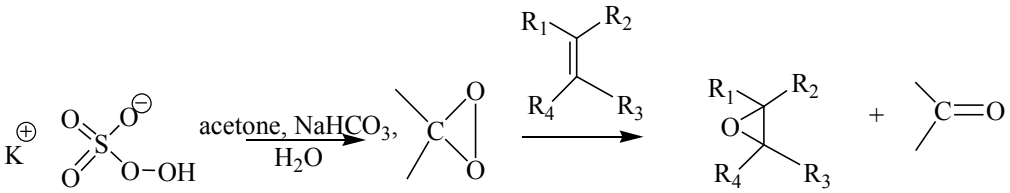

# CHAPTER 3

# RESULTS AND DISCUSSION

## 3.1 SYNTHESIS OF DIFFERENTIALLY PROTECTED MONOSACCHARIDE UNITS 24 AND 25

Synthesis of the target compounds **22** and **23** (Scheme 1, p. 32) was initiated by the syntheses of known compounds **24** and **25** *via* literature procedures (Section 2.2.1).[53,82,86,87] Initial attempts to synthesize **24** *via* Scheme 3a were unsuccessful probably due to the interconversion between the cyclic and acyclic forms of the glucosamine derivative (Figure 18). Due to this interconversion, benzylation of **38** resulted in a mixture of various benzylated products. Scheme 3b, however, was successful, probably due to the higher stability of the phenyl thioglycoside group.[86]

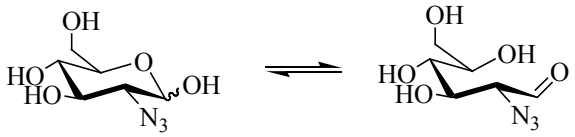


Cyclic form Acyclic form

Figure 18. Interconversion between cyclic and acyclic forms of **38**.

## 3.2 COUPLING OF 25 WITH 24

Following a previously known procedure, α-selective glycosylation of **25** with **24** resulted in a 58% yield of olefin pseudodisaccharide **26** with a 3:1 ratio of the α and β anomers (Figure 19).[35]

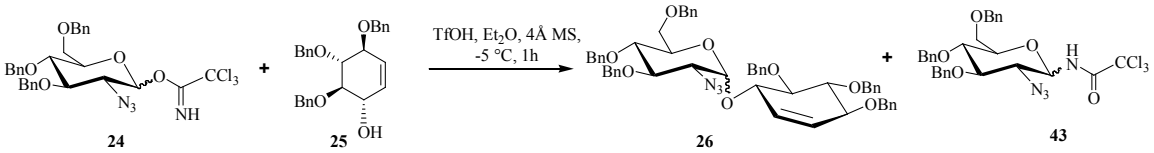


Figure 19. Glycosydic coupling of the trichloroacetimidate donor **24** and the *myo*-inositol derived acceptor **25**.

Chromatographic separation of the two anomers using a EtOAc/heptane solvent system (as reported in the literature)[35] was not very efficient. The spots for the starting material **24** and products were observed at the same $R_f$ on TLC using this solvent system. However, much better separation was observed when the reaction progress was monitored by TLC using a 1:1 hexane: ether solvent system. Also, careful observation revealed that the donor stained olive green, but the disaccharide product stained red in p-anisaldehyde stain. An amide side product **43** was also isolated from the reaction mixture.[96] This impurity almost co-elutes with the β-anomer of the olefin pseudodisaccharide in the 1:1 hexane: ether solvent system. However, the two can be separated efficiently using a 7:1 benzene: acetonitrile solvent system. Another side product from this glycosylation reaction could be a homodimer of the trichloroacetimidate donor, **44** (Figure 20). Use of old TfOH (may be wet), in one experiment, resulted in almost 80% conversion of the donor into homodimer **44** instead of it being converted into the desired disaccharide. Thus for the most efficient glycosylation, it is absolutely necessary to use completely anhydrous reagents and dry conditions.

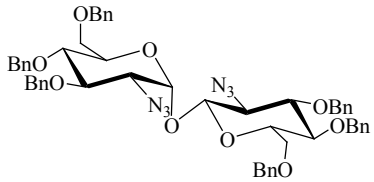


**44**

Figure 20. Possible structure of the homodimer of trichloroacetimidate donor **24**.

## 3.3 ATTEMPTED SYNTHESIS OF 27 *VIA* EPOXIDATION OF THE OLEFIN PSEUDODISACCHARIDE 26

Before doing the epoxidation reaction on the quite precious disaccharides, practice epoxidation reactions were done on the model compounds styrene and 3-cyclohexene-1-methanol using mCPBA, Jacobsen's catalyst, and N-methylmorpholine-N-oxide (NMO). Both substrates provided the corresponding epoxides in decent yields (40-50%). However, trial epoxidation on the beta-anomer of olefin pseudodisaccharide **26β** did not give the corresponding epoxide under any of those conditions (Table 1, entries 3-5). There is the possibility of decomposition of the epoxide under acidic conditions, so the reaction was performed in buffered solutions. But still there was no desired product obtained.

| Table 1. Epoxidation reaction on different substrates under different conditions | | | |
|---|---|---|---|
| **No.** | **Substrate** | **Conditions**[a] | **Yield %** |
| 1. | **Styrene** | R,R catalyst (4 mol %), NMO (5 equiv), mCPBA (2 equiv), -78 ˚C[91] | 59 |
| 2. | **3-cyclohexene-1-methanol** | R,R catalyst (5 mol %), NMO (5 equiv), mCPBA (2 equiv), 10% $Na_2CO_3$ solution, 0 ˚C[97] | 40 |
| 3. | **26β** | R,R catalyst (4 mol %), NMO (5 equiv), mCPBA (2 equiv), -78 ˚C | NR[b] |
| 4. | **26β** | R,R / S,S catalyst (5 mol %), NMO (5 equiv), mCPBA (2 equiv), 0 ˚C | NP[c] |
| 5. | **26β** | R,R catalyst (5 mol %), NMO (5 equiv), mCPBA (2 equiv), 10% $Na_2CO_3$ solution, 0 ˚C | NP[c] |
| 6. | **3-cyclohexene-1-methanol** | *In situ* reaction: Oxone (5 equiv), acetone (31 equiv), $Bu_4NHSO_4$ (0.2 equiv), buffered water (pH 7.2), 2-4 ˚C, 30 min | 90 |
| 7. | **25** | *In situ* reaction: Oxone (5 equiv), acetone (31 equiv), $Bu_4NHSO_4$ (0.2 equiv), buffered water (pH 7.2), 2-4 ˚C, very slow reaction | NP[c] |
| 8. | **25** | DMDO solution (large excess) | NP[c] |
| 9. | **26α** | DMDO solution (large excess) | NP[c] |

[a] reference of literature procedure; [b] no reaction; [c] no product could be isolated due to decomposition

Alternatively, the epoxidation reaction was also tried using freshly prepared DMDO solution in acetone.[93,94] Assuming a low concentration of the DMDO solution, a large volume was used to ensure the addition of an excess of this solution. The reaction

proceeded relatively quickly with model compound 3-cyclohexene-1-methanol under the reported conditions (Table 1, entry 6).[94] We also tried to epoxidize conduritol acceptor **25** under similar conditions. However, with **25** the reaction proceeded very slowly (suggesting that the substrate might be sterically hindered). Increasing the reaction time resulted in complete decomposition of the products. An attempt was also made to epoxidize the alpha-anomer of the olefin pseudodisaccharide, **26α,** using the higher concentration DMDO solution. There was some trace of "product-like" compound formed during the initial few hours of the reaction, but soon there was complete decomposition of the product spot into several different compounds. NMR spectra of all the compounds were taken, one of the spots could have been the desired product. However, considering the extent of decomposition observed in this reaction, and the limitation on the availability of the olefin pseudodisaccharide **26α**, it was decided to wait on the epoxidation scheme and try the alternate approach via dihydroxylation.

## 3.4 ATTEMPTED SYNTHESIS OF TARGET COMPOUND 22 *VIA* DIHYDROXYLATION OF 26

After several unsuccessful attempts at epoxidation of **26**, we decided to run the dihydroxylation reaction on **26α** using the known procedure (Figure 21).[35] Initially the reaction was started with the reported equivalents of the reagents. However, the reaction proceeded very slowly, so it was pushed to completion at the expense of adding more reagents and increasing the reaction time. The resulting cis-dihydroxylated product was a mixture of two isomers, **32** and **45**, with the two OH groups "up" and "down"

respectively. Careful separation using PTLC (45% EtOAc in heptane) yielded an almost 1:1 ratio of the two isomers in a combined yield of 58%.

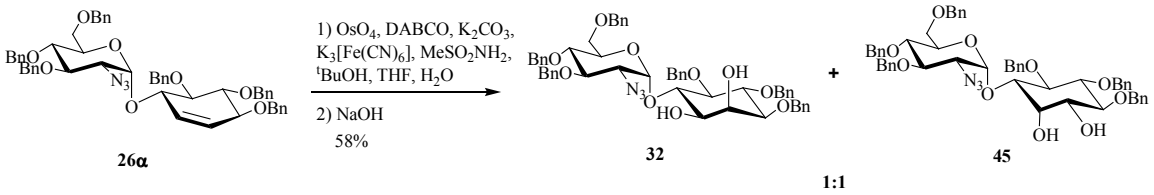


Figure 21. Asymmetric dihydroxylation of pseudodisaccharide **26α**.

### 3.4.1 Identification and characterization of the two diols 32 and 45

The next challenge was to identify the two dihydroxylated products. NMR spectra of the two compounds were ambiguous for this purpose. The identities of **32** and **45** were established by running a palmitoylation reaction on one of the isomers, **45**, Figure 22. Comparing the NMR spectrum of the resulting product **46** to a known compound (**90** in Azev's thesis)[35] confirmed the position of the hydroxyl groups in **45** to be "down".[35]

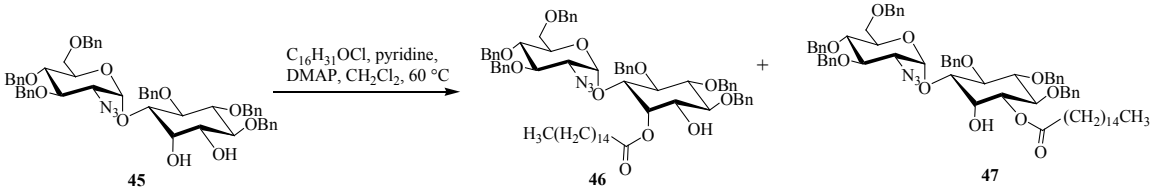


Figure 22. Palmitoylation of the diol **45.**

Once identified, the desired diol **32** was subjected to selective monobenzylation *via* stannylene intermediate **48** (Figure 23).[89] The two product isomers, **49** and **50**, were isolated in a 4:1 ratio and 65% combined yield.

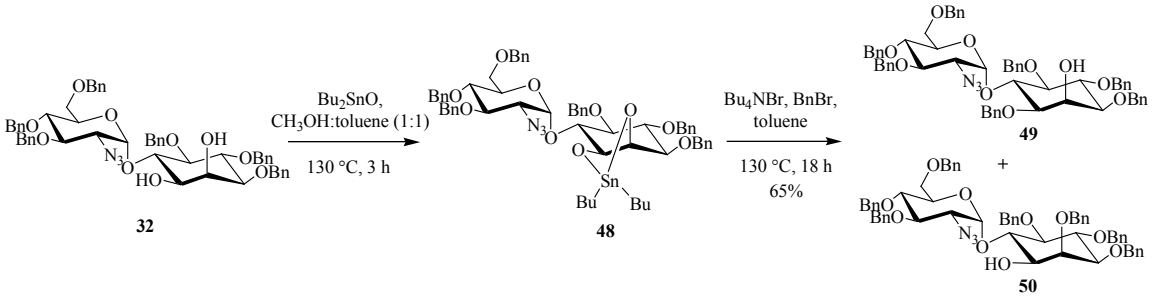


Figure 23. Selective monoalkylation of diol **32**.

### 3.4.2 Identification and characterization of the two isomers 49 and 50

Exact mass determination of the products by mass spectrometry indicated molecular formulae consistent with **49** and **50**. The next challenge was to identify which of the two isomers was the desired one (i.e. **49**, the isomer with a benzyl group at the 1-position and a free –OH group at 2-position of the *myo*-inositol ring). Based on the fact that stannylene mediated alkylation is generally favored at the equatorial position, it was suspected that the major product was **49**. $^{1}$H NMR and 2D COSY analysis of the minor isomer was used for further confirmation of this assumption. If the minor isomer were assumed to be **50** (Figure 24), then Ins-H1 should be coupled with the –OH proton and its signal should be a ddd, which upon the removal of –OH coupling by deuterium exchange should change to a dd with a small and a large coupling constant. The $^{1}$H NMR spectrum

of the minor isomer was recorded first in deuterated DMSO (DMSO-$d_6$) solvent, and then in DMSO-$d_6$ with a drop of $D_2O$. The doublet at δ 5.22 ppm in the DMSO-$d_6$ spectrum disappears on addition of $D_2O$ (Figure 25) indicating that this signal is due to the –OH hydrogen. A 2D COSY spectrum of the minor isomer in DMSO-$d_6$ was used to identify the proton that was coupled to the –OH group. This proton could either be Ino-H1 (if **50**) or Ino-H2 (if **49**). The signal for this proton was observed as a ddd at δ 3.71 ppm in DMSO-$d_6$. But, upon addition of $D_2O$, the coupling between the –OH hydrogen and this proton disappeared and the multiplicity of the signal changed to a doublet of doublet with a small and a large coupling constant (Figure 25). This indicated that the proton that is coupled to the –OH group in the minor isomer is Ino-H1, thus confirming our hypothesis that the minor isomer was actually **50**.

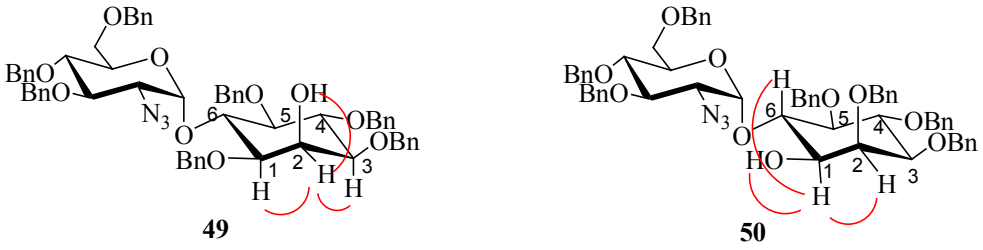


Figure 24. Structures of compound **49** and **50** showing coupling with OH group.

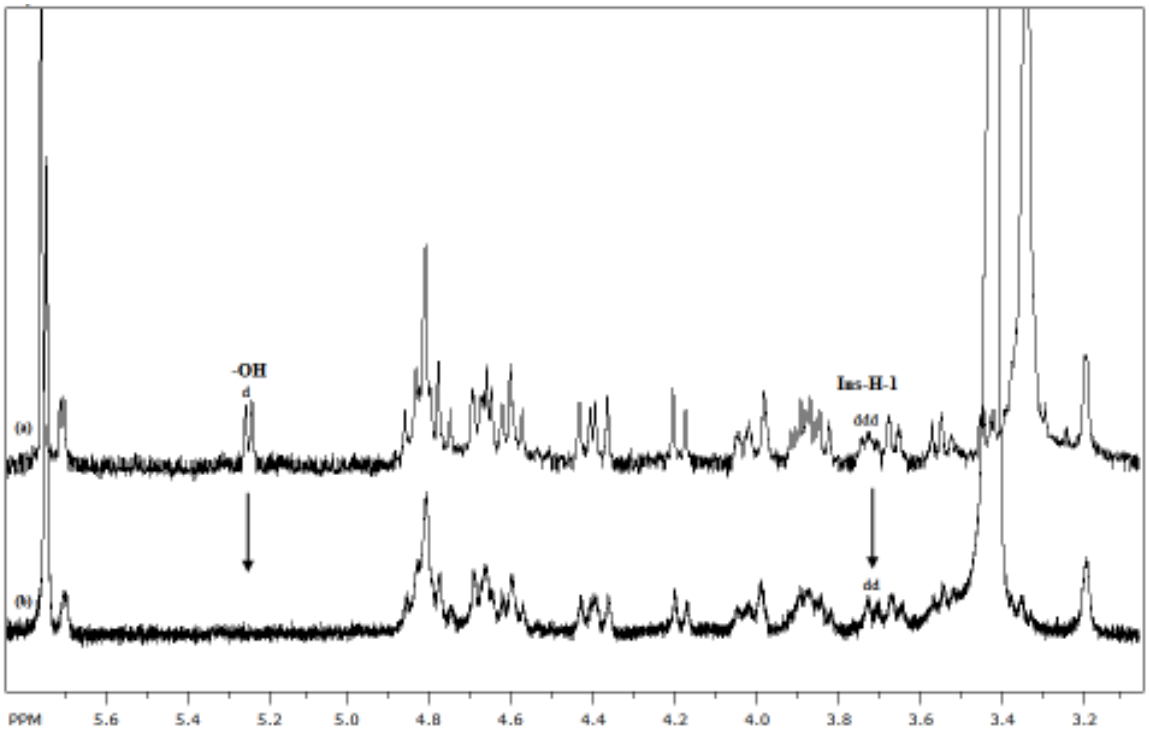


Figure 25. Deuterium exchange experiment with **50**.

### 3.4.3 Palmitylation of monobenzylated isomer 49

The next step was to attach a palmityl chain to the free –OH group on the 2-position of the *myo*-inositol ring of **49**. Cesium hydroxide based *O*-alkylation of alcohols was used as an initial approach.[98] The advantage of using cesium bases over the other metal hydrides/hydroxides is their relatively high solubility in dipolar aprotic solvents like dimethyl formamide (DMF), appropriate basicity, and their high degree of dissociation into solvated cations and relatively "free" anions that are the reactive species for further nucleophilic substitution.[99] The *in situ* generated cesium alkoxides are better nucleophiles that facilitate the $S_N2$ type replacement. The presence of added nucleophiles

like tetrabutylammonium iodide (TBAI) and activated molecular sieves are known to accelerate nucleophilic substitutions considerably. TBAI acts as a phase transfer catalyst and also provides a better leaving group ($I^-$) for the electrophile. Molecular sieves remove water from the reaction mixture thus preventing the protonation of alkoxides.

Before attempting the alkylation reaction on the most precious compound, **49**, it was desirable to practice the cesium hydroxide-promoted alkylation on a model compound. Alpha-methylbenzyl alcohol **51** was used for this purpose (Figure 26). Compound **51** was treated with the desired electrophile, palmityl bromide ($C_{16}H_{33}Br$), under slightly modified conditions from those described in the literature to give the corresponding ether **52**.[100] The reaction was very slow at room temperature. Heating the reaction to 60 ˚C accelerated the rate of formation of the product. However, the yield was moderate (20-30 %), possibly due to the E-2 elimination reaction in **51**. So this was not an ideal model for the practice of alkylation.

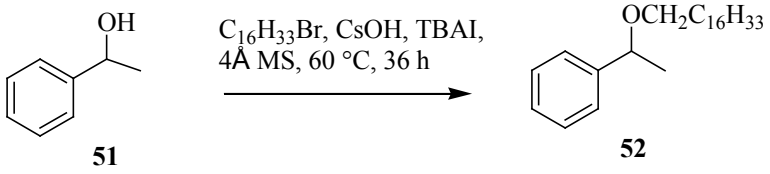


Figure 26. Model palmitylation reaction.

### 3.4.4 Palmitylation of the monobenzylated product obtained from the undesired ("down") diol

Compound **45**, being an isomer of **32**, was subjected to the monobenzylation reaction *via* stannylene intermediate (Figure 27). Only one isomer of the monobenzylated product could be isolated. Repeated reactions have to be done to find out the details.

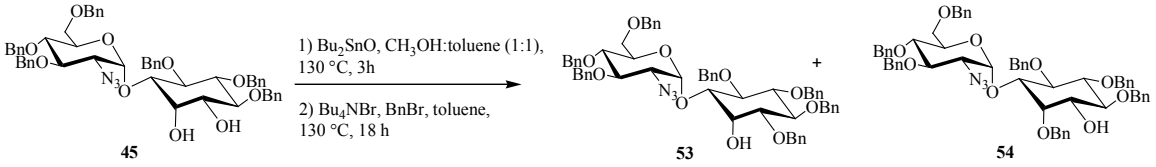


Figure 27. Selective monoalkylation of "undesired" diol **45**.

The resulting product, **53** with an axial –OH group on *myo*-inositol, was predicted to be a good model for practicing the alkylation reaction. Both CsOH and NaH bases were tried under different experimental conditions, but unfortunately none of them gave the desired product (Figure 28).

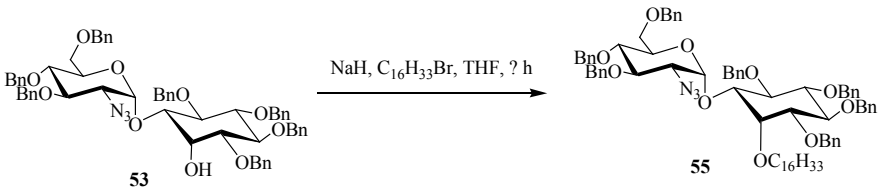


Figure 28. Practice alkylation on **53**.

Interestingly, alkylation of **49** using NaH base and TBAI in THF solvent proved to be a successful trial (Figure 29). High-resolution mass spectrometric analysis and the $^1$H NMR spectrum of the resulting product proved its structure to be **29**.

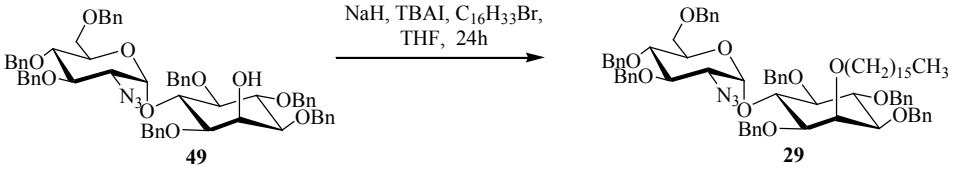


Figure 29. Palmitylation of **49**.

Finally, deprotection of the fully benzylated **29** by dissolving metal reduction using the established procedure[55] yielded the final lipid linked IG, **22**, which was further desalted using a Sephadex® G-10 size exclusion column to afford pure **22** (Figure 30).

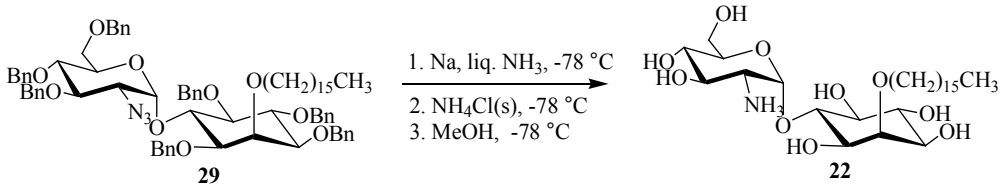


Figure 30. Deprotection of fully protected **29**

All of the reactions in the synthetic schemes were monitored by thin layer chromatography, and the products were characterized by $^1$H NMR spectroscopy. Some products were further analyzed by high-resolution mass spectrometry.

# CHAPTER 4

# CONCLUSIONS AND FUTURE GOALS

Synthesis of a non-hydrolyzable, palmitylated inositol glycan has been partially accomplished. Initial attempts to synthesize **22** and **23** *via* an epoxidation pathway (Scheme 1, p. 32) were not successful, probably due to the sterically hindered olefin pseudodisaccharide, **26**. However, an alternate pathway *via* dihydroxylation of **26** gave promising results. The two dihydroxylated isomers **32** and **45** were successfully isolated (1:1 ratio) and characterized. The position of the – OH groups ("up" or "down") in the two isomers was determined by running a palmitoylation reaction on one of the isomers. The desired diol (with both –OH groups "up") was successfully subjected to selective monobenzylation *via* a stannylene acetal intermediate. The two isomers **49** and **50** were successfully isolated and characterized using $^{1}$H NMR and COSY analysis. Palmitylation of **49** at the free hydroxyl group yielded fully protected lipid-linked disaccharide **29**. Deprotection of the resulting product by reduction with sodium and liquid ammonia yielded the target compound **22**.

Future goals include optimization of the synthesis of **22**, followed by biological testing for anti-cancer and anti-diabetic activities. Another goal is to retry epoxidation of **26** followed by the ring opening reaction. Success of this reaction would enable the synthesis of **23**, the thiol analogue of **22**.

# CHAPTER 5

# EXPERIMENTAL PROCEDURES

**General methods:** Solvents and reagents obtained from commercial sources (Fisher Scientific or Sigma Aldrich) were used without further purification with the following exceptions: DMF, and pyridine were distilled under reduced pressure from barium oxide. Tetrahydrofuran (THF), toluene, and diethyl ether were distilled from sodium benzophenone ketyl. Thiophenol was distilled using calcium chloride. Acetic anhydride and methylene chloride were distilled at their boiling points. Methanol was distilled using magnesium metal and iodine. Compound **35** was provided by Prof. Marc d'Alarcao (work of his previous student). All non-aqueous reactions were carried out under an argon or nitrogen atmosphere. Organic extracts were dried with anhydrous $Na_2SO_4$ or $MgSO_4$ and solvents were removed *in vacuo* on a rotary evaporator. Rotary evaporation was accomplished at 10-15 Torr and 23 ˚C. The carbohydrate intermediates were co-evaporated with toluene several times to make them completely anhydrous. Reactions were routinely monitored by thin layer chromatography (TLC) on Baker glass-backed silica gel plates (0.25-mm thickness) with a 254-nm fluorescent indicator. Compounds were visualized by one or more of the following techniques: ultraviolet illumination; dipping the TLC plates in ethanolic solution of 2.5% p-anisaldehyde, 3.5% sulfuric acid, and 1% acetic acid followed by heating; dipping the TLC plates in ethanolic solution of Hanes-Isherwood stain (ammonium molybdate/HCl/perchloric acid/acetone); subjecting the TLC plates to iodine vapors. Preparative separations were performed

either by flash chromatography on Baker silica gel (particle size 40-60 nm) or by preparative TLC. Nuclear magnetic resonance (NMR) data for $^{1}H$ were obtained on Inova-400 MHz or Inova-300 MHz NMR spectrometer and were reported in parts per million (δ) relative to TMS. High-resolution mass spectrometry (HRMS) data were obtained using electrospray ionization mass spectrometer (ESI-MS) method at the Scripps Centre for Mass Spectrometry located in La Jolla, California.

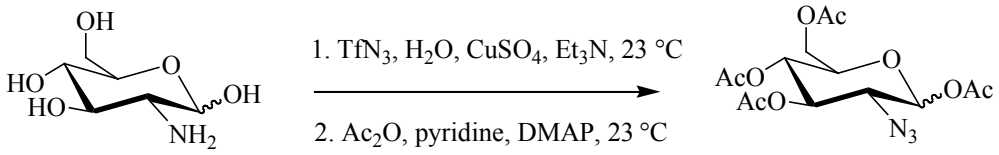


**36** **37**

**1,3,4,6-Tetra-*O*-acetyl-2-azido-2-deoxy- α/β-D-glucopyranoside (37).**[101] (a) *Preparation of $TfN_3$:* The reaction was set up under an argon atmosphere. A solution of $NaN_3$ (3.26 g, 0.05 mol) in dry acetonitrile (60 mL) was stirred vigorously at 0 ˚C for 10 min. Trifluoromethanesulfonic anhydride (7 mL, 6.67 x $10^{-2}$ mol) was added slowly to the reaction mixture over 10 min. The reaction mixture was stirred over an ice bath for about 2 h or until it turned milky white in color (the resulting $TfN_3$ solution should not be evaporated as $TfN_3$ is explosive when not in solution).[102] (b) *Diazo-transfer:* To a solution of D-glucosamine hydrochloride (11.05 g, 5.6 x $10^{-2}$ mol) in water (55 mL) was added $CuSO_4$ (140 mg, 5.6 x $10^{-4}$ mol) with vigorous stirring at 0 ˚C until a clear blue solution was formed. After 15 min, distilled triethylamine (15.6 mL, 11.2 x $10^{-2}$ mol) was added to the reaction mixture at 0 ˚C. The color of the solution turned ink blue. The triflic azide solution was then added to the glucosamine solution dropwise using a pressure equalizing dropping funnel. The color of the solution turned yellowish brown. After 30 min, the ice bath was removed and the reaction mixture was allowed to stir at room temperature for 16 h. The reaction mixture was then evaporated under vacuum to afford brown oil (Caution was exercised due to the explosive nature of $TfN_3$). The oil was coevaporated with toluene twice to remove any excess water. (c) *Acetylation:* To a solution of the brown oil in pyridine (45 mL) at 0 ˚C was added DMAP (35 mg, 0.23 mmol) and dry acetic anhydride (50 mL). The mixture was stirred over an ice bath until

the reaction was no longer exothermic, and then stirred at room temperature until TLC (silica, 5% EtOAc in $CH_2Cl_2$) showed completion of the reaction, about 24 h. The reaction mixture was then quenched with a saturated solution of $NaHCO_3$, extracted with $CH_2Cl_2$ (4 x 250 mL), the combined organic phases were dried over $MgSO_4$, filtered and concentrated *in vacuo*. The crude product from the reaction was purified by flash chromatography (2% EtOAc in $CH_2Cl_2$) yielding **37** (8.5 g, 40%) as light brown oil. $R_f$ = 0.17 (2% EtOAc in $CH_2Cl_2$). $^1$H NMR (400 MHz, $CDCl_3$): δ 2.02 (s, 3H, C**H**$_3$CO), 2.07 (s, 3H, C**H**$_3$CO), 2.09 (s, 3H, C**H**$_3$CO), 2.18 (s, 3H, C**H**$_3$CO), 3.66 (m, 1H, **H**-7), 3.79 (ddd, J = 1.2, 2.8, 4.8, 1H, **H**-5), 4.07 (dd, J = 2.1, 12.8, 1H, **H**-6), 4.29 (dd, J = 4.4, 12.8, 1H, **H**-2), 5.12-4.99 (m, 2H, **H**-3, **H**-4), 5.54 (d, J = 8.8,1H, **H**-1). Data is consistent with the literature values.[102]

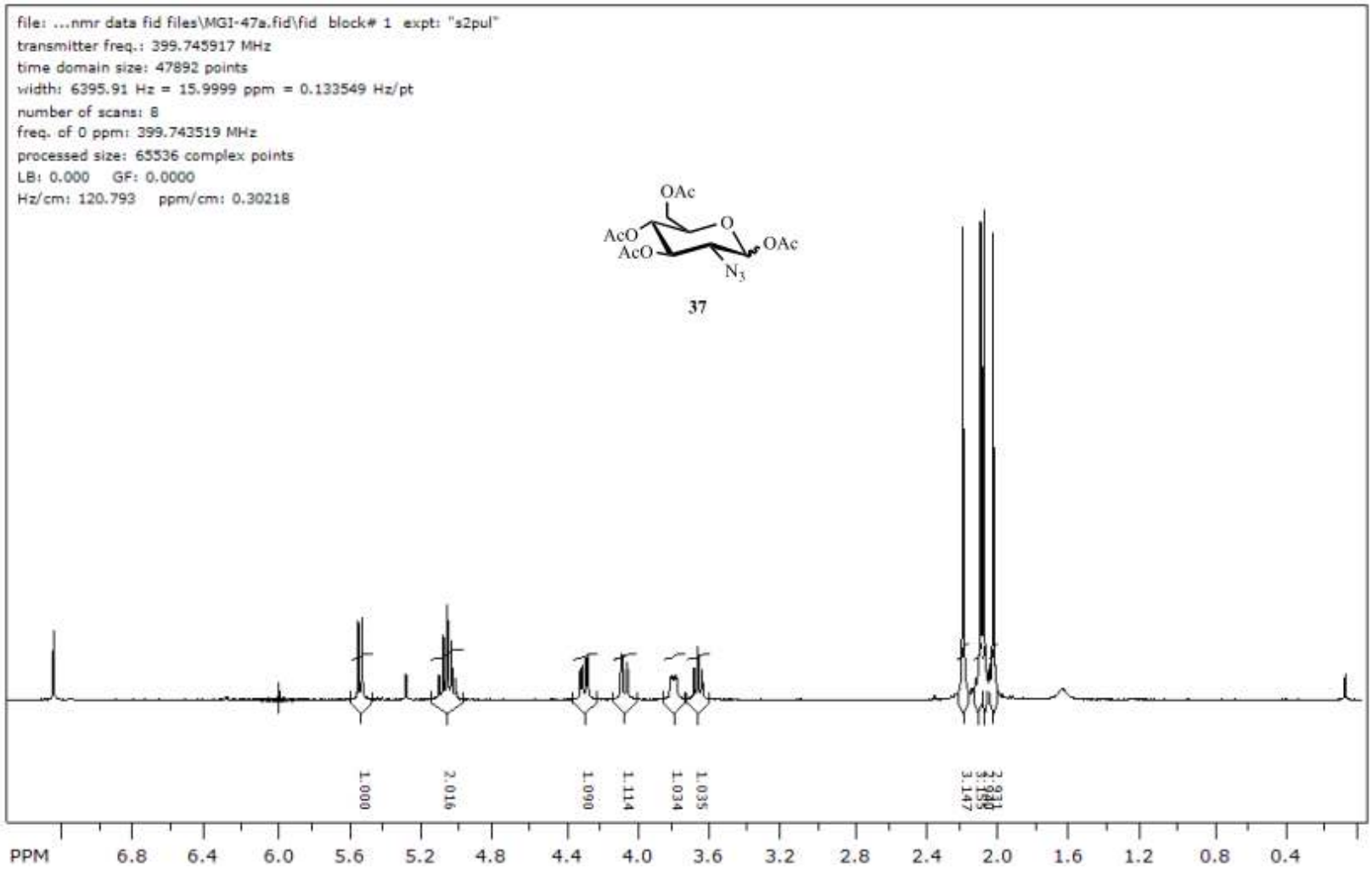
file: ...nmr data fid files\MGI-47a.fid\fid block# 1 expt: "s2pul"
transmitter freq.: 399.745917 MHz
time domain size: 47892 points
width: 6395.91 Hz = 15.9999 ppm = 0.133549 Hz/pt
number of scans: 8
freq. of 0 ppm: 399.743519 MHz
processed size: 65536 complex points
LB: 0.000 GF: 0.0000
Hz/cm: 120.793 ppm/cm: 0.30218
OAc
AcO
AcO
O
OAc
N3
37
1.000
2.016
1.090
1.114
1.034
1.035
3.147
PPM
6.8
6.4
6.0
5.6
5.2
4.8
4.4
4.0
3.6
3.2
2.8
2.4
2.0
1.6
1.2
0.8
0.4

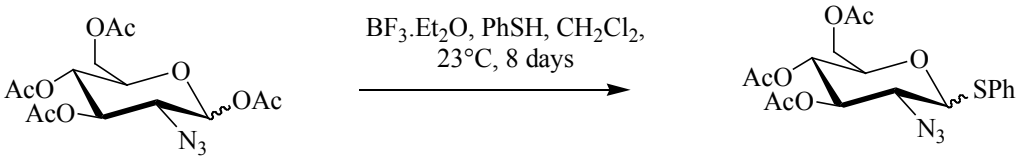


**37** **41**

**Phenyl-2-azido-3,4,6-tri-*O*-acetyl-2-deoxy-1-thio-α/β-D-glucopyranoside (41).**[86] To a solution of **37** (1.9 g, 5.1 mmol) in $CH_2Cl_2$ (41 mL) was added freshly distilled thiophenol (1.05 mL, 10.28 mmol) followed by boron-trifluoride etherate (2.85 mL, 23.12 mmol) with constant stirring under an argon atmosphere. The reaction mixture was stirred at room temperature until TLC (5% EtOAc in $CH_2Cl_2$) showed almost 98% conversion of the starting material into the product, approximately 8 days. The color of the reaction mixture changed from pale yellow to red to dark red as the reaction proceeded. The reaction mixture was diluted with $CH_2Cl_2$ (100 mL) and washed with brine (8 x 50 mL). The organic layer was dried over $MgSO_4$, filtered and concentrated *in vacuo* to afford a light brown oil. Purification of crude reaction product by flash chromatography (2% EtOAc in $CH_2Cl_2$) yielded **41** (1.13g, 52%) as a 3:1 α/β mixture ($R_f$ of the mixture = 0.62 (5% EtOAc in $CH_2Cl_2$)). Unreacted **37** (0.3g, 16% yield) was also recovered ($R_f$ = 0.43 (5% EtOAc in $CH_2Cl_2$)). $^1$H NMR for **41α** (400 MHz, $CDCl_3$): δ 2.02 (s, 3H, C**H**$_3$CO), 2.05 (s, 3H, C**H**$_3$CO), 2.11 (s, 3H, C**H**$_3$CO), 4.02 (dd, $J_{6a,6b}$ = 12.0, $J_{6a,5}$ = 2.0, 1H, **H**-6a), 4.08 (dd, J = 10.8, 5.6, 1H, **H**-2), 4.29 (dd, $J_{6a,6b}$ = 12.0, $J_{6b,5}$ = 5.4, 1H, **H**-6b), 4.59 (ddd, J = 7.2, 4.8, 2.0, 1H, **H**-5), 5.02 (Ψt, J = 12.8, 12.0, 1H, **H**-4), 5.33 (dd, J = 10.4, 9.2, 1H, **H**-3), 5.64 (d, J = 5.6, 1H, **H**-1), 7.26-7.51 (m, 5H, Ar**H**). $^1$H NMR for **41β** (400 MHz, $CDCl_3$): δ 1.99 (s, 3H, C**H**$_3$CO), 2.02 (s, 3H, C**H**$_3$CO), 2.07 (s, 3H, C**H**$_3$CO), 3.39 (Ψt, J = 9.8 Hz, 1H, **H**-2), 3.68 (ddd, J = 9.8, 4.7, 2.3 Hz, 1H, **H**-5),

4.16 (dd, $J_{6a,6b}$ = 12.1, $J_{6a,5}$ = 2.6, 1H, **H**-6a), 4.21 (dd, $J_{6a,6b}$ = 12.4, $J_{6b,5}$ = 4.9, 1H, **H**-6b), 4.48 (d, J = 10.2 Hz, 1H, **H**-1), 4.91 (Ψt, J = 9.64 Hz, 1H, **H**-4), 5.06 (dd, J = 9.6, 9.6, 1H, **H**-3), 7.20-7.63 (m, 5H, Ar**H**).

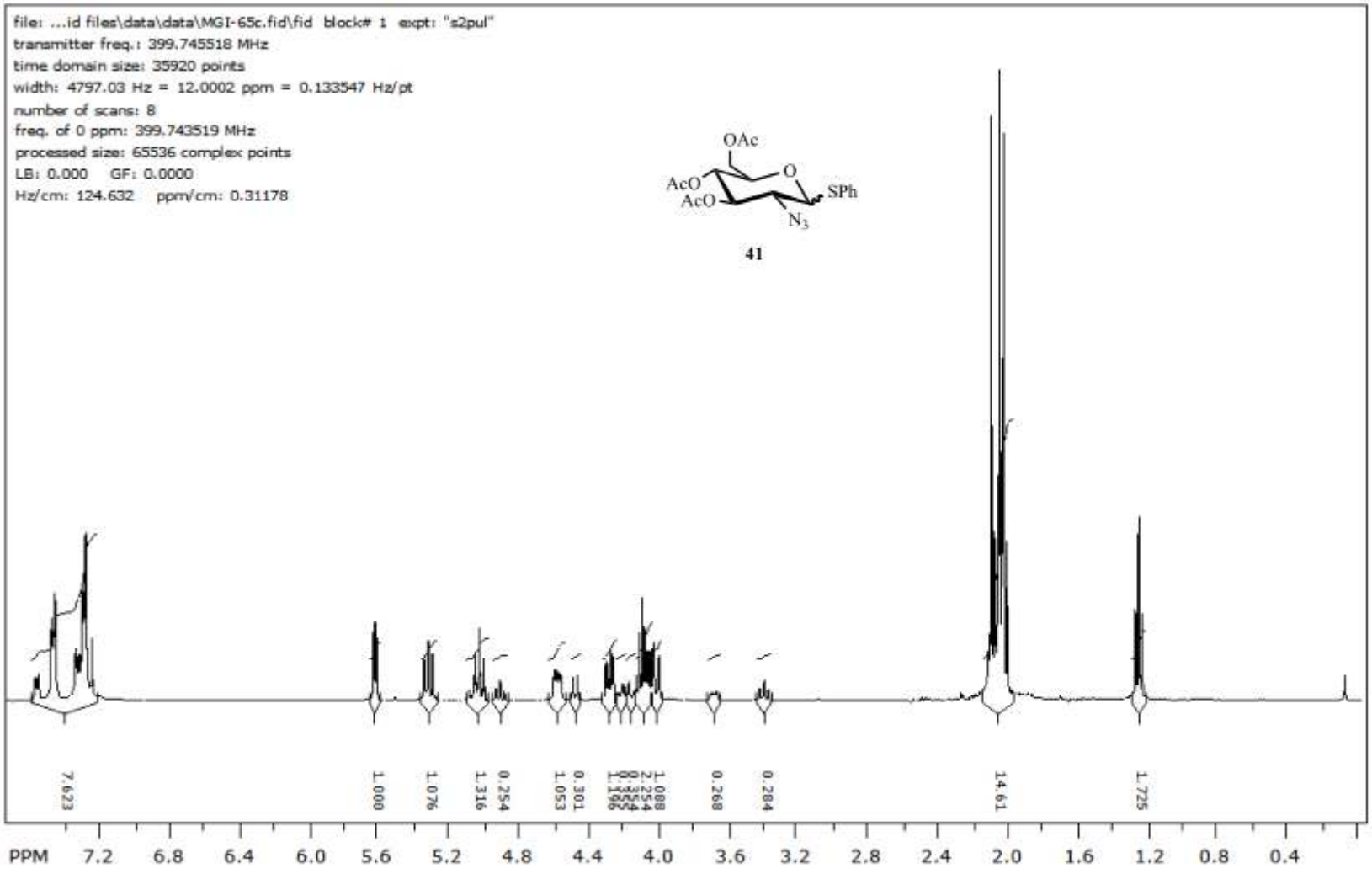
file: ...id files\data\data\MGI-65c.fid\fid block# 1 expt: "s2pul"
transmitter freq.: 399.745518 MHz
time domain size: 35920 points
width: 4797.03 Hz = 12.0002 ppm = 0.133547 Hz/pt
number of scans: 8
freq. of 0 ppm: 399.743519 MHz
processed size: 65536 complex points
LB: 0.000 GF: 0.0000
Hz/cm: 124.632 ppm/cm: 0.31178
OAc
AcO
AcO
O
SPh
N3
41
7.623
1.000
1.076
1.316
0.254
1.053
0.301
1.088
2.254
0.268
0.284
14.61
1.725
PPM
7.2
6.8
6.4
6.0
5.6
5.2
4.8
4.4
4.0
3.6
3.2
2.8
2.4
2.0
1.6
1.2
0.8
0.4

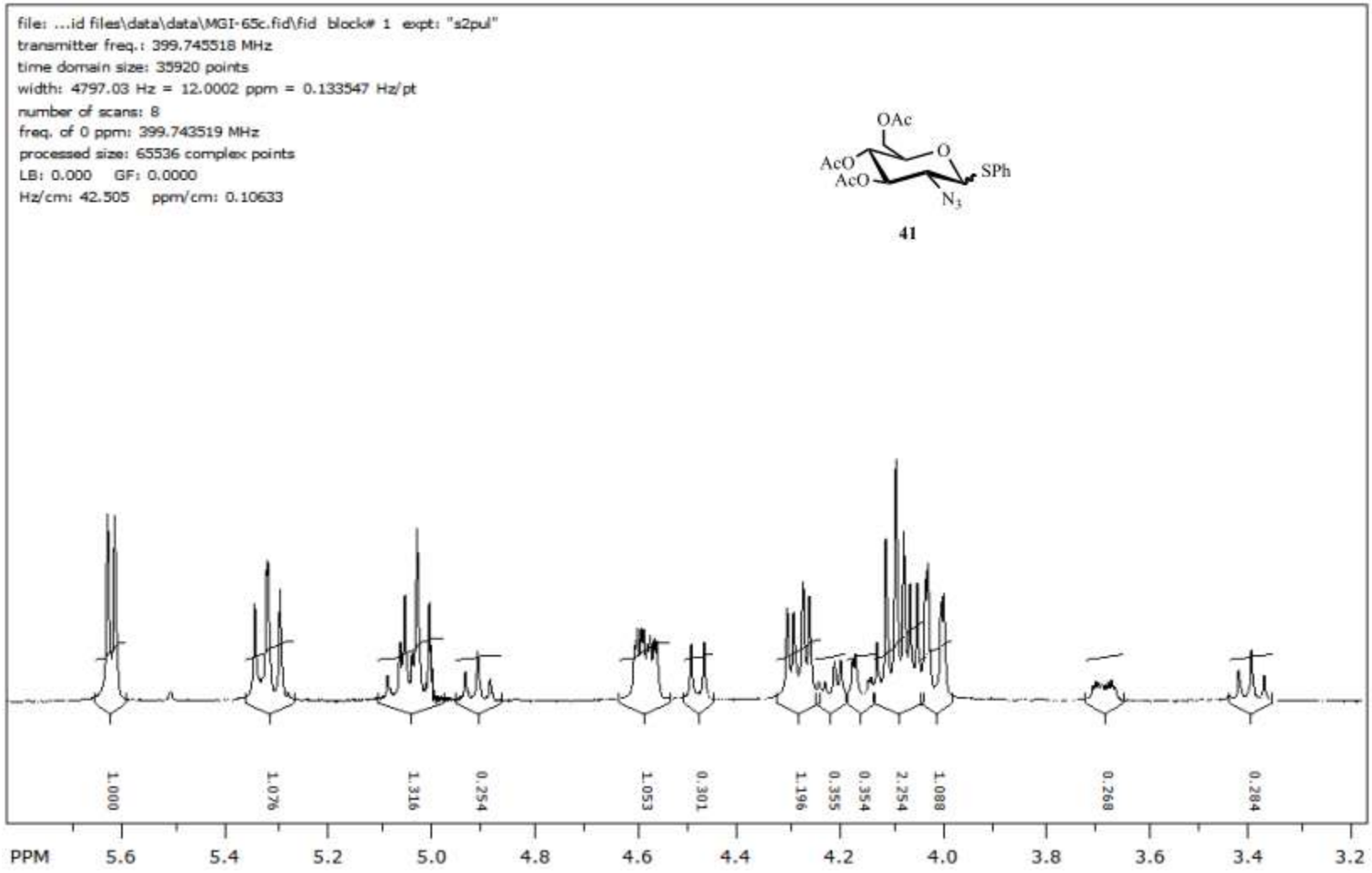
file: ...id files\data\data\MGI-65c.fid\fid block# 1 expt: "s2pul"
transmitter freq.: 399.745518 MHz
time domain size: 35920 points
width: 4797.03 Hz = 12.0002 ppm = 0.133547 Hz/pt
number of scans: 8
freq. of 0 ppm: 399.743519 MHz
processed size: 65536 complex points
LB: 0.000 GF: 0.0000
Hz/cm: 42.505 ppm/cm: 0.10633
OAc
AcO
AcO
O
SPh
N3
41
1.000
1.076
1.316
0.254
1.053
0.301
1.196
0.355
0.354
2.254
1.088
0.268
0.284
PPM
5.6
5.4
5.2
5.0
4.8
4.6
4.4
4.2
4.0
3.8
3.6
3.4
3.2

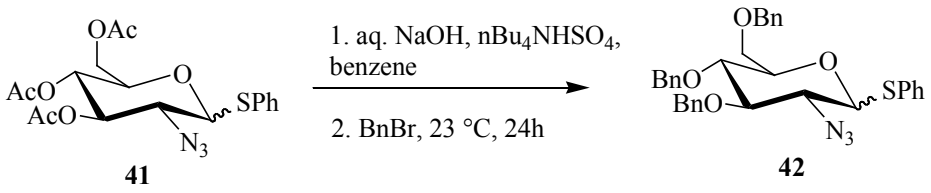


**41** **42**

**Phenyl-2-azido-3,4,6-tri-*O*-benzyl-2-deoxy-1-thio-α/β-D-glucopyranoside (42).**[87] To a pale yellow solution of **41** (1.13g, 2.62 mmol) in benzene (50 mL) was added 20% aqueous NaOH (25 mL) followed by tetra-n-butylammonium bisulfate ($nBu_4NHSO_4$, 0.48 g, 1.52 mmol). The heterogeneous mixture was stirred vigorously under argon atmosphere at room temperature (23 ˚C) for 1h. Then BnBr (1.5 mL, 12.5 mmol) was transferred slowly into the reaction mixture over a period of 10 min. The reaction mixture was stirred at room temperature until TLC (2% EtOAc in $CH_2Cl_2$) showed complete disappearance of the starting material, approximately 24h. The reaction mixture was quenched with distilled water (160 mL) and diluted with toluene (400 mL). The organic layer was separated, washed successively with $H_2O$ (80 mL), 1M HCl (2 x 80 mL), and $H_2O$ (2 x 80 mL), dried over $MgSO_4$, filtered and concentrated *in vacuo*. Purification of the crude reaction product (a few drops of DMF were added to dissolve the crude product) by flash chromatography (9:1 hexane:EtOAc, $R_f = 0.3$) yielded a mixture of the two isomers of **42** (1.3 g, 87% yield). $R_f$ of the mixture = 0.8 (2% EtOAc in $CH_2Cl_2$). $^1$H NMR for **42α** (400 MHz, $CDCl_3$): δ 3.63 (dd, J = 2.0, 10.8 Hz, 1H, **H**-6a), 3.75 (Ψt, J = 8.9, 9.6 Hz, 1H, **H**-3), 3.81 (dd, J = 3.8, 7.7 Hz, 1H, **H**-2), 3.82 (Ψt, J = 8.8, 9.8 Hz, 1H, **H**-4), 3.95 (dd, J = 10.0, 5.4 Hz, 1H, **H**-6b), 4.36 (ddd, J = 2.1, 3.6, 7.9 Hz, 1H, **H**-5), 4.44 (d, J = 11.8 Hz, 1H, Ph**CH$_2$**O), 4.53 (d, J = 10.8 Hz, 1H, Ph**CH$_2$**O), 4.60 (d, J = 11.8 Hz, 1H, Ph**CH$_2$**O), 4.81 (d, J = 10.9 Hz, 1H, Ph**CH$_2$**O), 4.87 (d, J = 10.6

Hz, 1H, Ph**C**$\mathbf{H_2}$O), 4.92 (d, J = 10.8 Hz, 1H, Ph**C**$\mathbf{H_2}$O), 5.61 (d, J = 5.4 Hz, 1H, **H**-1), 7.14-7.52 (m, 30H, **Ph**$CH_2O$ (20H) + C**H**$Cl_3$). $^1$H NMR for **42β** (400 MHz, $CDCl_3$): δ 3.34 (Ψt, J = 9.2, 9.3 Hz, 1H, **H**-2), 3.47 (m, 1H, **H**-5), 3.51 (Ψt, J = 9.2, 9.0 Hz, 1H, **H**-3), 3.56-3.64 (m, 2H, **H**-4, **H**-6a), 3.76 (dd, J = 3.6, 8.8 Hz, 1H, **H**-6b), 4.38-4.46 (m, 1H, Ph**C**$\mathbf{H_2}$O), 4.52-4.66 (m, 3H, Ph**C**$\mathbf{H_2}$O), 4.76 (d, J = 9.6 Hz, 1H, **H**-1), 4.82-4.88 (m, 2H, Ph**C**$\mathbf{H_2}$O), 7.14-7.62 (m, **Ph**$CH_2O$ (20H) + C**H**$Cl_3$).

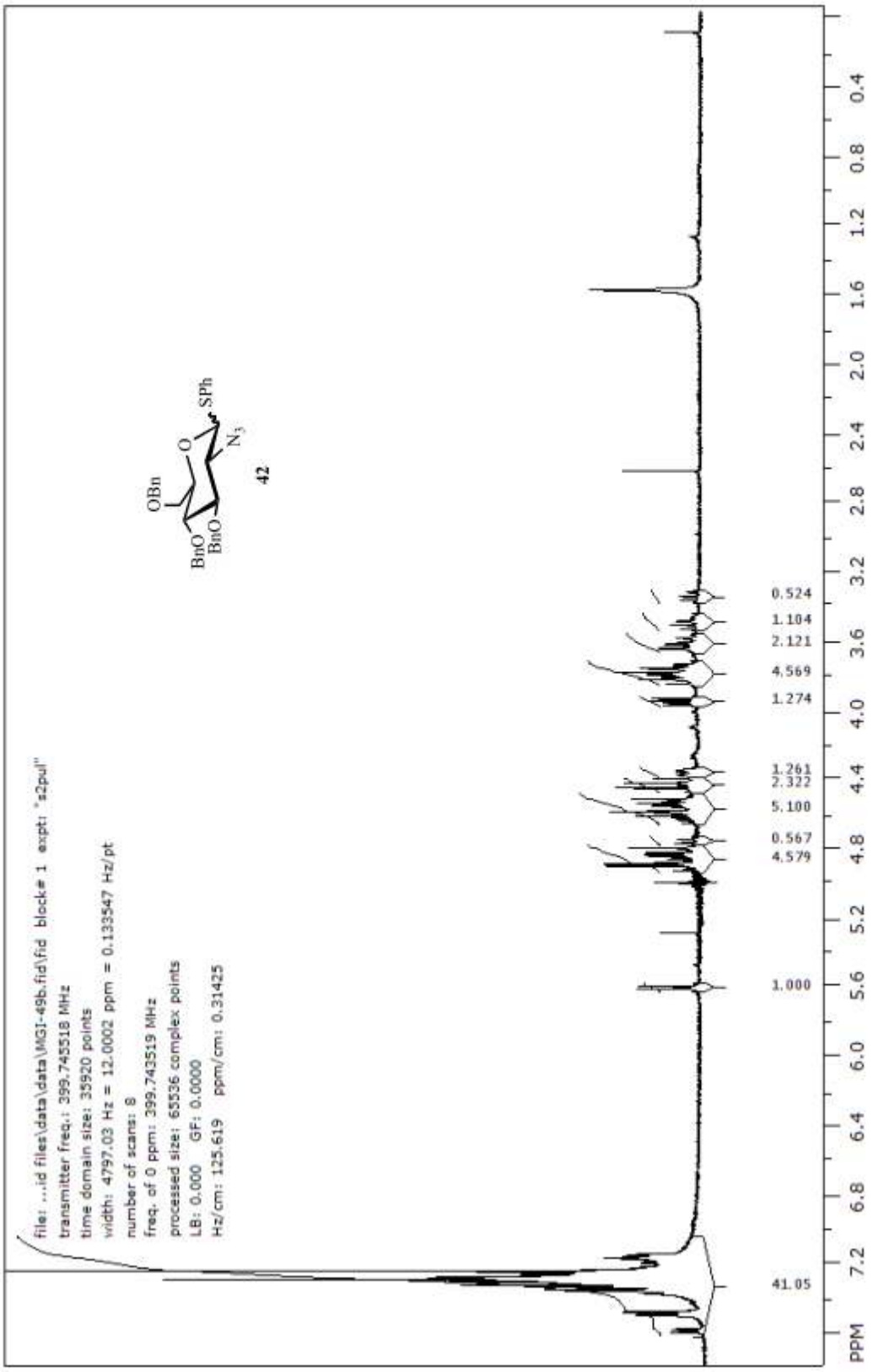
file: ...id files\data\data\MGI-49b.fid\fid block# 1 expt: "s2pul"
transmitter freq.: 399.745518 MHz
time domain size: 35920 points
width: 4797.03 Hz = 12.0002 ppm = 0.133547 Hz/pt
number of scans: 8
freq. of 0 ppm: 399.743519 MHz
processed size: 65536 complex points
LB: 0.000 GF: 0.0000
Hz/cm: 125.619 ppm/cm: 0.31425
OBn
BnO
BnO
O
SPh
N3
42
0.524
1.104
2.121
4.569
1.274
1.261
2.322
5.100
0.567
4.579
1.000
41.05
PPM
7.2
6.8
6.4
6.0
5.6
5.2
4.8
4.4
4.0
3.6
3.2
2.8
2.4
2.0
1.6
1.2
0.8
0.4

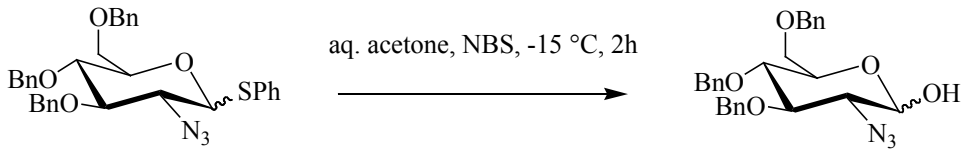


**42** **40**

**2-Azido-3,4,6-tri-*O*-benzyl-2-deoxy-α/β-D-glucopyranose (40).**[87] To a solution of **42** (1.77 g, 3.08 mmol) in acetone/water (99:1, 170 mL) under an argon atmosphere was added N-bromosuccinimide (NBS, 0.90 g, 5.08 mmol) with vigorous stirring at –15 ˚C (using a cold bath of 30% methanol in water and dry ice). Reaction flask was covered with an aluminum foil to avoid light. The color change from yellow to orange was observed as the reaction proceeded. Progress of the reaction was monitored by TLC (3:1 hexane: EtOAc) until all the starting material had reacted, approximately 2h. The reaction mixture was quenched with a saturated solution of $NaHCO_3$ (250 mL). The aqueous phase was extracted with EtOAc (4 x 100 mL). The combined organic layers were washed with brine (2 x 100 mL), dried over $MgSO_4$, filtered and concentrated *in vacuo*. Purification of the crude reaction product by flash chromatography (3:1 hexane:EtOAc, $R_f = 0.28$) yielded **40** as a white shiny powder (1.15g, 77%). $R_f = 0.28$ (3:1 hexane:EtOAc). $^1$H NMR for mixture of **40α** and **40β** (300 MHz, $CDCl_3$): δ 3.24 (dd, 1H, J = 1.9, 4.6 Hz, **α** -O**H**), 3.37 (dd, J = 10.1, 12.4 Hz, 1H, **β**-**H**-2), 3.40-3.47 (m, 3H, **α**-**H**-2, **α**-**H**-6a, **β**-**H**-3), 3.49 (m, 1H, **β**-**H**-5 ), 3.52-3.72 (m, 5H, **α**-**H**-4, **α**-**H**-6b, **β**-**H**-4, **β**-**H**-6a, **β**-**H**-6b), 3.76 (d, J = 7.4 Hz, **β**-O**H**), 4.02 (dd, 1H, J = 11.7, 13.4 Hz, **α**-**H**-3), 4.08 (m, 1H, **α**-**H**-5), 4.44-4.64 (m, 7H, **β**-**H**-1 (1H), Ph**C**$\mathbf{H_2}$O (6H)), 4.74-4.95 (m, 6H, Ph**C**$\mathbf{H_2}$O), 5.32 (dd, J = 4.8, 4.76 Hz, **α**-**H**-1), 7.09-7.44 (m, 33H, **Ph**$CH_2O$ (30H) + C**H**$Cl_3$).

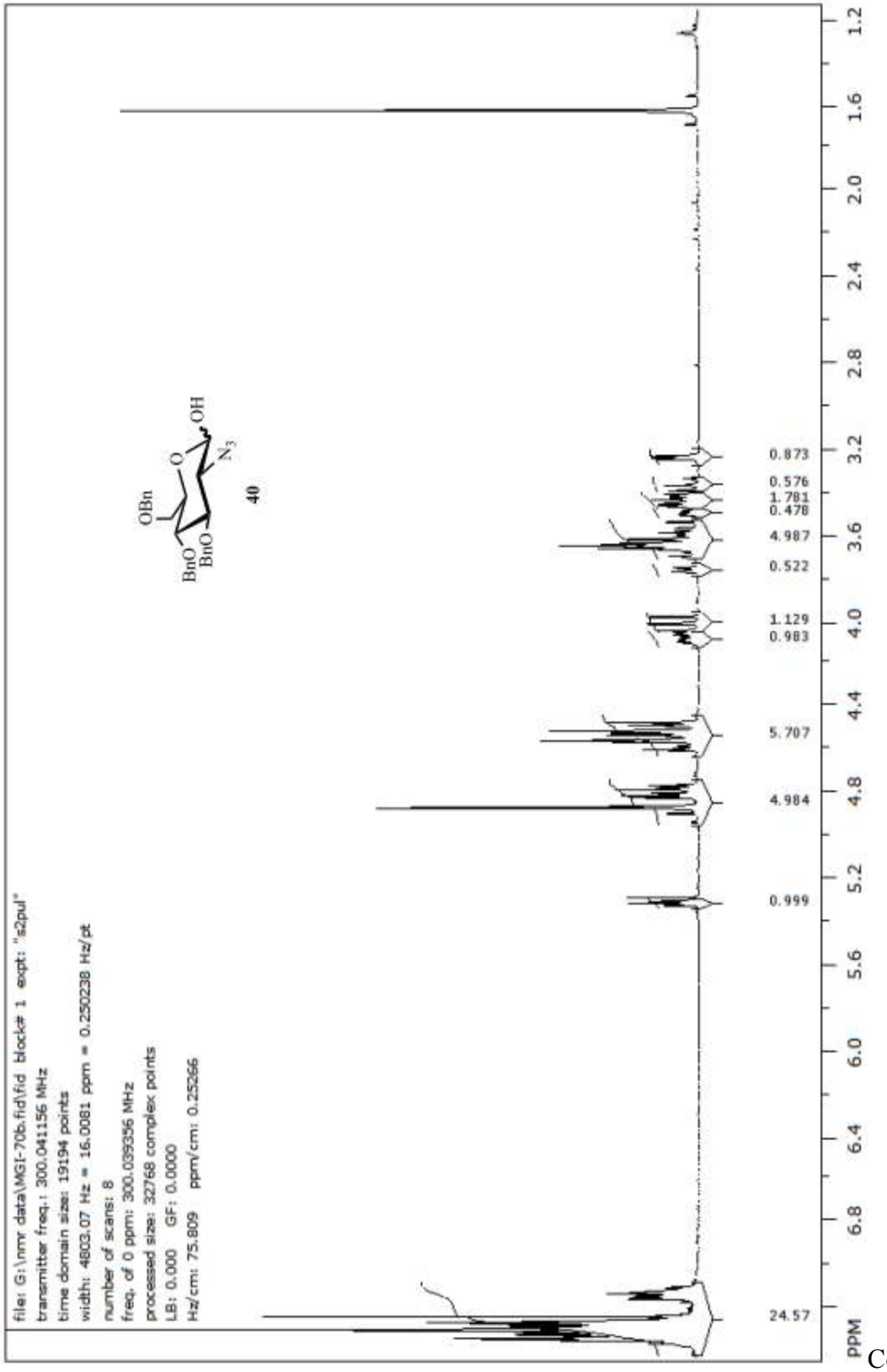
file: G:\nmr data\MGI-70b.fid\fid block# 1 expt: "s2pul"
transmitter freq.: 300.041156 MHz
time domain size: 19194 points
width: 4803.07 Hz = 16.0081 ppm = 0.250238 Hz/pt
number of scans: 8
freq. of 0 ppm: 300.039356 MHz
processed size: 32768 complex points
LB: 0.000 GF: 0.0000
Hz/cm: 75.809 ppm/cm: 0.25266
OBn
BnO
BnO
O
OH
N3
40
24.57
0.999
4.984
5.707
1.129
0.983
0.522
4.987
0.478
1.781
0.576
0.873
PPM
6.8
6.4
6.0
5.6
5.2
4.8
4.4
4.0
3.6
3.2
2.8
2.4
2.0
1.6
1.2

Comp

OBn
BnO
BnO
O
OH
N3
40

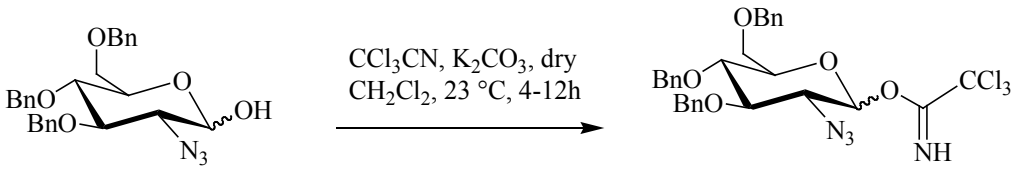


**40** **24**

**2-Azido-3,4,6-tri-*O*-benzyl-2-deoxy-α/β-D-glucopyranosyl trichloroacetimidate (24).**[103] To a solution of **40** (97 mg, 0.21 mmol) in dry $CH_2Cl_2$ (1.6 mL) under an argon atmosphere was added flame dried $K_2CO_3$ (0.14 g, 1.05 mmol) and trichloroacetonitrile ($CCl_3CN$, 0.17 mL, 1.68 mmol). The reaction mixture was stirred vigorously at room temperature and monitored by TLC (3:1 hexane:EtOAc) until the product formation was completed, about 4-12h. 2-D TLC proved some decomposition of the product on silica gel. Complete disappearance of the starting material was not achieved. The reaction mixture was filtered through a bed of silica gel over Celite using excess $CH_2Cl_2$ and evaporated under vacuum to yield a crude reaction product **24** (88 mg, 67%). $R_f$ of mixture = 0.46 (3:1 hexane:EtOAc). Integrals from the $^1$H NMR of this mixture showed 9:1 **α/β** ratio. $^1$H NMR for **24 β** (400 MHz, $CDCl_3$): δ 3.55 (Ψt, J = 9.2, 9.5 Hz, 1H, **H**-2), 3.59 (m, 1H, **H**-5), 3.69 (m, 1H, **H**-6a), 3.73-3.80 (m, 3H, **H**-3, **H**-4, **H**-6b), 4.53 (d, J = 12.16, 1H, Ph**C**$\mathbf{H_2}$O), 4.59 (d, J = 8.12, 1H, Ph**C**$\mathbf{H_2}$O), 4.62 (d, J = 9.6, 1H, Ph**C**$\mathbf{H_2}$O), 4.81 (d, J = 10.88, 1H, Ph**C**$\mathbf{H_2}$O), 4.85 (d, J = 10.92, 1H, Ph**C**$\mathbf{H_2}$O), 4.90 (d, J = 10.97, 1H, Ph**C**$\mathbf{H_2}$O), 5.62 (d, J = 8.52, 1H, **H**-1 ), 7.12-7.44 (m, 20H, **Ph**$CH_2O$ (15H) + **C**$\mathbf{H}Cl_3$), 8.73 (s, 1H, N**H**). Data is consistent with the literature.[103]

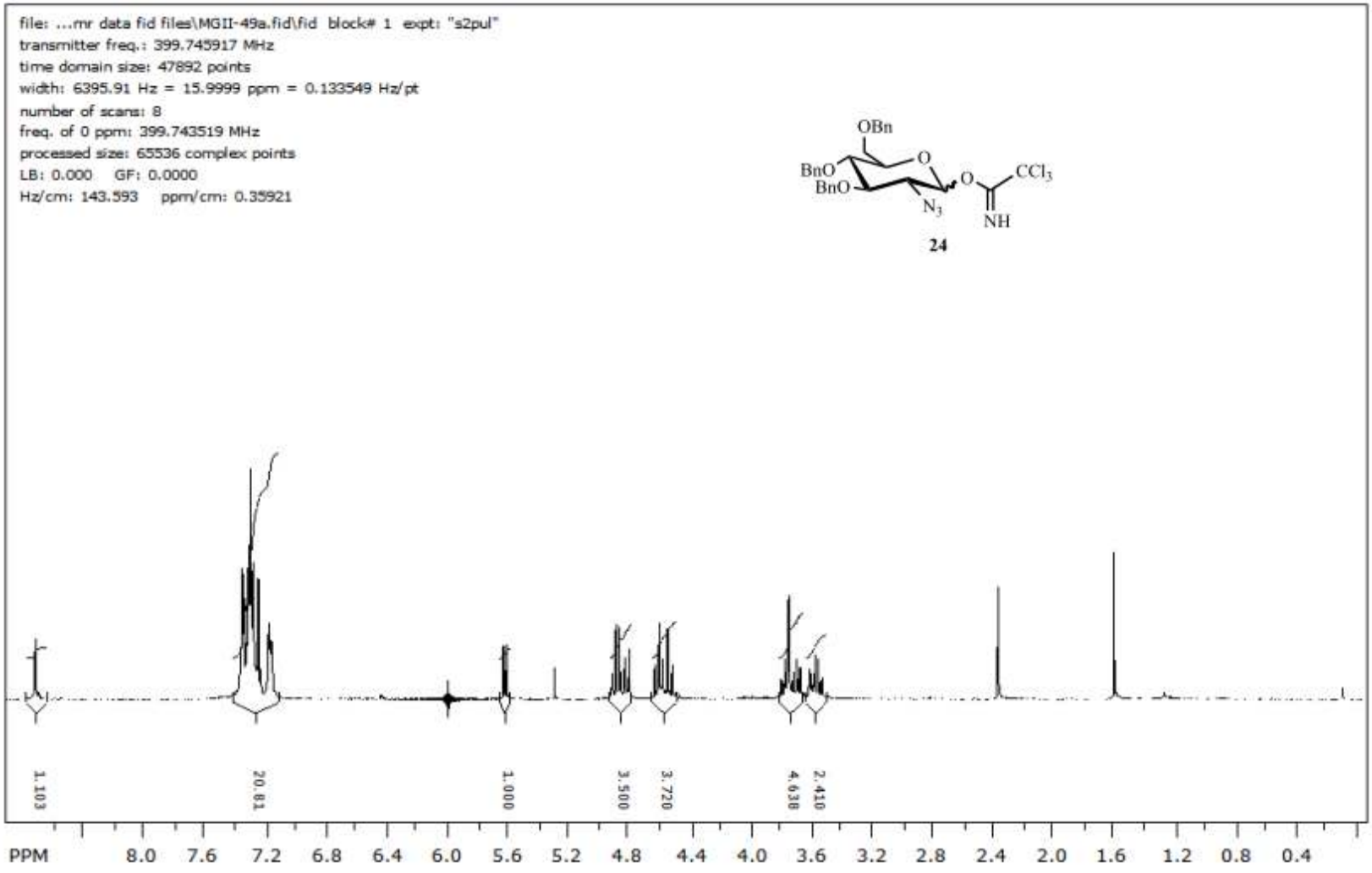
file: ...mr data fid files\MGII-49a.fid\fid block# 1 expt: "s2pul"
transmitter freq.: 399.745917 MHz
time domain size: 47892 points
width: 6395.91 Hz = 15.9999 ppm = 0.133549 Hz/pt
number of scans: 8
freq. of 0 ppm: 399.743519 MHz
processed size: 65536 complex points
LB: 0.000 GF: 0.0000
Hz/cm: 143.593 ppm/cm: 0.35921
OBn
BnO
BnO
O
O
CCl3
N3
NH
24
1.103
20.81
1.000
3.500
3.720
4.638
2.410
PPM
8.0
7.6
7.2
6.8
6.4
6.0
5.6
5.2
4.8
4.4
4.0
3.6
3.2
2.8
2.4
2.0
1.6
1.2
0.8
0.4

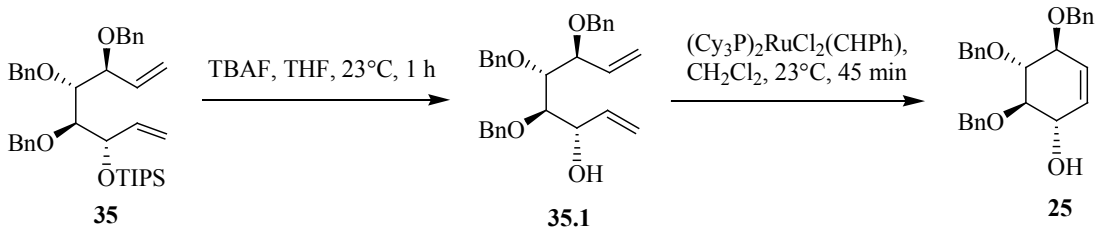


**35** **35.1** **25**

**(a) 3(S)-Hydroxy-4(S),5(R),6(S)-tribenzyloxy-1,7-octadiene (35.1).**[104] To a solution of compound **35** (114.7 mg, 0.192 mmol) in THF (1.4 mL) was added t-butyl ammonium fluoride (TBAF, 0.92 mL, 0.912 mmol) at 0 ˚C under an atmosphere of argon. The reaction mixture turns pale yellow and then golden yellow in color. After 10 min the reaction mixture was warmed to room temperature. The progress of the reaction was monitored by TLC (6:1 hexane:EtOAc) until the completion of the reaction, about 1 h. The reaction mixture was evaporated under reduced pressure to give an orange-brown residue. Purification of the crude reaction product by flash chromatography (6:1 hexane:EtOAc) yielded pure **35.1** (94 mg, 80%). $R_f$ = 0.25 (6:1 hexane:EtOAc). $^1$H NMR (400 MHz, $CDCl_3$) δ 2.63 (d, J = 7.4, 1H), 3.74 (m, 2H), 4.10 (m, 2H), 4.36 (d, J = 11.9, 1H), 4.77-4.61 (m, 5H), 5.37-5.14 (m, 4H), 6.02-5.82 (m, 2H), 7.32-7.25 (m, 16H, **Ph**$CH_2O$ + C**H**$Cl_3$). Data is consistent with the literature.[104]

**(b) 3(S),4(R),5(R)-Tribenzyloxy-6(S)-hydroxycyclohexene (25).**[82] To a solution of compound **35.1** (94 mg, 0.21 mmol) in $CH_2Cl_2$ (10.0 mL) was added the first generation Grubb's catalyst, $(Cy_3P)_2RuCl_2(CHPh)$, (17.12 mg, 20.75 μmol) at room temperature under an atmosphere of argon. The color of the reaction mixture turned pink and then brown. The reaction was monitored by TLC (7:3 hexane:EtOAc) until all the starting material was reacted, about 45 min. Then the reaction mixture was opened to the

atmosphere for 4 h. Thereafter, the reaction mixture was evaporated under reduced pressure to give a crude residue. The residue was further purified by flash chromatography (7:3 hexane:EtOAc) to yield pure compound **25** (52 mg, 60%). For **25**: $R_f$ = 0.32 (7:3 hexane:EtOAc); $^1$H NMR (400 MHz, $CDCl_3$) δ 2.13 (m, 1H), 3.52 (dd, J = 8.0, 10.1, 1H), 3.78 (dd, J = 7.4, 10.2, 1H), 4.34-4.23 (m, 2H), 4.75-4.66 (m, 2H), 4.94-4.87 (m, 2H), 5.02 (d, J = 11.4, 1H), 5.70 (m, 2H), 7.19-7.45 (m, 15H, **Ph**$CH_2O$). Data is consistent with the literature.[82]

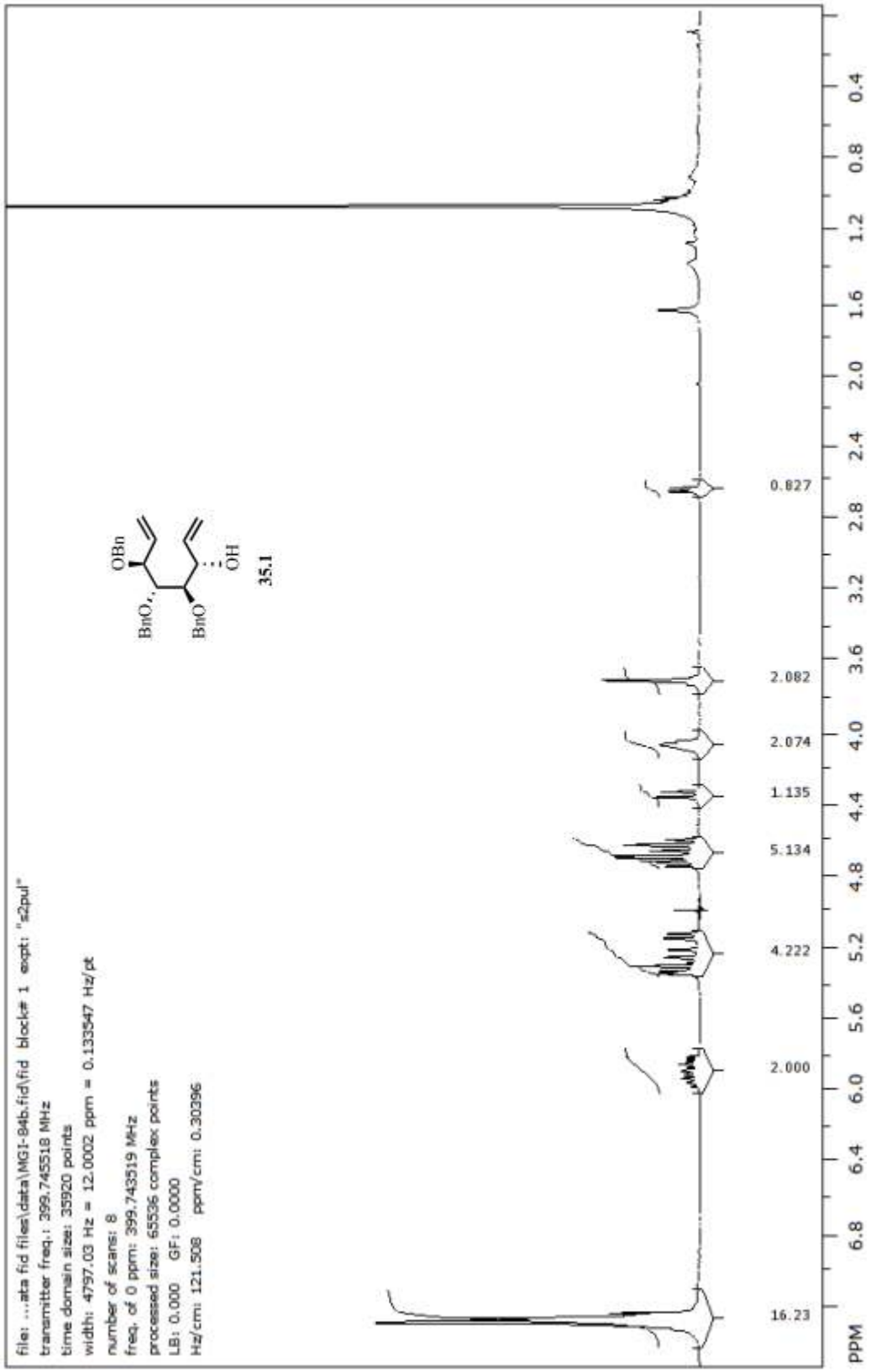
file: ...ata fid files\data\MGI-84b.fid\fid block# 1 expt: "s2pul"
transmitter freq.: 399.745518 MHz
time domain size: 35920 points
width: 4797.03 Hz = 12.0002 ppm = 0.133547 Hz/pt
number of scans: 8
freq. of 0 ppm: 399.743519 MHz
processed size: 65536 complex points
LB: 0.000 GF: 0.0000
Hz/cm: 121.508 ppm/cm: 0.30396
OBn
BnO
BnO
OH
35.1
16.23
2.000
4.222
5.134
1.135
2.074
2.082
0.827
PPM
6.8
6.4
6.0
5.6
5.2
4.8
4.4
4.0
3.6
3.2
2.8
2.4
2.0
1.6
1.2
0.8
0.4

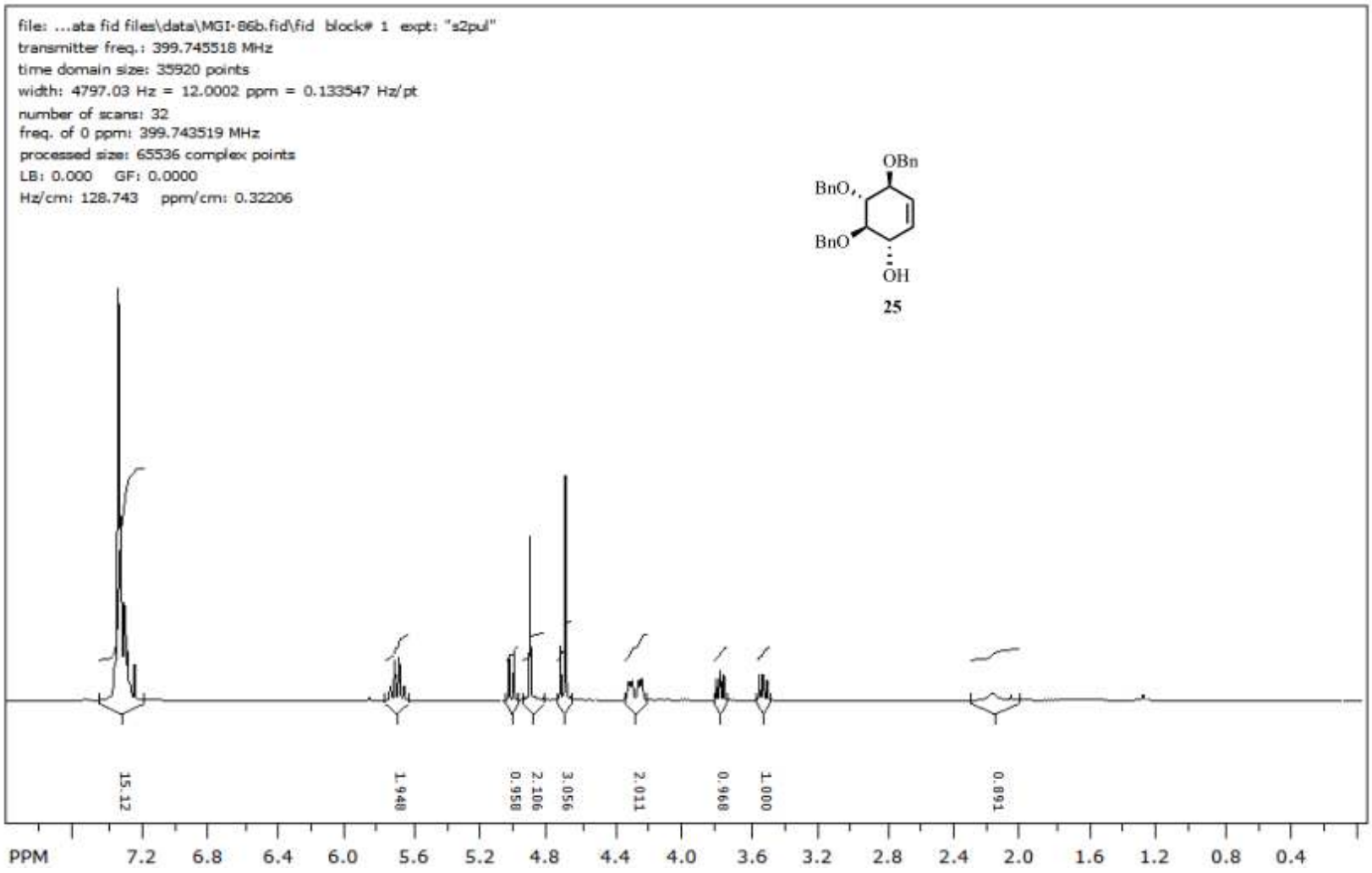
file: ...ata fid files\data\MGI-86b.fid\fid block# 1 expt: "s2pul"
transmitter freq.: 399.745518 MHz
time domain size: 35920 points
width: 4797.03 Hz = 12.0002 ppm = 0.133547 Hz/pt
number of scans: 32
freq. of 0 ppm: 399.743519 MHz
processed size: 65536 complex points
LB: 0.000 GF: 0.0000
Hz/cm: 128.743 ppm/cm: 0.32206
OBn
BnO
BnO
OH
25
15.12
1.948
0.958
2.106
3.056
2.011
0.968
1.000
0.891
PPM
7.2
6.8
6.4
6.0
5.6
5.2
4.8
4.4
4.0
3.6
3.2
2.8
2.4
2.0
1.6
1.2
0.8
0.4

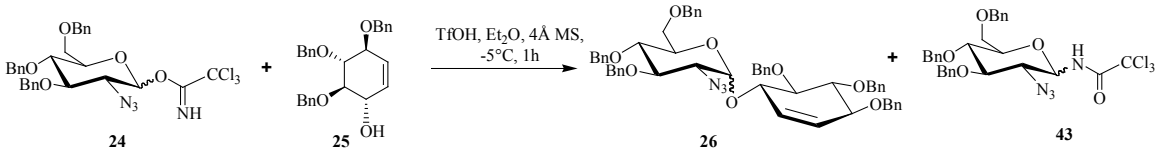


**2-Azido-3,4,6-tri-*O*-benzyl-2-deoxy-D-glucopyranosyl-α/β-(1 → 6)-3,4,5-tri-*O*-benzyl-1,2-didehydro-1,2-dideoxy-D-*myo*-inositol (26α/β) and N-(2-azido-3,4,6-tri-*O*-benzyl-1,2-dideoxy- α/β-D-glucopyranosyl) trichloroacetamide (43).**[35] Mixture of donor **24** (216 mg, 0.34 mmol) and acceptor **25** (156 mg, 0.37 mmol) were coevaporated three times with toluene to remove any traces of water. Anhydrous ether (14 mL) and crushed activated molecular seives (4 Å, 230 mg) were added to the reaction mixture under an atmosphere of argon. After stirring for 15 min the reaction mixture was cooled to -5 ˚C and a TfOH solution in ether (0.0626 M*, 0.51 mL, 0.1 equiv) was added dropwise. The reaction mixture was stirred at -5 ˚C until TLC (1:1 hexane: ether) showed almost complete disappearance of the starting materials, about 1 h. The reaction mixture was warmed to room temperature, quenched with solid $NaHCO_3$ (230 mg), stirred for about 15 minutes, and then filtered into a separatory funnel. The filtrate was washed successively with cold 5% aq. $Na_2CO_3$ (3 x 8 mL), water (2 x 8 mL) and then with brine (2 x 8 mL). The ether layer was separated, dried over $Mg_2SO_4$, filtered, and evaporated under reduced pressure. The crude residue was purified by flash chromatography (4:1 → 2:5 → 1:1 v/v hexane:ether) yielding most of the fractions with pure coupling products along with some impure fractions. The impure fractions were combined and purified further by PTLC (1:1 v/v hexane:ether).

* 0.0626 M TfOH solution was prepared by dissolving 56 µL of pure TfOH (11.3 M) in 10 mL of anhydrous ether.

All the pure fractions were combined separately yielding 140 mg of **26α** ($R_f$ =0.48 in 1:1 v/v hexane:ether) and 40 mg of **26β** ($R_f$ =0.62 in 1:1 v/v hexane:ether) with a combined yield of 58%. For **26α**: $R_f$ =0.51 (3:1 hexane:EtOAc); $^1$H NMR (400 MHz, $CDCl_3$) δ 3.34 (dd, J = 10.9, 1.9 Hz, 1H, GluN-**H**-6a), 3.4 (dd, J = 11.1, 2.7 Hz, 1H, GluN-**H**-6b), 3.45 (dd, J = 10.5, 3.5 Hz, 1H, GluN-**H**-2), 3.65-3.79 (m, 3H, GluN-**H**-4, Ino-**H** (2H)), 3.96 (dd, J = 10.1, 9.1 Hz, 1H, GluN-**H**-3), 4.02 (ddd, 1H, GluN-**H**-5), 4.25 (m, 1H, Ino-**H**), 4.29 (d, J = 11.9 Hz, 1H, Ph**C**$\mathbf{H_2}$O), 4.4 (m, 1H, Ino-**H**), 4.45 (d, J = 11.1 Hz, 1H, Ph**C**$\mathbf{H_2}$O), 4.54 (d, J = 12 Hz, 1H, Ph**C**$\mathbf{H_2}$O), 4.65-4.74 (m, 3H, Ph**C**$\mathbf{H_2}$O), 4.77 (d, J = 11.1 Hz, 1H, Ph**C**$\mathbf{H_2}$O), 4.83-4.99 (m, 5H, Ph**C**$\mathbf{H_2}$O), 5.1 (d, J = 3.6 Hz, 1H, GluN-**H**-1), 5.7-5.83 (m, 2H, Ino-**H** (2H)), 7.05-7.39 (m, 36H, **Ph**$CH_2O$ (30H) + C**H**$Cl_3$). For **26β**: $R_f$ =0.56 (3:1 hexane:EtOAc), $R_f$ =0.71 (7:1 benzene:acetonitrile); $^1$H NMR (400 MHz, $CDCl_3$) δ 3.32-3.49 (m, 3H, GluN-**H**-2, GluN-**H**-3, GluN-**H**-5), 3.61-3.84 (m, 5H, GluN-**H**-4, GluN-**H**-6a, GluN-**H**-6b, Ino-**H** (2H)), 4.26 (m, 1H, Ino-**H**), 4.46 (m, 1H, Ino-**H**), 4.48-4.62 (m, 3H, Ph**C**$\mathbf{H_2}$O), 4.65 (d, J = 7.6 Hz, 1H, GluN-**H**-1), 4.67-4.75 (m, 2H, Ph**C**$\mathbf{H_2}$O), 4.77-4.93 (m, 6H, Ph**C**$\mathbf{H_2}$O), 4.97 (d, J = 10.16 Hz, 1H, Ph**C**$\mathbf{H_2}$O), 5.68-5.83 (m, 2H, Ino-**H** (2H)), 7.15-7.21 (m, 2H, **Ph**$CH_2O$), 7.21-7.49 (m, 28.8H, **Ph**$CH_2O$ (28H) + C**H**$Cl_3$). For **43**: $R_f$ =0.57 (3:1 hexane:EtOAc), $R_f$ =0.66 (7:1 benzene:acetonitrile); $^1$H NMR (400 MHz, $CDCl_3$) δ 3.57-3.73 (m, 3H, **H**-3, **H**-5, **H**-6a), 3.78-3.94 (m, 3H, **H**-6b, **H**-4, **H**-2), 4.49 (d, J = 11.94 Hz, 1H, Ph**C**$\mathbf{H_2}$O), 4.58 (d, J = 10.63 Hz, 1H, Ph**C**$\mathbf{H_2}$O), 4.64 (d, J = 11.95 Hz, 1H, Ph**C**$\mathbf{H_2}$O), 4.77 (d, J = 10.62 Hz, 1H, Ph**C**$\mathbf{H_2}$O), 4.85 (d, J = 10.66 Hz, 1H, Ph**C**$\mathbf{H_2}$O), 4.92 (d, J = 10.67 Hz, 1H, Ph**C**$\mathbf{H_2}$O), 5.66 (dd, J = 6.55, 5.37

Hz, 1H, **H**-1), 7.00 (d, J = 6.48 Hz, 1H, N**H**), 7.1-7.2 (m, 2H, **Ph**$CH_2O$), 7.2-7.4 (m, 23H, **Ph**$CH_2O$ (13H) + C**H**$Cl_3$). Data is consistent with the literature.[35]

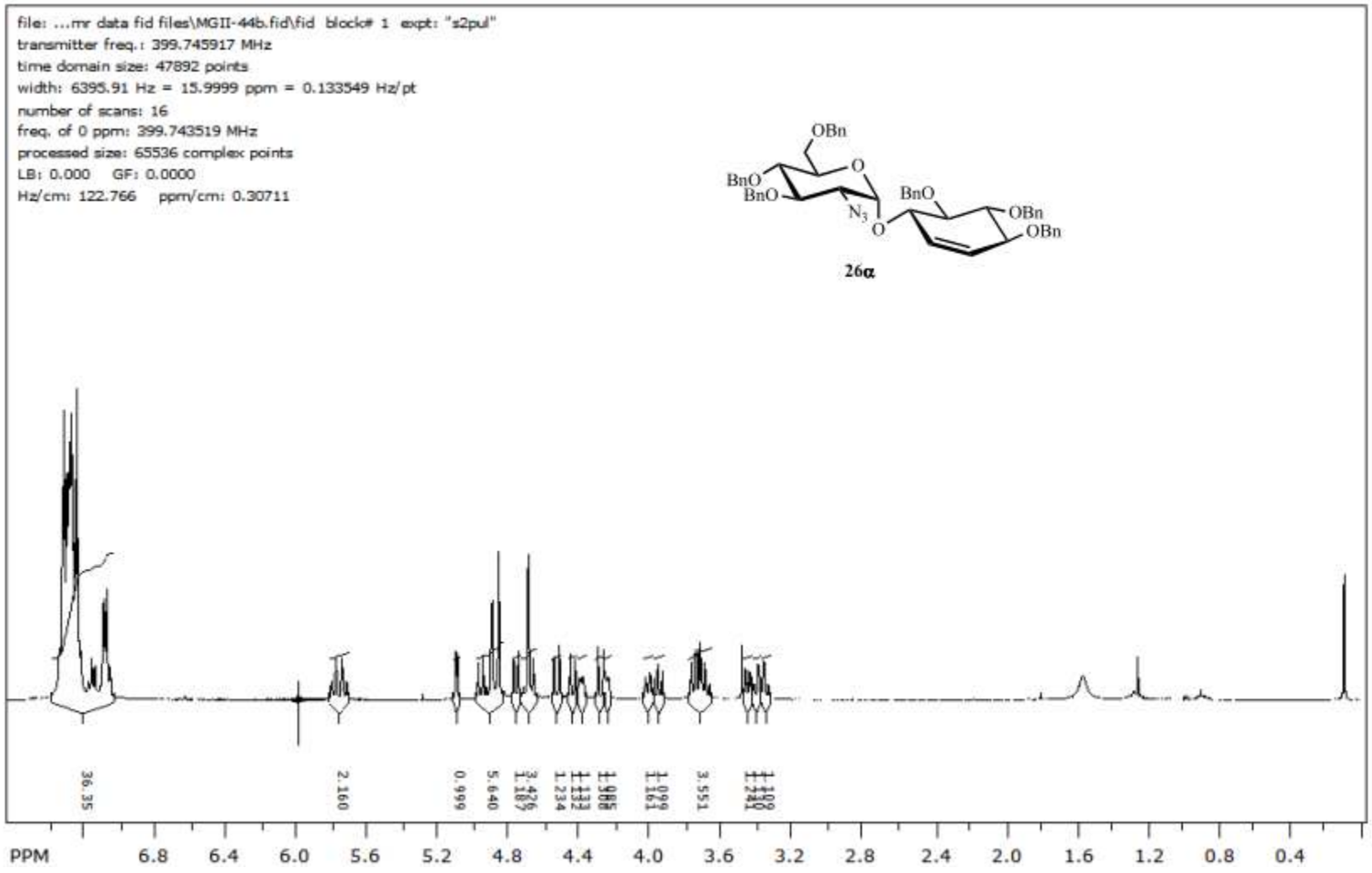
file: ...mr data fid files\MGII-44b.fid\fid block# 1 expt: "s2pul"
transmitter freq.: 399.745917 MHz
time domain size: 47892 points
width: 6395.91 Hz = 15.9999 ppm = 0.133549 Hz/pt
number of scans: 16
freq. of 0 ppm: 399.743519 MHz
processed size: 65536 complex points
LB: 0.000 GF: 0.0000
Hz/cm: 122.766 ppm/cm: 0.30711
OBn
BnO
BnO
O
N3
O
BnO
OBn
OBn
26α
36.35
2.160
0.999
5.640
3.426
1.189
1.234
1.132
1.161
1.099
3.551
PPM
6.8
6.4
6.0
5.6
5.2
4.8
4.4
4.0
3.6
3.2
2.8
2.4
2.0
1.6
1.2
0.8
0.4

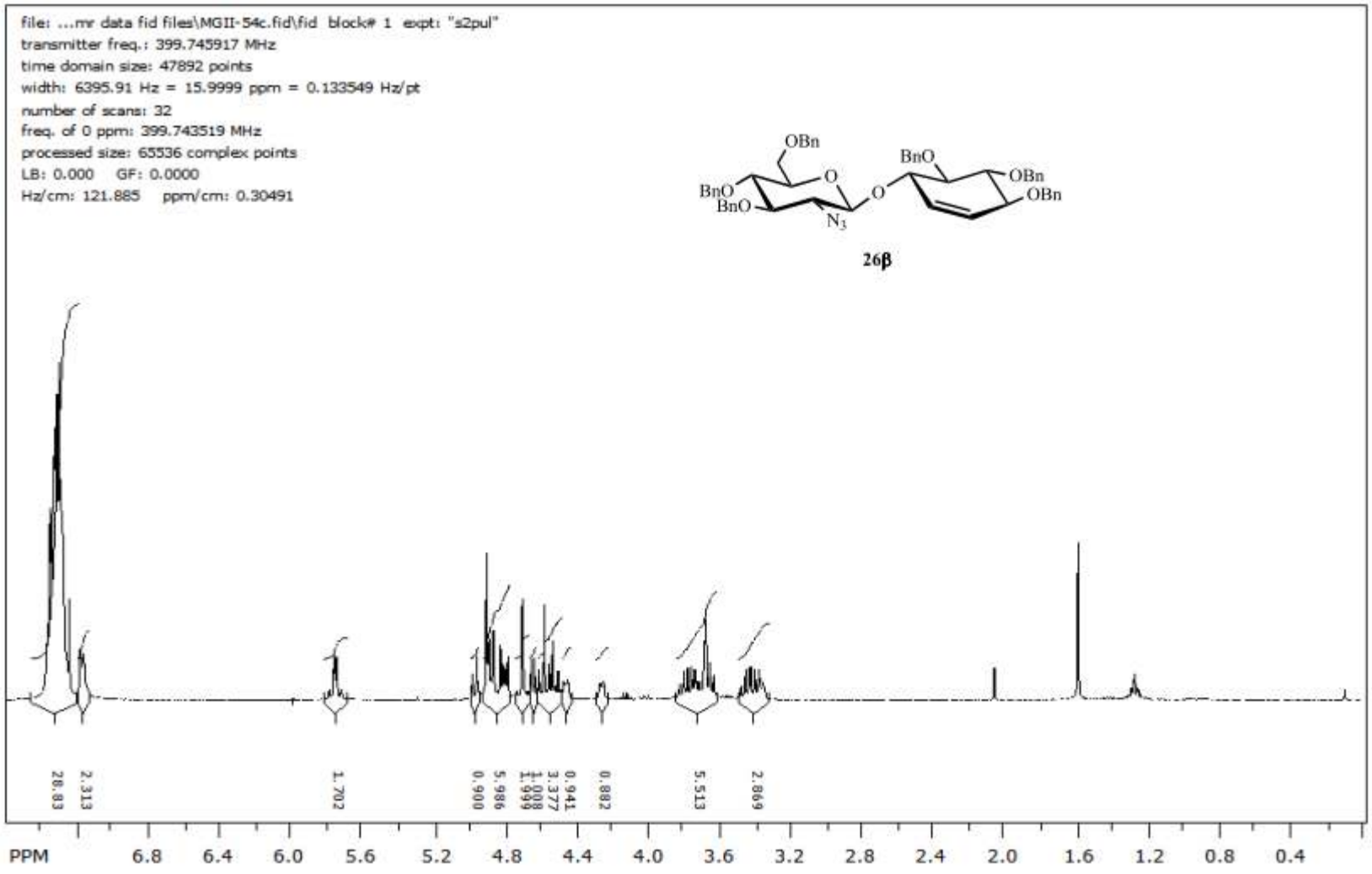
file: ...mr data fid files\MGII-54c.fid\fid block# 1 expt: "s2pul"
transmitter freq.: 399.745917 MHz
time domain size: 47892 points
width: 6395.91 Hz = 15.9999 ppm = 0.133549 Hz/pt
number of scans: 32
freq. of 0 ppm: 399.743519 MHz
processed size: 65536 complex points
LB: 0.000 GF: 0.0000
Hz/cm: 121.885 ppm/cm: 0.30491
OBn
BnO
BnO
O
N3
O
BnO
OBn
OBn
26β
28.83
2.313
1.702
0.900
5.986
1.000
1.999
3.377
0.941
0.882
5.513
2.869
PPM
6.8
6.4
6.0
5.6
5.2
4.8
4.4
4.0
3.6
3.2
2.8
2.4
2.0
1.6
1.2
0.8
0.4

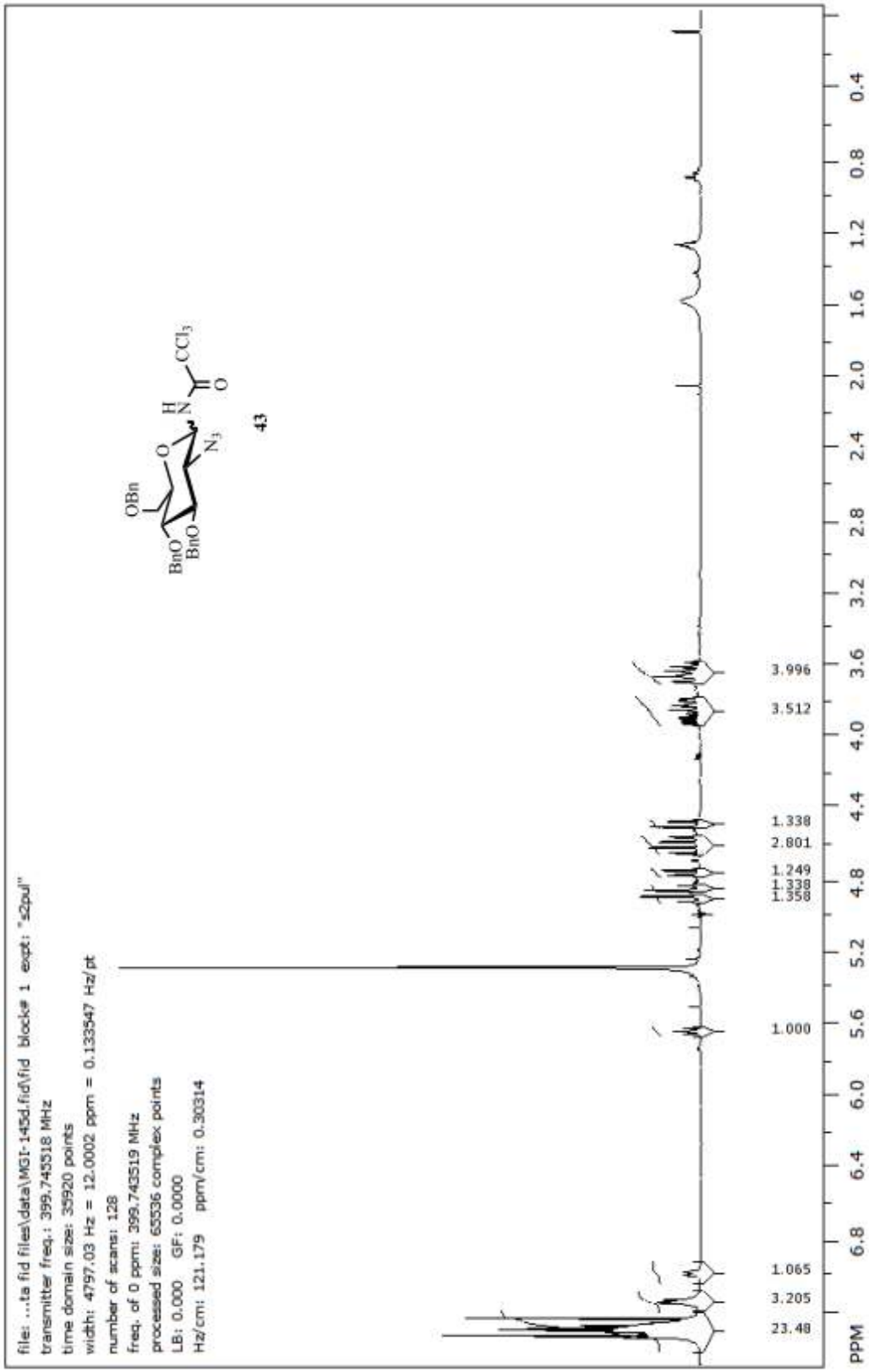
file: ...ta fid files\data\MGI-145d.fid\fid block# 1 expt: "s2pul"
transmitter freq.: 399.745518 MHz
time domain size: 33920 points
width: 4797.03 Hz = 12.0002 ppm = 0.133547 Hz/pt
number of scans: 128
freq. of 0 ppm: 399.743519 MHz
processed size: 65536 complex points
LB: 0.000 GF: 0.0000
Hz/cm: 121.179 ppm/cm: 0.30314
OBn
BnO
BnO
O
N3
H
N
CCl3
O
43
1.065
3.205
23.48
1.000
1.338
2.801
1.249
1.338
1.358
3.996
3.512
PPM
6.8
6.4
6.0
5.6
5.2
4.8
4.4
4.0
3.6
3.2
2.8
2.4
2.0
1.6
1.2
0.8
0.4

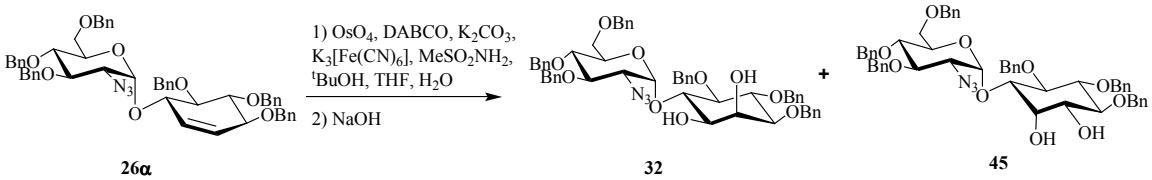


**2-Azido-3,4,6-tri-*O*-benzyl-2-deoxy-D-glucopyranosyl-(1 → 6)-3,4,5-tri-*O*-benzyl-D-*myo* inositol (32 and 45).**[35] To a solution of **26α** (36.2 mg, 41.4 μmol) in THF (0.57 mL) and $^{t}$BuOH (0.65 mL) was added water (408 μL) followed by $K_3[Fe(CN)_6]$ (40.8 mg, 124.2 μmol, 3 equiv), $K_2CO_3$ (124 μL of 1 M aq solution, 124.2 μmol, 3 equiv), DABCO (139 μL of 0.089 M aq solution, 12.42 μmol, 0.3 equiv), $OsO_4$ (72.64 μL of 0.056 M aq solution, 4.1 μmol, 0.1 equiv), and $MeSO_2NH_2$ (7.79 mg, 82.8 μmol in 4.5 mL of $H_2O$, 2 equiv) at vigorous stirring under an argon atmosphere at 23 ˚C. The reaction was monitored by TLC (45 % EtOAc in heptane, for **26α** $R_f$ =0.73, for **32** and **45** $R_f$ =0.25-0.35). After 24 h 40-50 % conversion of the starting material was observed. Addition of another batch of the reagents in the same proportion, however, pushed the formation of the osmate ester to completion, additional 24 h. NaOH (63 μL of 1 M aq solution) was added followed by an additional stirring for about 12 h. The reaction mixture was quenched by addition of solid $Na_2SO_3$ (100 mg). The upper organic phase changed from yellow to colorless and the lower aqueous phase turned black.* After stirring for additional 15 min the organic layer was separated. The aqueous layer was extracted with toluene (3 x 1 mL) and the combined organic layers were washed successively with 1 M NaOH (2 x 1 mL), water (2 x 1 mL), 1 M $Na_2S_2O_3$ (3 x 1 mL), water (1 x 1 mL), and brine (2 x 1 mL).

* This color change was not observed in some cases.

The organic phase was dried over $MgSO_4$, filtered, and evaporated to give a crude mixture of two diols **32** and **45**. The two diols had a very close $R_f$ and were separated by PTLC (45 % EtOAc in heptane, 10-15 mg maximum loading) yielding 10.6 mg of pure **32** and 10.8 mg of pure **45** with a combined yield of 58%. For **32**: $R_f$ = 0.29 (45 % EtOAc in heptane); $^1$H NMR (400 MHz, $CDCl_3$) δ 2.49 (m, 1H, O**H**), 3.03 (dd, J = 11.0, 1.6 Hz, 1H, GluN-**H**-6a), 3.27 (dd, J = 11.0, 2.4 Hz, 1H, GluN-**H**-6b), 3.36 (Ψt, J = 9.7 Hz, 1H, Ino-**H**-4), 3.47 (dd, J = 9.6, 2.7 Hz, 1H, Ino-**H**-3), 3.55 (dd, J = 10.1, 3.6 Hz, 1H, GluN-**H**-2), 3.57-3.62 (m, 1H, Ino-**H**-1), 3.69-3.83 (m, 2H, GluN-**H**-4, O**H**), 3.84-4.05 (m, 4H, GluN-**H**-3, GluN-**H**-5, Ino-**H**-5, Ino-**H**-6), 4.11 (d, J = 12.5 Hz, 1H, Ph**C**$\mathbf{H_2}$O), 4.18 (m, 1H, Ino-**H**-2), 4.41 (d, J = 10.6 Hz, 1H, Ph**C**$\mathbf{H_2}$O), 4.43 (d, J = 12.0 Hz, 1H, Ph**C**$\mathbf{H_2}$O), 4.65 (d, J = 11.2 Hz, 1H, Ph**C**$\mathbf{H_2}$O), 4.68-4.81 (m, 4H, Ph**C**$\mathbf{H_2}$O), 4.86 (d, J = 12.0 Hz, 1H, Ph**C**$\mathbf{H_2}$O), 4.83 (d, J = 10.9 Hz, 1H, Ph**C**$\mathbf{H_2}$O), 4.91 (d, J = 10.6 Hz, 1H, Ph**C**$\mathbf{H_2}$O), 5.00 (d, J = 10.9 Hz, 1H, Ph**C**$\mathbf{H_2}$O), 5.35 (d, J = 3.18 Hz, 1H, GluN-**H**-1), 7.01-7.46 (m, 36.8H, **Ph**$CH_2O$ (30H) + C**H**$Cl_3$). For **45**: $R_f$ = 0.25 (45 % EtOAc in heptane); $^1$H NMR (400 MHz, $CDCl_3$) δ 2.47 (m, 1H, O**H**), 3.05 (m, 1H, O**H**), 3.31 (dd, J = 10.9, 1.55 Hz, 1H, GluN-**H**-6a), 3.39 (dd, J = 11.1, 2.7 Hz, 1H, GluN-**H**-6b), 3.48 (Ψt, J = 9.28 Hz, 1H, Ino-**H**-4), 3.51 (dd, J = 9.6, 2.9 Hz, 1H, Ino-**H**-6), 3.58 (dd, J = 10.1, 3.6 Hz, 1H, GluN-**H**-2), 3.65 (dd, J = 9.7, 2.7 Hz, 1H, Ino-**H**-2), 3.74 (Ψt, J = 9.6 Hz, 1H, GluN-**H**-4), 3.86 (Ψt, J = 9.76, 9.68 Hz, 1H, Ino-**H**-3), 3.87-4.00 (m, 3H, GluN-**H**-3, GluN-**H**-5, Ino-**H**-5), 4.22 (Ψt, J = 2.8, 2.6 Hz, 1H, Ino-**H**-1), 4.29 (d, J = 12.1 Hz, 1H, Ph**C**$\mathbf{H_2}$O), 4.46 (d, J = 11.0 Hz, 1H, Ph**C**$\mathbf{H_2}$O), 4.51 (d, J = 12.1 Hz, 1H, Ph**C**$\mathbf{H_2}$O), 4.70 (d, J = 10.7 Hz, 1H, Ph**C**$\mathbf{H_2}$O), 4.76 (d, J = 11.0 Hz, 1H, Ph**C**$\mathbf{H_2}$O), 4.80 (d, J = 11.1 Hz,

1H, Ph**C**$\mathbf{H_2}$O), 4.83-4.91 (m, 4H, Ph**C**$\mathbf{H_2}$O), 4.90 (d, J = 10.6 Hz, 1H, Ph**C**$\mathbf{H_2}$O), 4.92 (d, J = 10.9 Hz, 1H, Ph**C**$\mathbf{H_2}$O), 4.99 (d, J = 3.7, 1H, GluN-**H**-1), 7.01-7.49 (m, 35H, **Ph**$CH_2O$ (30H) + C**H**$Cl_3$).

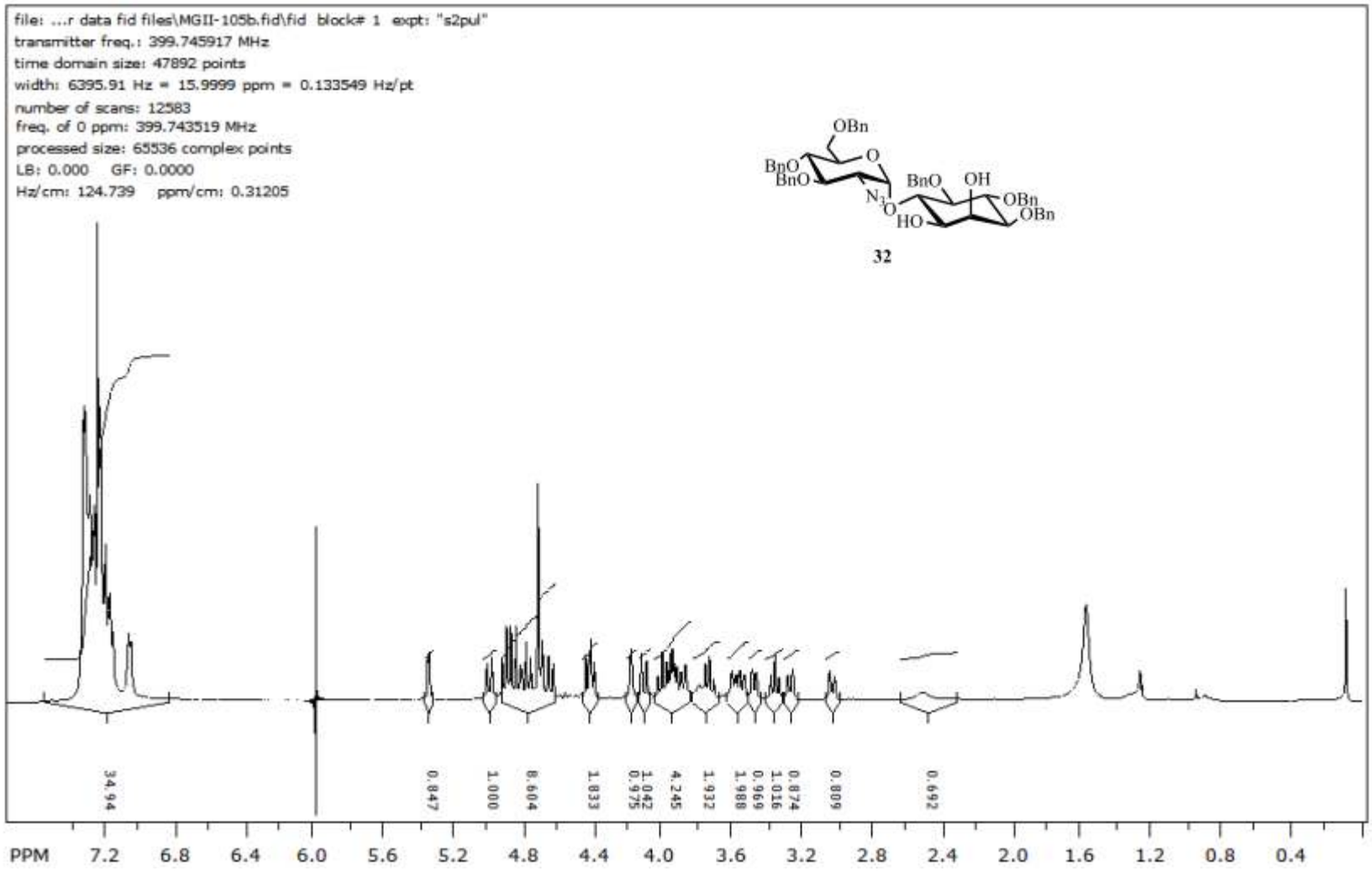
file: ...r data fid files\MGII-105b.fid\fid block# 1 expt: "s2pul"
transmitter freq.: 399.745917 MHz
time domain size: 47892 points
width: 6395.91 Hz = 15.9999 ppm = 0.133549 Hz/pt
number of scans: 12583
freq. of 0 ppm: 399.743519 MHz
processed size: 65536 complex points
LB: 0.000 GF: 0.0000
Hz/cm: 124.739 ppm/cm: 0.31205
OBn
BnO
BnO
O
N3
O
BnO
OH
OBn
OBn
HO
32
34.94
0.847
1.000
8.604
1.833
1.042
0.975
4.245
1.932
1.988
0.969
1.016
0.874
0.809
0.692
PPM
7.2
6.8
6.4
6.0
5.6
5.2
4.8
4.4
4.0
3.6
3.2
2.8
2.4
2.0
1.6
1.2
0.8
0.4

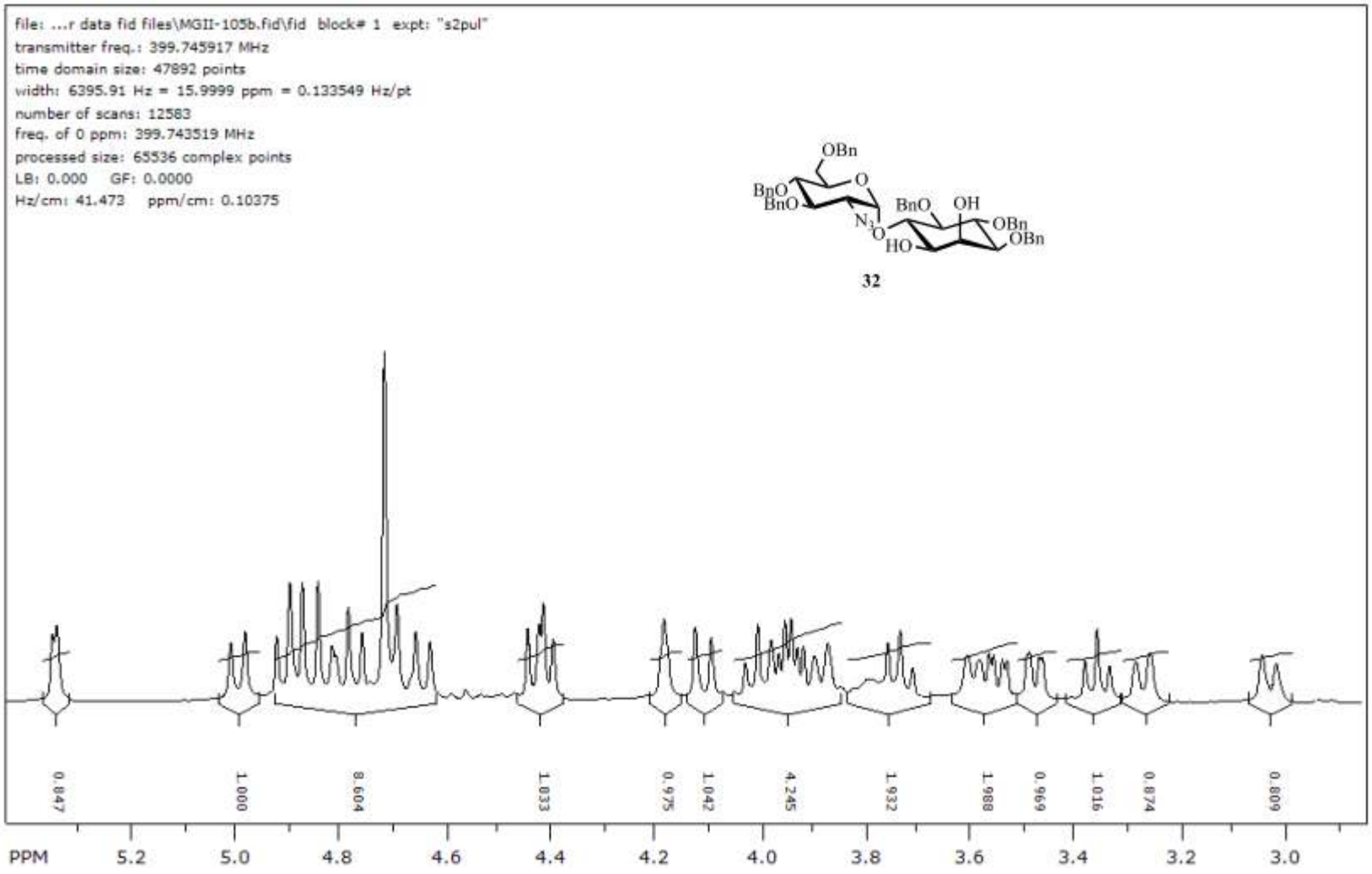
file: ...r data fid files\MGII-105b.fid\fid block# 1 expt: "s2pul"
transmitter freq.: 399.745917 MHz
time domain size: 47892 points
width: 6395.91 Hz = 15.9999 ppm = 0.133549 Hz/pt
number of scans: 12583
freq. of 0 ppm: 399.743519 MHz
processed size: 65536 complex points
LB: 0.000 GF: 0.0000
Hz/cm: 41.473 ppm/cm: 0.10375
OBn
BnO
BnO
O
N3
O
HO
BnO
OH
OBn
OBn
32
0.847
1.000
8.604
1.033
0.975
1.042
4.245
1.932
1.988
0.969
1.016
0.874
0.809
PPM
5.2
5.0
4.8
4.6
4.4
4.2
4.0
3.8
3.6
3.4
3.2
3.0

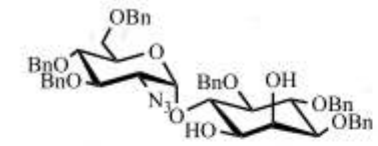


**32**

```
Pulse Sequence: gCOSY
 Solvent: CDCl3
 Ambient temperature
INOVA-400  "inova400"
 Relax. delay 1.000 sec
 Acq. time 0.213 sec
 Width     4797.0 Hz
 2D Width 4797.0 Hz
 8 repetitions
 128 increments
OBSERVE    H1, 399.7435482 MHz
DATA PROCESSING
 Sq. sine bell 0.107 sec
F1 DATA PROCESSING
 Sq. sine bell 0.027 sec
FT size 2048 x 2048
Total time 21 min, 29 sec
```

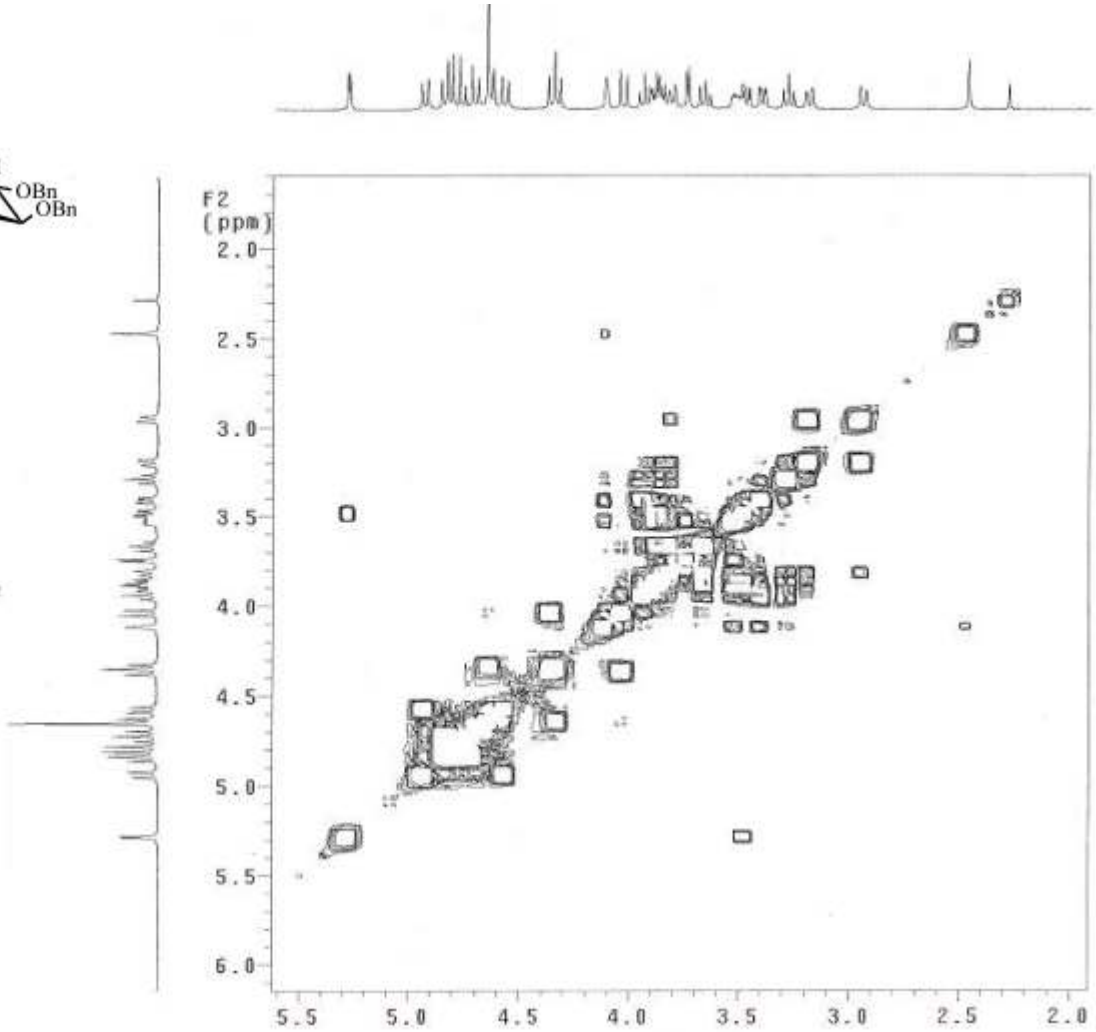

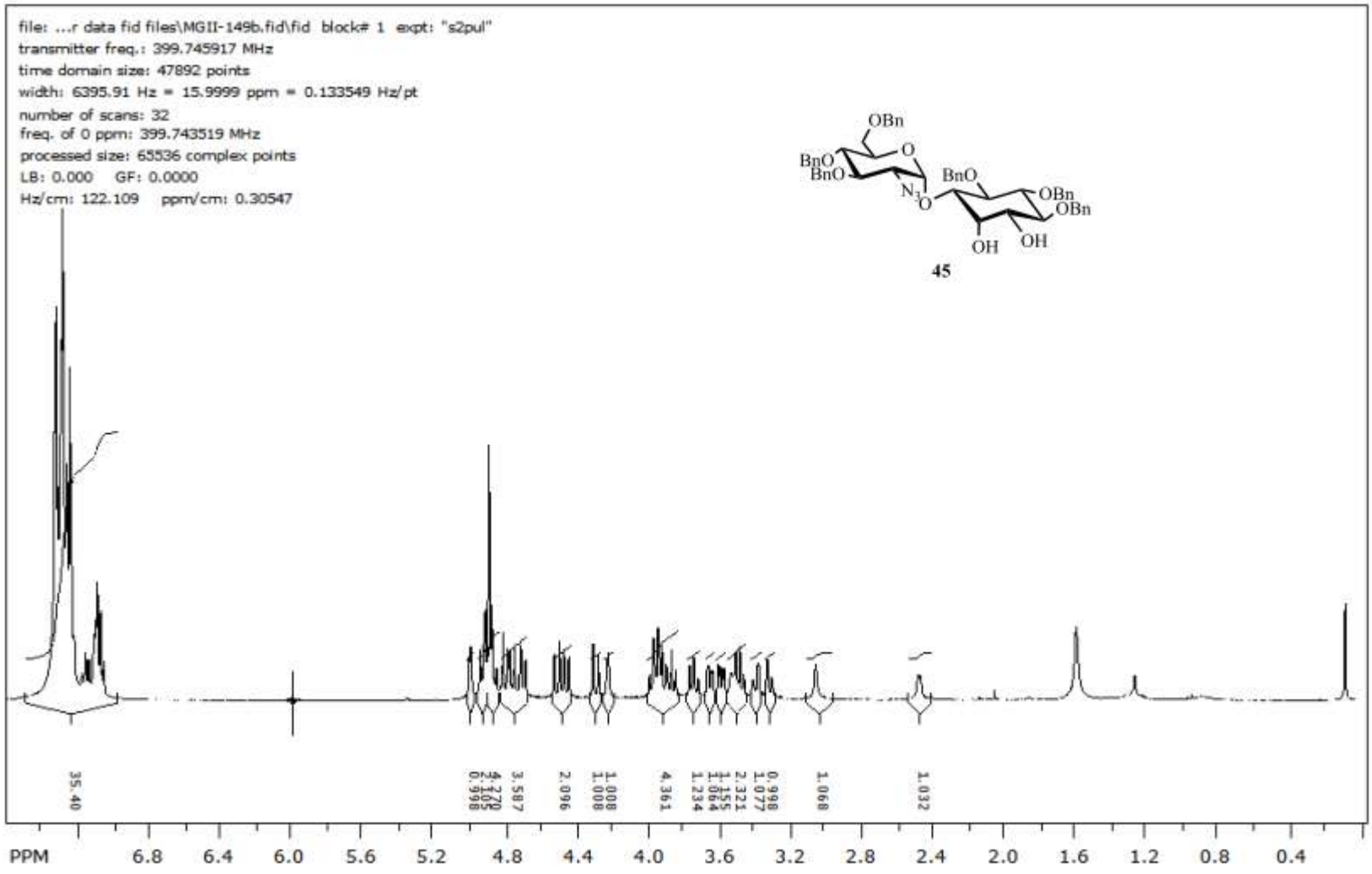
file: ...r data fid files\MGII-149b.fid\fid block# 1 expt: "s2pul"
transmitter freq.: 399.745917 MHz
time domain size: 47892 points
width: 6395.91 Hz = 15.9999 ppm = 0.133549 Hz/pt
number of scans: 32
freq. of 0 ppm: 399.743519 MHz
processed size: 65536 complex points
LB: 0.000 GF: 0.0000
Hz/cm: 122.109 ppm/cm: 0.30547
OBn
BnO
BnO
BnO
OBn
OBn
OH
OH
45
35.40
0.998
4.270
3.587
2.096
1.008
1.008
4.361
1.234
1.155
1.064
2.321
1.077
0.998
1.068
1.032
PPM
6.8
6.4
6.0
5.6
5.2
4.8
4.4
4.0
3.6
3.2
2.8
2.4
2.0
1.6
1.2
0.8
0.4

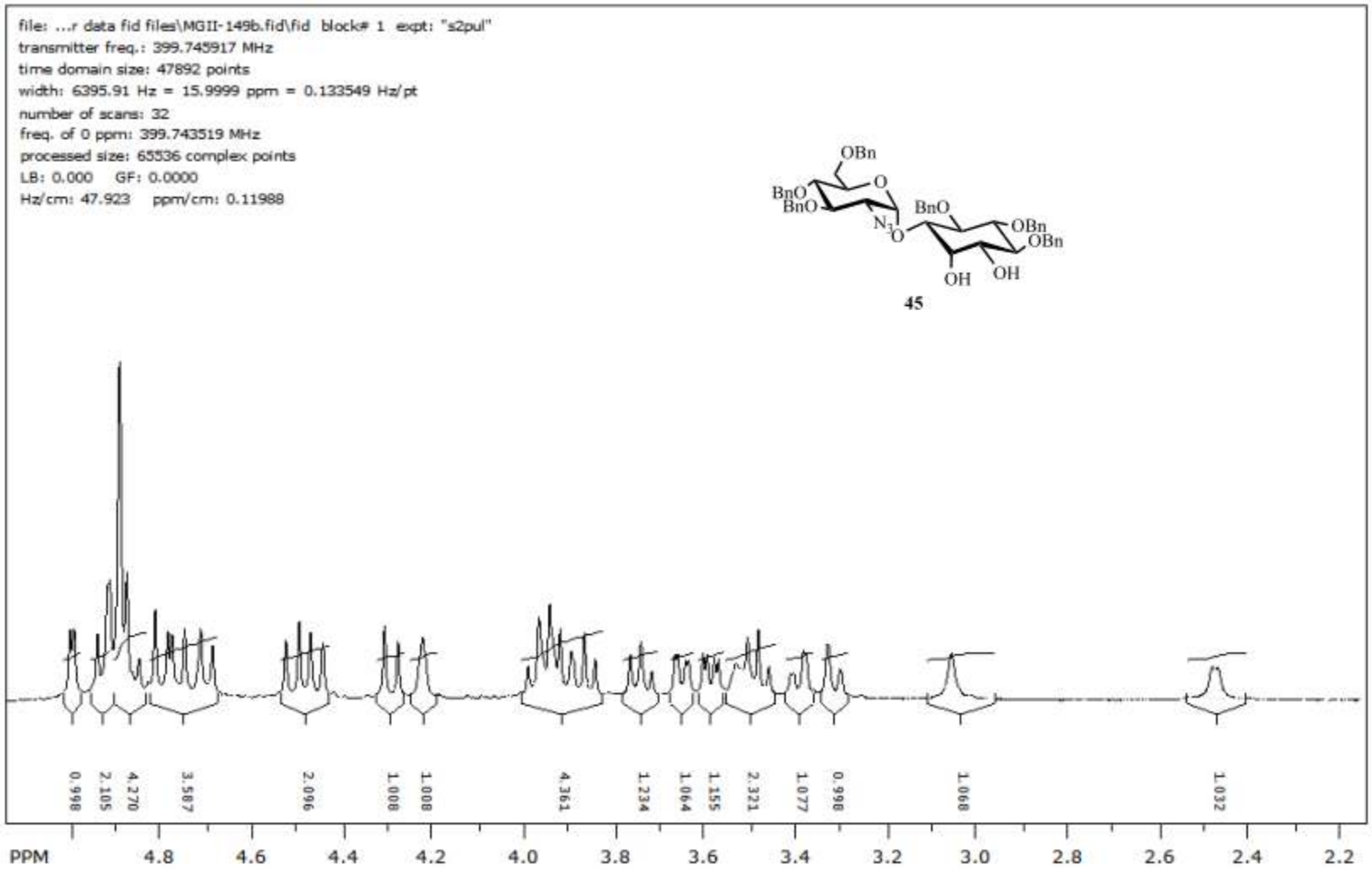
file: ...r data fid files\MGII-149b.fid\fid block# 1 expt: "s2pul"
transmitter freq.: 399.745917 MHz
time domain size: 47892 points
width: 6395.91 Hz = 15.9999 ppm = 0.133549 Hz/pt
number of scans: 32
freq. of 0 ppm: 399.743519 MHz
processed size: 65536 complex points
LB: 0.000 GF: 0.0000
Hz/cm: 47.923 ppm/cm: 0.11988
OBn
BnO
BnO
O
N3
O
BnO
OBn
OBn
OH
OH
45
0.998
2.105
4.270
3.587
2.096
1.008
1.008
4.361
1.234
1.064
1.155
2.321
1.077
0.998
1.068
1.032
PPM
4.8
4.6
4.4
4.2
4.0
3.8
3.6
3.4
3.2
3.0
2.8
2.6
2.4
2.2

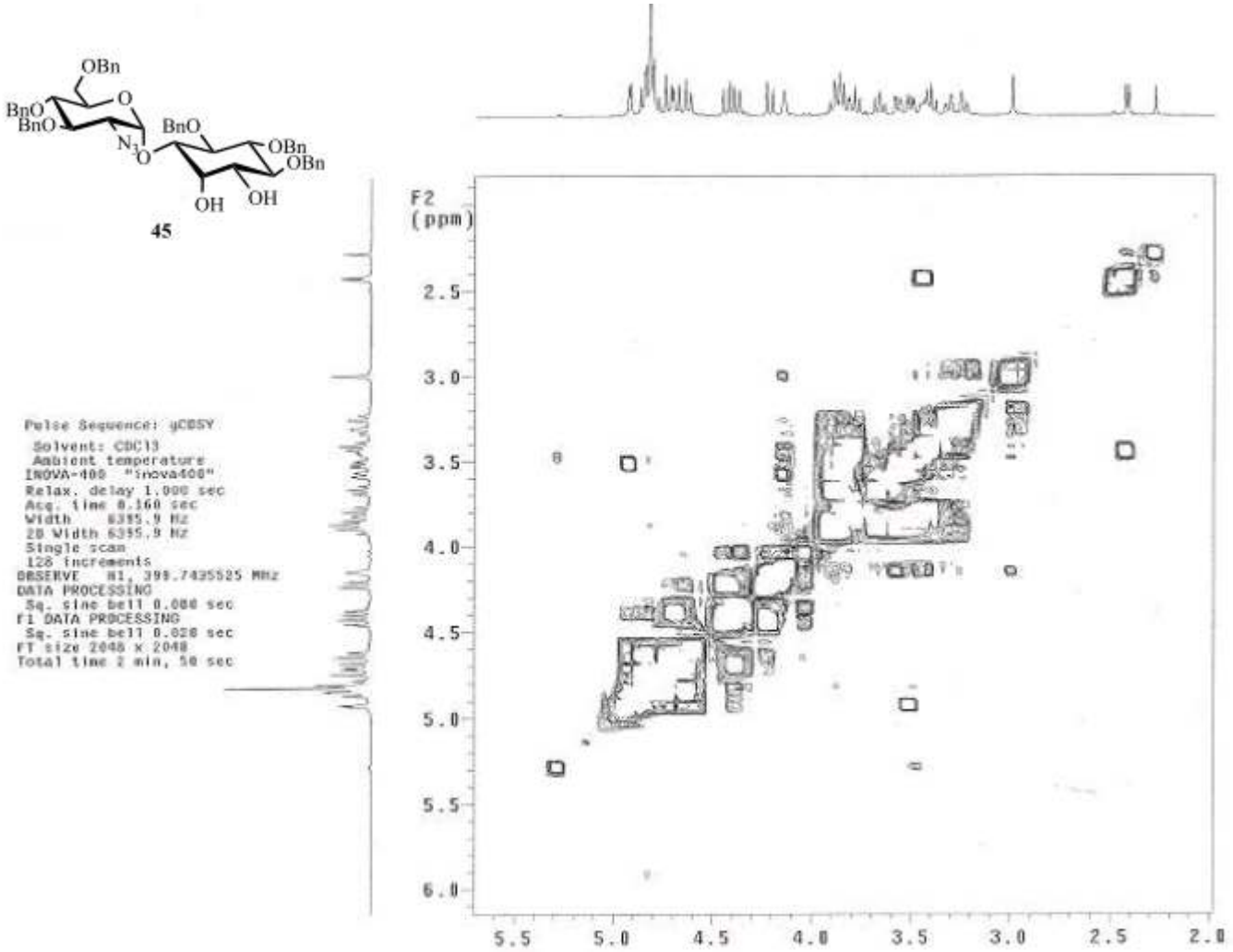
OBn
BnO
BnO
O
N3
O
BnO
OBn
OBn
OH
OH
45
Pulse Sequence: gCOSY
Solvent: CDCl3
Ambient temperature
INOVA-400 "inova400"
Relax. delay 1.000 sec
Acq. time 0.160 sec
Width 6385.9 Hz
2D Width 6385.9 Hz
Single scan
128 increments
OBSERVE H1, 399.7435525 MHz
DATA PROCESSING
Sq. sine bell 0.080 sec
F1 DATA PROCESSING
Sq. sine bell 0.020 sec
FT size 2048 x 2048
Total time 2 min, 50 sec
F2
(ppm)
2.5
3.0
3.5
4.0
4.5
5.0
5.5
6.0
5.5
5.0
4.5
4.0
3.5
3.0
2.5
2.0

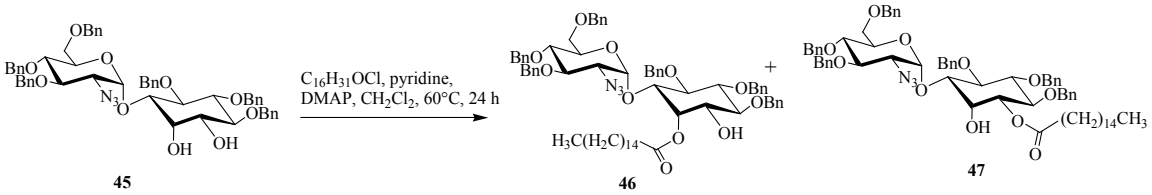


**2-Azido-3,4,6-tri-*O*-benzyl-2-deoxy-D-glucopyranosyl-(1 → 6)-3,4,5-tri-*O*-benzyl-1-palmitoyl-D-*myo*-inositol (46)** and **2-azido-3,4,6-tri-*O*-benzyl-2-deoxy-D-glucopyranosyl-(1 → 6)-3,4,5-tri-*O*-benzyl-2-palmitoyl-D-*myo*-inositol (47).** To a solution of diol **45** (10 mg, 0.01 mmol) in distilled pyridine (21 μL, 0.25 mmol) was added DMAP catalyst (0.125 mg, 0.001 mmol, 10 mol %) and palmitoyl chloride (6.05 μL, 0.02 mmol, 2 equiv*). The reaction mixture was stirred under an argon atmosphere at 60 ˚C and was monitored by TLC (40 % EtOAc in heptane). The reaction was heated to about 110 ˚C to accelerate the conversion of the starting material. However, even after prolonged periods of reflux (36-48 h) the conversion was never completed. Pyridine was evaporated under vacuum. The reaction mixture was diluted with $CH_2Cl_2$ and washed successively with water (2 x 10 mL), 0.1 M HCl (1 x 10 mL), water (2 x 10 mL), saturated $NaHCO_3$ (3 x 10 mL), and brine (1 x 10 mL). The organic phase was dried over $MgSO_4$, filtered, and evaporated to give a crude reaction product. Further purification of the crude reaction product by PTLC (45 % EtOAc in heptane) yielded 0.3 mg of **46** and 1.3 mg of **47**, with a combined yield of 24 % (after recovery of 3.0 mg of starting material). For **46**: $^1$H NMR (400 MHz, $CDCl_3$).[35] For **47**: $^1$H NMR (400 MHz, $CDCl_3$).[35]

* Excess palmitoyl chloride was added to push the reaction to completion

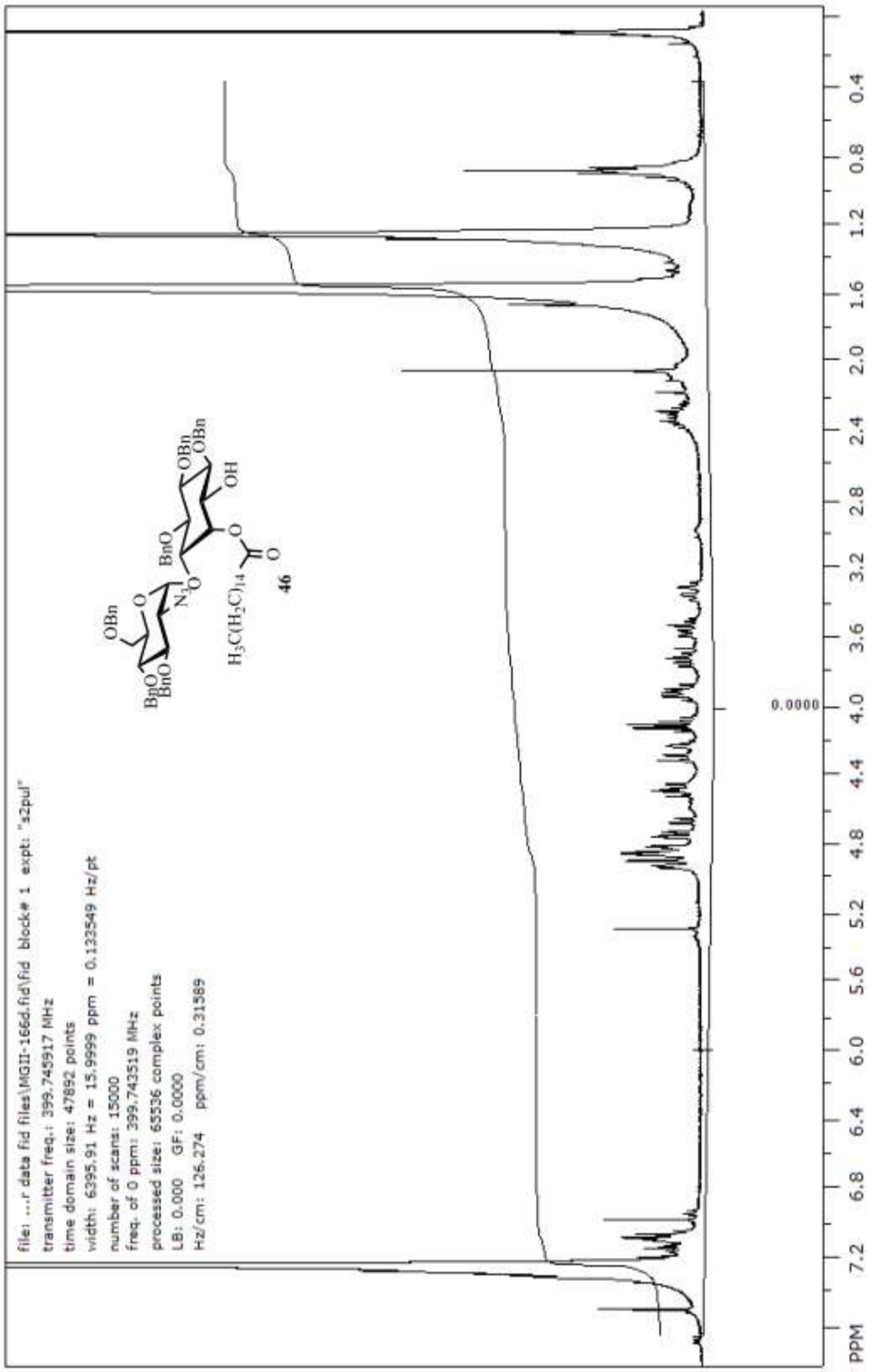
file: ...r data fid files\MGII-166d.fid\fid block# 1 expt: "s2pul"
transmitter freq.: 399.745917 MHz
time domain size: 47892 points
width: 6395.91 Hz = 15.9999 ppm = 0.133549 Hz/pt
number of scans: 15000
freq. of 0 ppm: 399.743519 MHz
processed size: 65536 complex points
LB: 0.000 GF: 0.0000
Hz/cm: 126.274 ppm/cm: 0.31589
OBn
BnO
BnO
O
N3
BnO
OBn
OBn
OH
O
O
H3C(H2C)14
O
46
0.0000
PPM
7.2
6.8
6.4
6.0
5.6
5.2
4.8
4.4
4.0
3.6
3.2
2.8
2.4
2.0
1.6
1.2
0.8
0.4

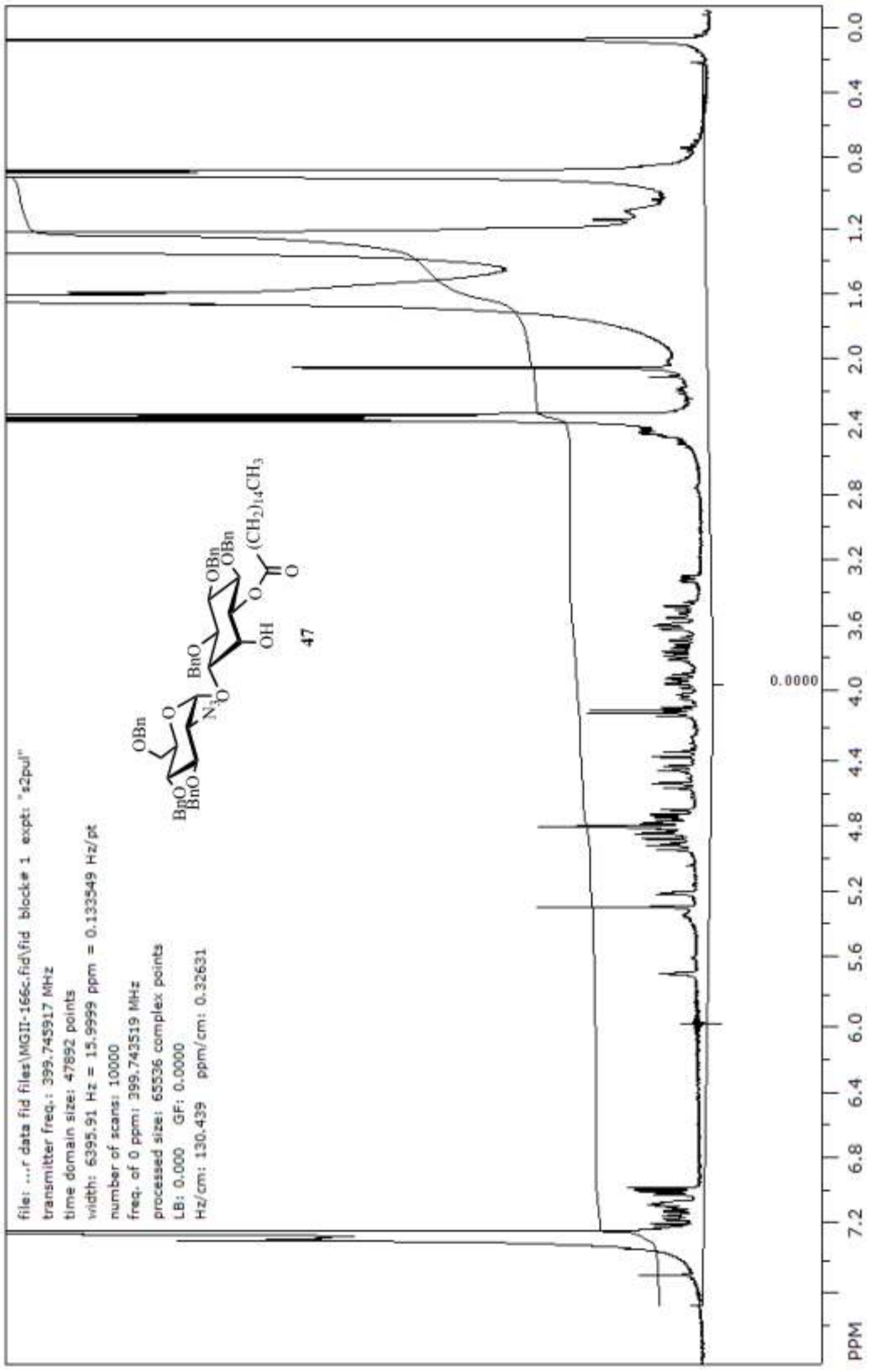
file: ...r data fid files\MGII-166c.fid\fid block# 1 expt: "s2pul"
transmitter freq.: 399.745917 MHz
time domain size: 47892 points
width: 6395.91 Hz = 15.9999 ppm = 0.133549 Hz/pt
number of scans: 10000
freq. of 0 ppm: 399.743519 MHz
processed size: 65536 complex points
LB: 0.000 GF: 0.0000
Hz/cm: 130.439 ppm/cm: 0.32631
OBn
BnO
BnO
O
N3
BnO
OBn
OBn
O
(CH2)14CH3
O
OH
47
0.0000
PPM
7.2
6.8
6.4
6.0
5.6
5.2
4.8
4.4
4.0
3.6
3.2
2.8
2.4
2.0
1.6
1.2
0.8
0.4
0.0

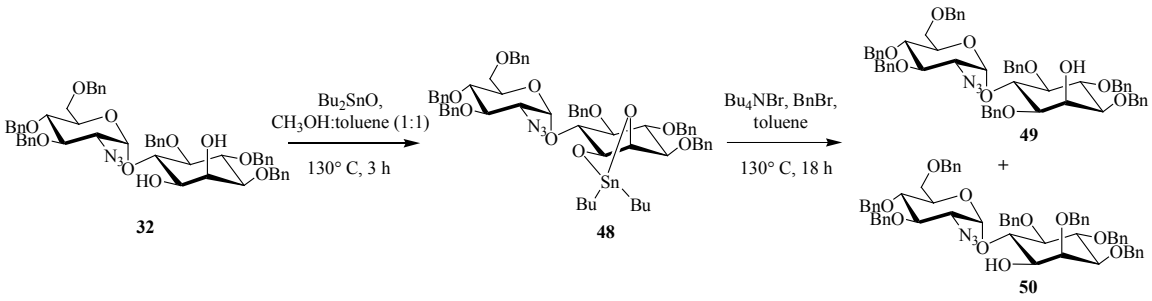


**2-Azido-3,4,6-tri-*O*-benzyl-2-deoxy-D-glucopyranosyl-(1 → 6)-1,3,4,5-tetra-*O*-benzyl-D-*myo*-inositol (49)** and **2-azido-3,4,6-tri-*O*-benzyl-2-deoxy-D-glucopyranosyl-(1 → 6)-2,3,4,5-tetra-*O*-benzyl-D-*myo*-inositol (50).** A mixture of diol **32** (10.6 mg, 12.35 μmol) and $Bu_2SnO$ (4.01 mg, 16.06 μmol, 1.3 equiv) in dry $CH_3OH$/toluene (1:1 v/v, 0.2 mL) was refluxed under an argon atmosphere at 130 ˚C for 3 h. The solvents were evaporated, dry toluene (1 mL) was added to the residue, and a second evaporation to dryness under high vacuum was effected. Then, a mixture of crude stannylene derivative, $Bu_4NBr$ (2.4 mg, 7.4 μmol, 0.6 equiv), and BnBr (5.2 μL, 43.23 μmol, 3.5 equiv) in dry toluene (0.2 mL) was refluxed under an argon atmosphere at 130 ˚C. Progress of the reaction was monitored by TLC (40 % EtOAc in hexane; for starting material $R_f = 0.23$, for products $R_f = 0.58$-$0.67$) until all the starting material was reacted, approximately 18 h. The solvent was evaporated under reduced pressure, and the crude reaction product was purified by PTLC (10 % EtOAc in toluene) yielding 6.2 mg of pure **49** and 1.6 mg of pure **50** with a combined yield of 64 %. For **49**: $R_f = 0.28$ (10 % EtOAc in toluene); $^1$H NMR (400 MHz, $CDCl_3$) δ 3.14 (dd, J = 11.3, 2.0 Hz, 1H, GluN-**H**-6a), 3.21 (dd, J = 11.2, 1.88 Hz, 1H, GluN-**H**-6b), 3.28 (dd, J = 10.3, 3.9 Hz, 1H, GluN-**H**-2), 3.37-3.45 (m, 2H, Ino-**H**-3, Ino-**H**-5), 3.52 (dd, J = 2.5, 9.5 Hz, 1H, Ino-**H**-1), 3.67 (Ψt, J = 9.5 Hz, 1H, GluN-**H**-4), 3.94 (Ψt, J = 9.2, 9.3 Hz, 1H, GluN-**H**-3), 3.99-4.09 (m, 2H,

GluN-**H**-5, Ino-**H**-4), 4.17 (Ψt, J = 9.3, 9.6 Hz, 1H, Ino-**H**-6), 4.22 (m, 1H, Ino-**H**-2), 4.24 (d, J = 11.8 Hz, 1H, Ph**CH$_2$**O), 4.38 (d, J = 11.0 Hz, 1H, Ph**CH$_2$**O), 4.51 (d, J = 12.1 Hz, 1H, Ph**CH$_2$**O), 4.62 (d, J = 10.9 Hz, 1H, Ph**CH$_2$**O), 4.66 (d, J = 11.3 Hz, 1H, Ph**CH$_2$**O), 4.66-4.74 (m, 4H, Ph**CH$_2$**O), 4.82 (d, J = 10.8 Hz, 1H, Ph**CH$_2$**O), 4.85 (d, J = 10.5 Hz, 1H, Ph**CH$_2$**O), 4.88 (d, J = 11.0 Hz, 1H, Ph**CH$_2$**O), 4.95 (d, J = 10.6 Hz, 1H, Ph**CH$_2$**O), 4.98 (d, J = 10.7 Hz, 1H, Ph**CH$_2$**O), 5.69 (d, J = 3.8 Hz, 1H, GluN-**H**-1), 7.00-7.43 (m, 42H, **Ph**$CH_2O$). HRMS (ESI): m/z calcd for $C_{61}H_{63}O_{10}N_3$: 998.4586. Found: 998.4577. For **50**: $R_f$ = 0.44 (10 % EtOAc in toluene); $^1$H NMR (400 MHz, $CDCl_3$) δ 3.03 (dd, J = 11.0, 2.0 Hz, 1H), 3.20 (dd, J = 11.3, 2.3 Hz, 1H), 3.23 (d, J = 6.3 Hz, 1H), 3.36 (Ψt, J = 9.2 Hz, 1H), 3.44-3.52 (m, 2H), 3.61 (ddd, J = 3.6, 5.9, 13.2 Hz, 1H), 3.67-3.76 (m, 2H), 3.86-4.03 (m, 5H), 4.38 (d, J = 11.0 Hz, 1H), 4.45 (d, J = 11.9 Hz, 1H), 4.62 (d, J = 11.2 Hz, 1H), 4.65-4.75 (m, 4H), 4.75-4.81 (m, 2H), 4.83 (d, J = 11.4 Hz, 1H), 4.88 (d, J = 11.7 Hz, 1H), 4.94 (d, J = 10.7 Hz, 1H), 4.98 (d, J = 11.9 Hz, 1H), 5.01 (d, J = 11.0 Hz, 1H), 5.43 (d, J = 3.8 Hz, 1H), 6.98-7.45 (m, 42H); $^1$H NMR (400 MHz, DMSO $d_6$) δ 3.27-3.37 (m, 63H, GluN-**H**-6a, GluN-**H**-6b, and $H_2O$), 3.38-3.46 (m, 2H, GluN-**H**-4, GluN-**H**-2), 3.54 (Ψt, J = 9.9, 8.9 Hz, 1H, Ino-**H**-4), 3.64-3.75 (m, 2H, Ino-**H**-5, Ino-**H**-1), 3.81-3.92 (m, 3H, GluN-**H**-5, Ino-**H**-3, Ino-**H**-6), 4.19 (d, J = 11.8 Hz, 1H, Ph**CH$_2$**O), 4.38 (d, J = 11.6 Hz, 1H, Ph**CH$_2$**O), 4.42 (d, J = 10.9 Hz, 1H, Ph**CH$_2$**O), 4.57-4.64 (m, 2H, Ph**CH$_2$**O), 4.64-4.71 (m, 3H, Ph**CH$_2$**O), 4.75-4.88 (m, 6H, Ph**CH$_2$**O), 5.25 (d, J = 5.9 Hz, 1H, -O**H**), 5.71 (d, J = 3.8 Hz, 1H, GluN-**H**-1), 6.96-7.45 (m, 42H, **Ph**$CH_2O$). HRMS (ESI): m/z calcd for $C_{61}H_{63}O_{10}N_3$: 998.4586. Found: 998.4575.

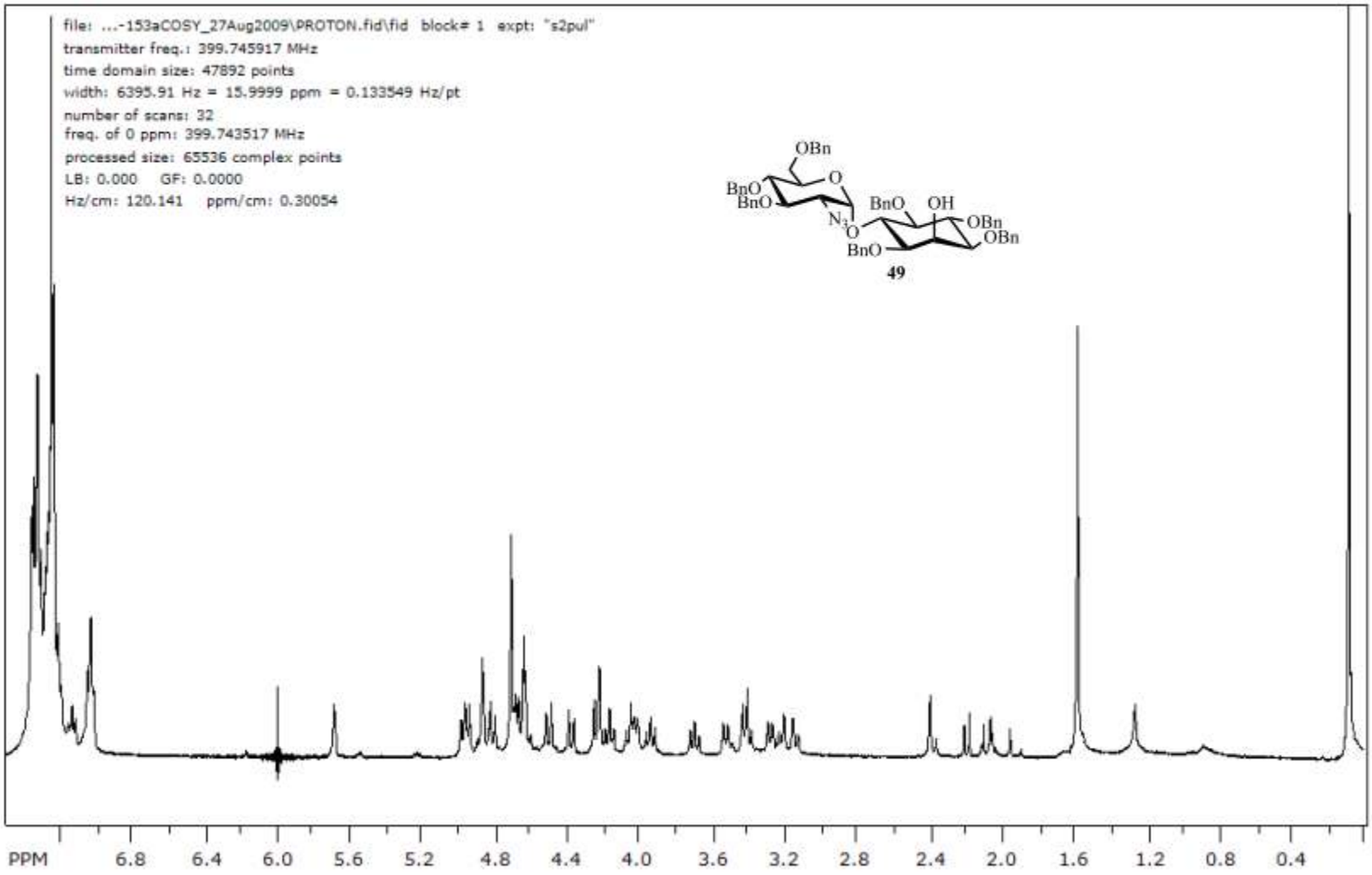
file: ...-153aCOSY_27Aug2009\PROTON.fid\fid block# 1 expt: "s2pul"
transmitter freq.: 399.745917 MHz
time domain size: 47892 points
width: 6395.91 Hz = 15.9999 ppm = 0.133549 Hz/pt
number of scans: 32
freq. of 0 ppm: 399.743517 MHz
processed size: 65536 complex points
LB: 0.000 GF: 0.0000
Hz/cm: 120.141 ppm/cm: 0.30054
OBn
BnO
BnO
O
N3
O
BnO
BnO
OH
OBn
OBn
49
PPM
6.8
6.4
6.0
5.6
5.2
4.8
4.4
4.0
3.6
3.2
2.8
2.4
2.0
1.6
1.2
0.8
0.4

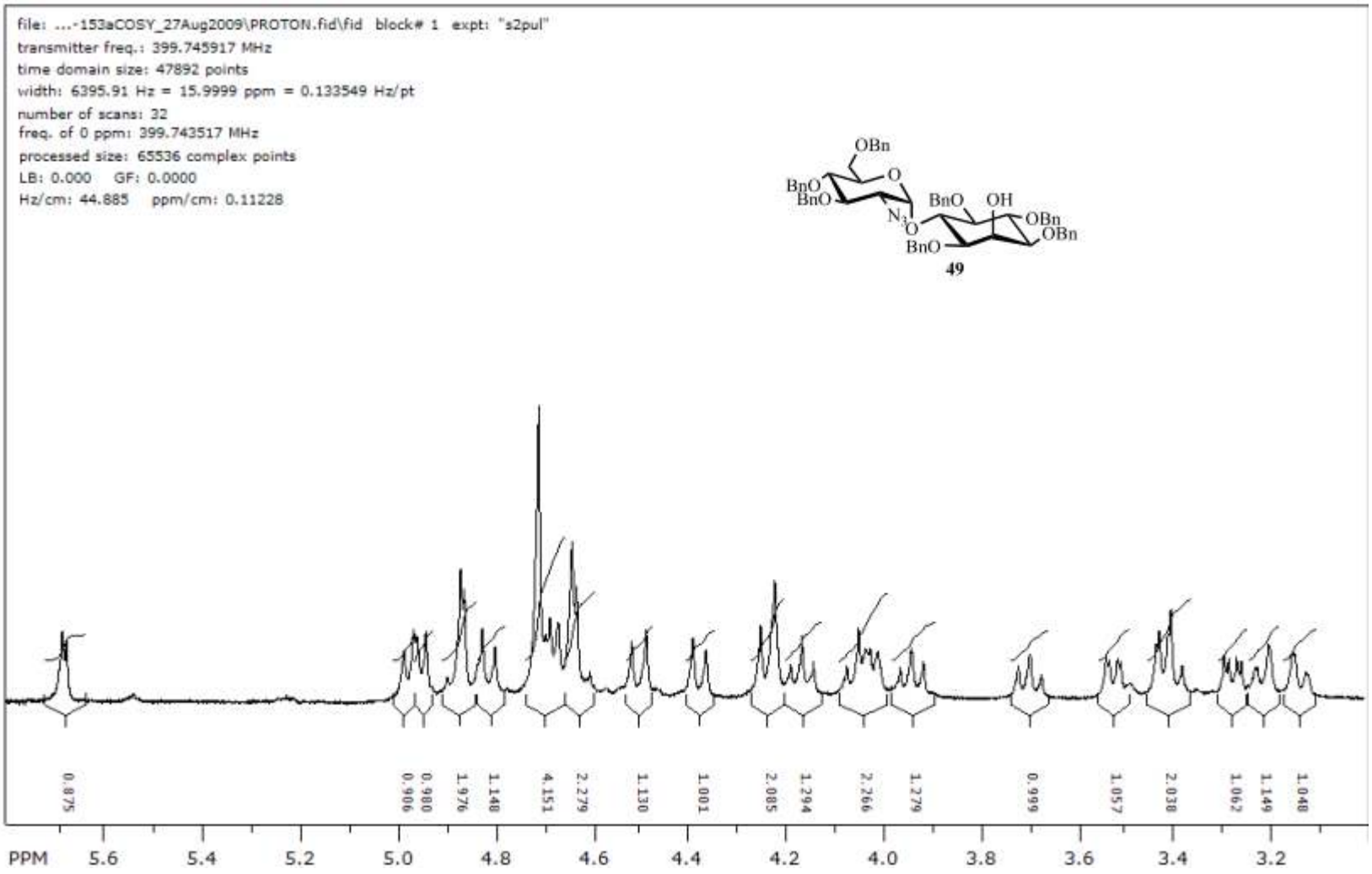
file: ...-153aCOSY_27Aug2009\PROTON.fid\fid block# 1 expt: "s2pul"
transmitter freq.: 399.745917 MHz
time domain size: 47892 points
width: 6395.91 Hz = 15.9999 ppm = 0.133549 Hz/pt
number of scans: 32
freq. of 0 ppm: 399.743517 MHz
processed size: 65536 complex points
LB: 0.000 GF: 0.0000
Hz/cm: 44.885 ppm/cm: 0.11228
OBn
BnO
BnO
O
N3
O
BnO
BnO
OH
OBn
OBn
49
0.875
0.906
0.980
1.976
1.148
4.151
2.279
1.130
1.001
2.085
1.294
2.266
1.279
0.999
1.057
2.038
1.062
1.149
1.048
PPM
5.6
5.4
5.2
5.0
4.8
4.6
4.4
4.2
4.0
3.8
3.6
3.4
3.2

OBn
BnO
BnO
O
N3
BnO
OH
OBn
OBn
49
F2 (ppm)
3.0
3.5
4.0
4.5
5.0
5.5
6.0
5.6
5.2
4.8
4.4
4.0
3.6
3.2
2.8
Pulse Sequence: gCOSY
Solvent: CDCl3
Ambient temperature
INOVA-400 "inova400"
Relax. delay 1.000 sec
Acq. time 0.213 sec
Width 4797.0 Hz
2D Width 4797.0 Hz
8 repetitions
512 increments
OBSERVE H1, 399.7435448 MHz
DATA PROCESSING
Sq. sine bell 0.107 sec
F1 DATA PROCESSING
Sq. sine bell 0.027 sec
FT size 2048 x 2048
Total time 1 hr, 27 min, 41 sec
Archive directory: /export/home/mrakshi/vnmrsys/data
Sample directory: MGII-161bCOSY_18Sep2003
File: gCOSY

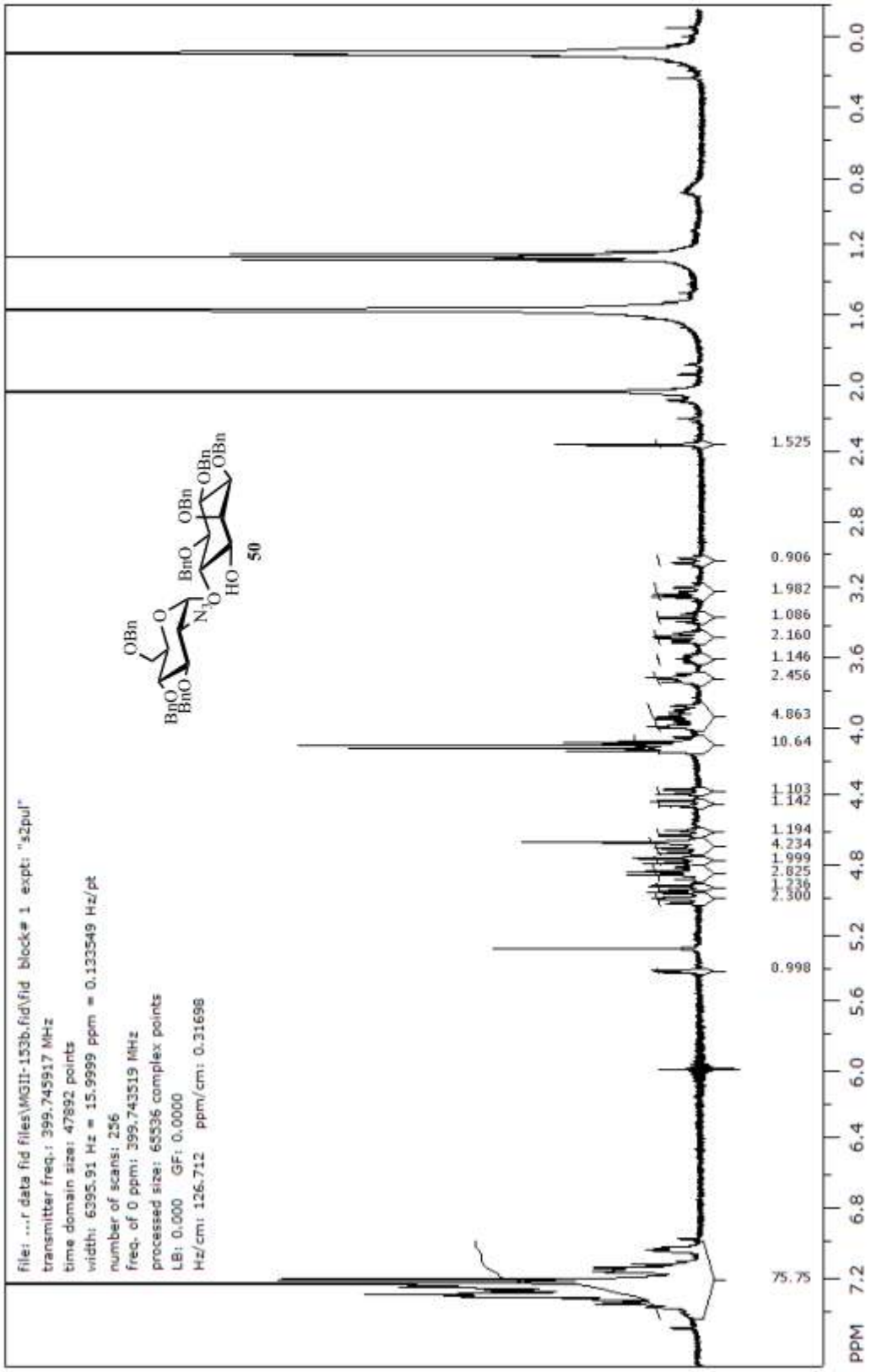
file: ...r data fid files\MGII-153b.fid\fid block# 1 expt: "s2pul"
transmitter freq.: 399.745917 MHz
time domain size: 47892 points
width: 6395.91 Hz = 15.9999 ppm = 0.133549 Hz/pt
number of scans: 256
freq. of 0 ppm: 399.743519 MHz
processed size: 65536 complex points
LB: 0.000 GF: 0.0000
Hz/cm: 126.712 ppm/cm: 0.31698
50
75.75
0.998
1.525
0.906
1.982
1.086
2.160
1.146
2.456
4.863
10.64
1.103
1.142
1.194
4.234
1.999
2.825
2.300
PPM

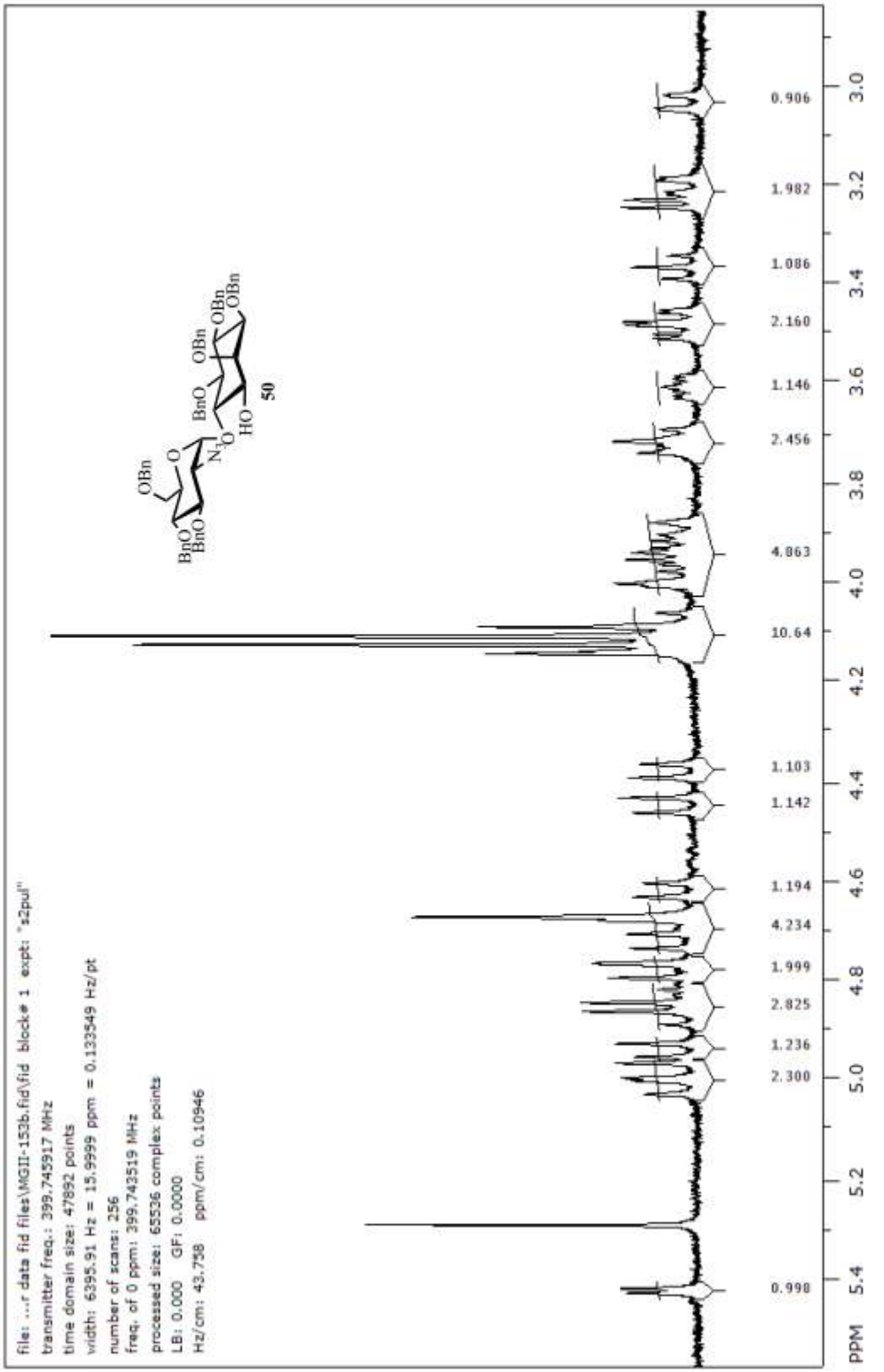
file: ...r data fid files\MGII-153b.fid\fid block# 1 expt: "s2pul"
transmitter freq.: 399.745917 MHz
time domain size: 47892 points
width: 6395.91 Hz = 15.9999 ppm = 0.133549 Hz/pt
number of scans: 256
freq. of 0 ppm: 399.743519 MHz
processed size: 65536 complex points
LB: 0.000 GF: 0.0000
Hz/cm: 43.758 ppm/cm: 0.10946
50
0.990
2.300
1.236
2.825
1.999
4.234
1.194
1.142
1.103
10.64
4.863
2.456
1.146
2.160
1.086
1.982
0.906
PPM
5.4
5.2
5.0
4.8
4.6
4.4
4.2
4.0
3.8
3.6
3.4
3.2
3.0

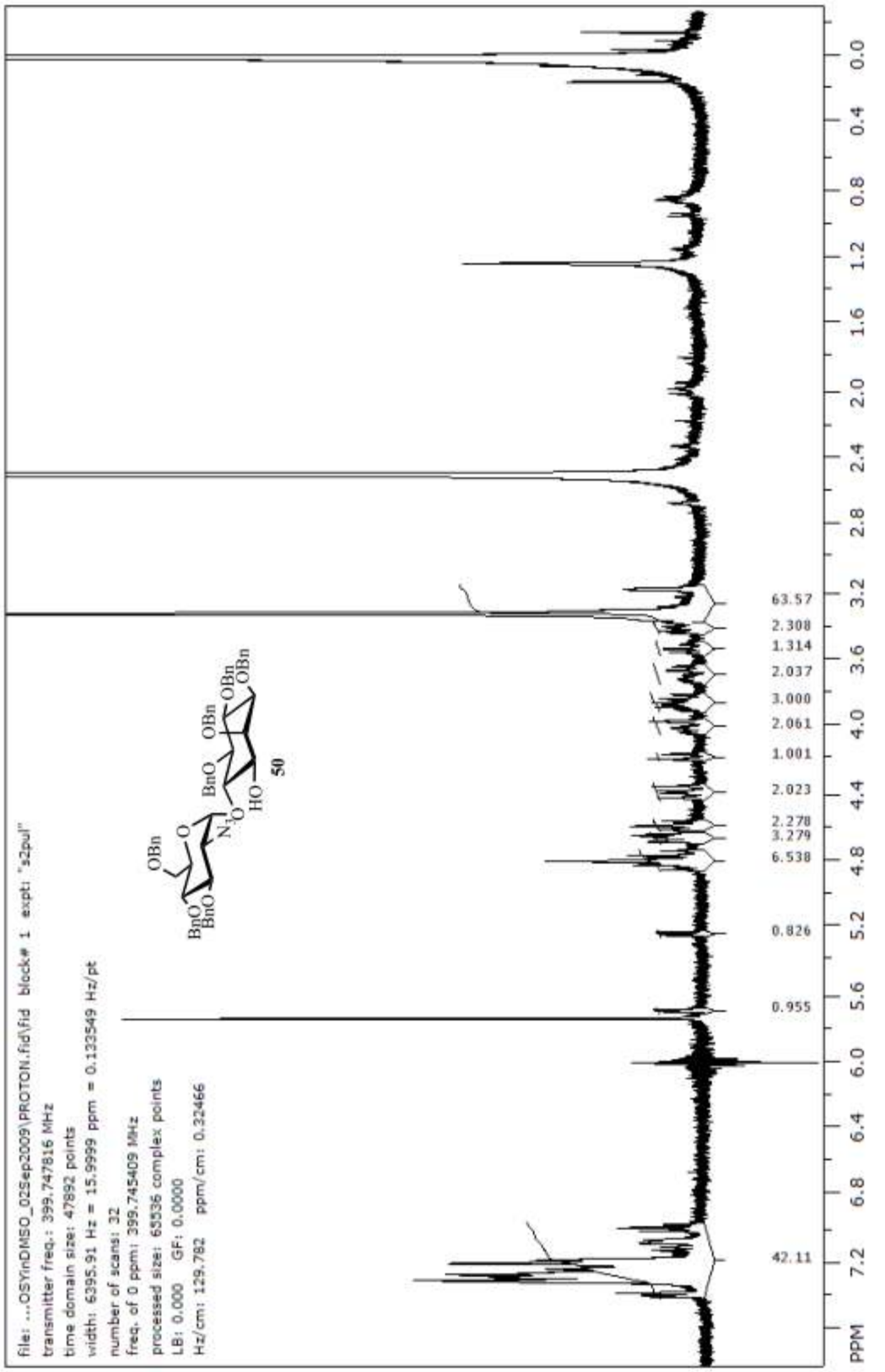
file: ...OSYinDMSO_02Sep2009\PROTON.fid\fid block# 1 expt: "s2pul"
transmitter freq.: 399.747816 MHz
time domain size: 47892 points
width: 6395.91 Hz = 15.9999 ppm = 0.133549 Hz/pt
number of scans: 32
freq. of 0 ppm: 399.745409 MHz
processed size: 65536 complex points
LB: 0.000 GF: 0.0000
Hz/cm: 129.782 ppm/cm: 0.32466
OBn
BnO
BnO
O
N3
BnO
OBn
OBn
HO
50
63.57
2.308
1.314
2.037
3.000
2.061
1.001
2.023
2.278
3.279
6.538
0.826
0.955
42.11
PPM
7.2
6.8
6.4
6.0
5.6
5.2
4.8
4.4
4.0
3.6
3.2
2.8
2.4
2.0
1.6
1.2
0.8
0.4
0.0

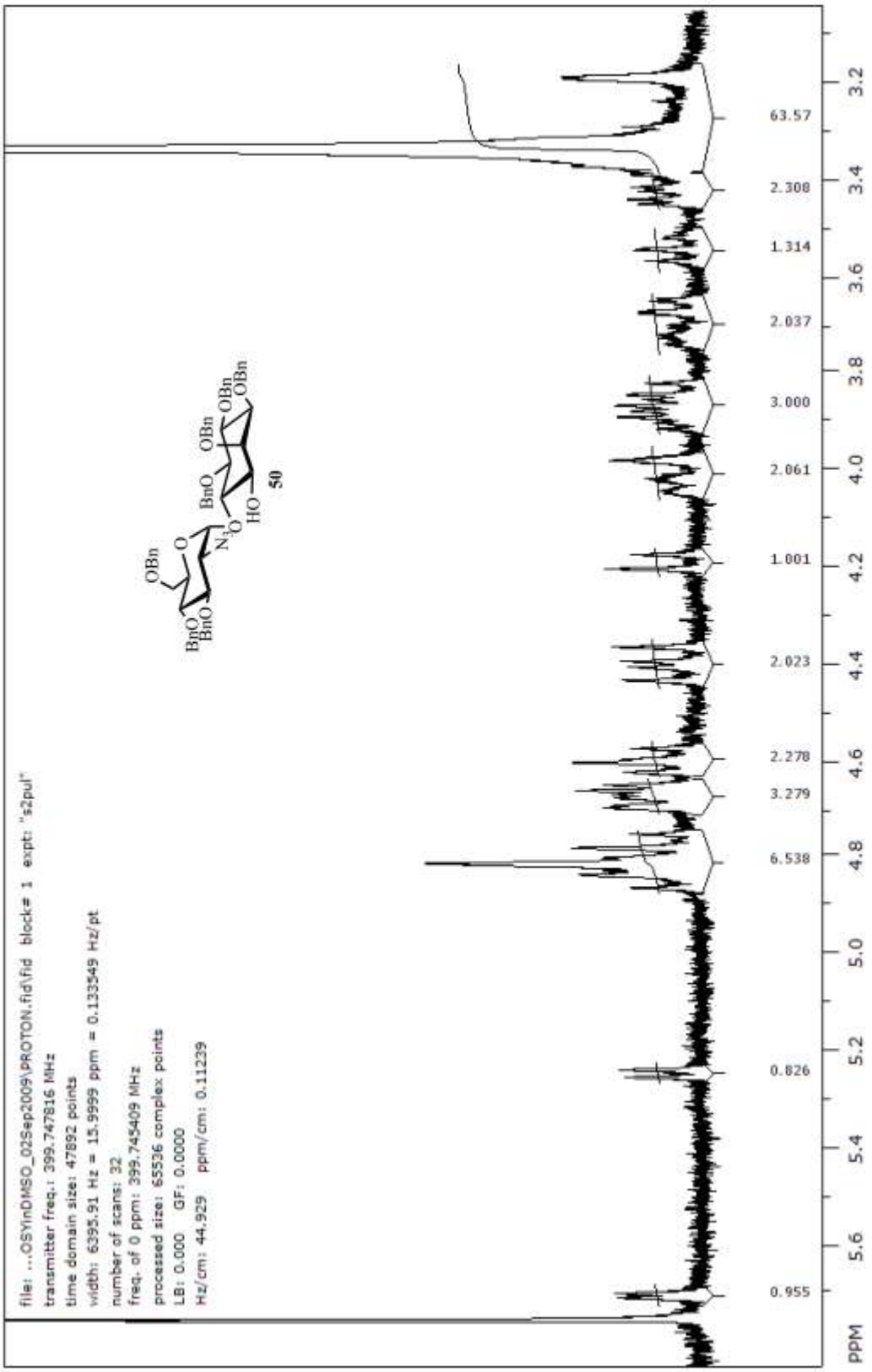
file: ...OSYinDMSO_02Sep2009\PROTON.fid\fid block# 1 expt: "s2pul"
transmitter freq.: 399.747816 MHz
time domain size: 47892 points
width: 6395.91 Hz = 15.9999 ppm = 0.133549 Hz/pt
number of scans: 32
freq. of 0 ppm: 399.745409 MHz
processed size: 65536 complex points
LB: 0.000 GF: 0.0000
Hz/cm: 44.929 ppm/cm: 0.11239
OBn
BnO
BnO
O
N3
BnO
OBn
OBn
OBn
HO
50
63.57
2.308
1.314
2.037
3.000
2.061
1.001
2.023
2.278
3.279
6.538
0.826
0.955
PPM
5.6
5.4
5.2
5.0
4.8
4.6
4.4
4.2
4.0
3.8
3.6
3.4
3.2

F2 (ppm)
3.5
4.0
4.5
5.0
5.5
6.0
6.0
5.5
5.0
4.5
4.0
3.5
3.0
OBn
BnO
BnO
O
N3
BnO
OBn
OBn
HO
50
Pulse Sequence: gCOSY
Solvent: DMSO
Ambient temperature
INOVA-400 "inova400-
Relax. delay 1.000 sec
Acq. time 0.160 sec
Width 6395.9 Hz
2D Width 6395.9 Hz
8 repetitions
512 increments
OBSERVE H1, 399.7454086 MHz
DATA PROCESSING
Sq. sine bell 0.080 sec
F1 DATA PROCESSING
Sq. sine bell 0.020 sec
FT size 2048 x 2048
Total time 1 hr, 23 min, 7 sec

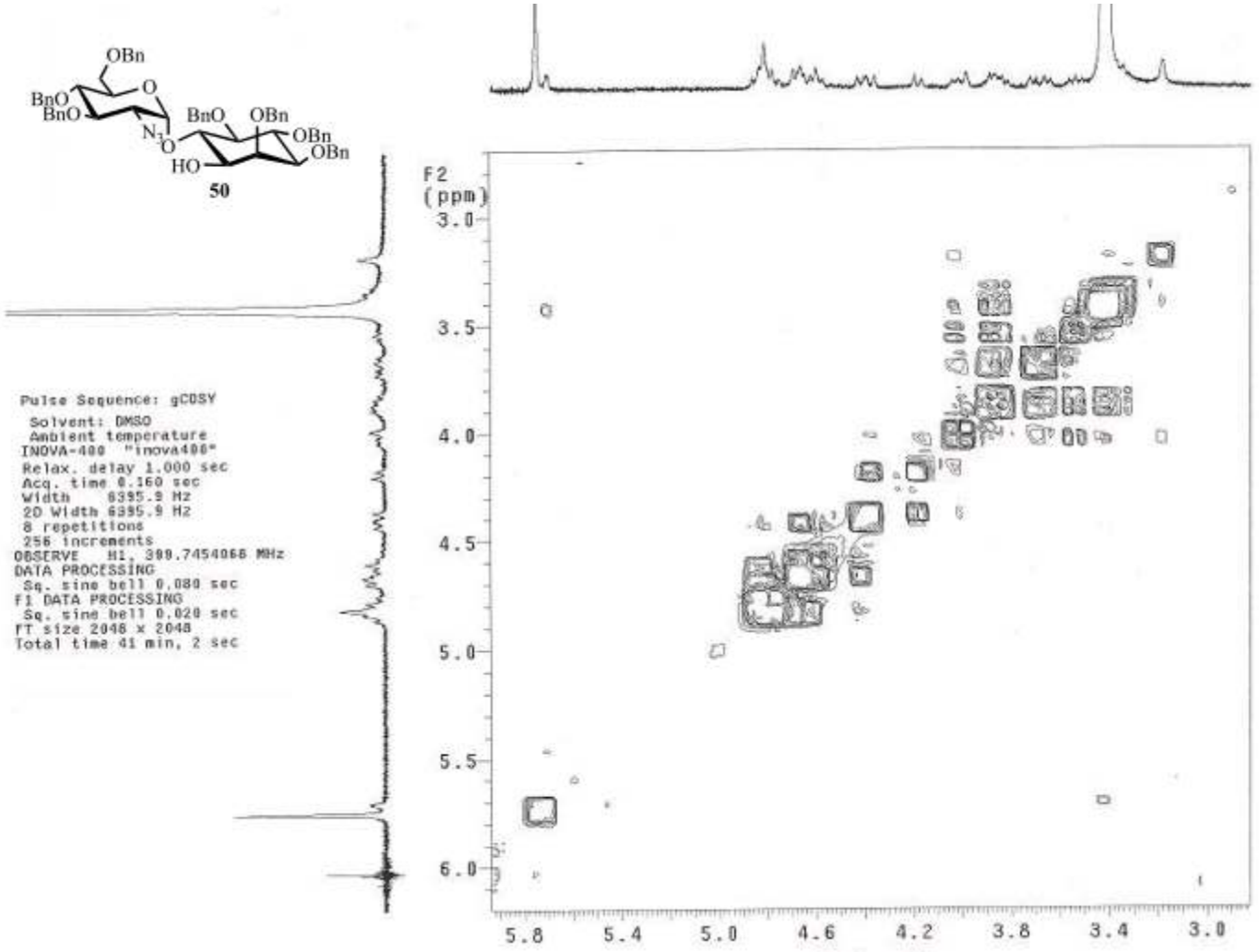
OBn
BnO
BnO
O
N3
O
BnO
OBn
OBn
OBn
HO
50
F2
(ppm)
3.0
3.5
4.0
4.5
5.0
5.5
6.0
5.8
5.4
5.0
4.6
4.2
3.8
3.4
3.0
Pulse Sequence: gCOSY
Solvent: DMSO
Ambient temperature
INOVA-400 "inova400"
Relax. delay 1.000 sec
Acq. time 0.160 sec
Width 6395.9 Hz
2D Width 6395.9 Hz
8 repetitions
256 increments
OBSERVE H1, 399.7454066 MHz
DATA PROCESSING
Sq. sine bell 0.080 sec
F1 DATA PROCESSING
Sq. sine bell 0.020 sec
FT size 2048 x 2048
Total time 41 min, 2 sec

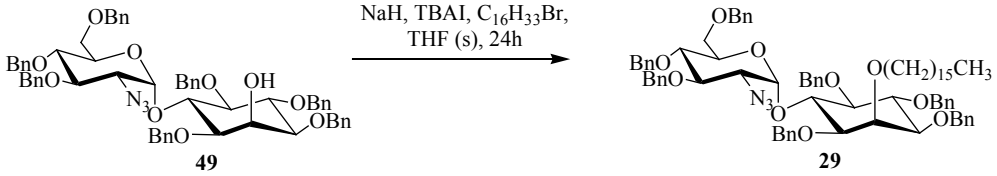


**2-Azido-3,4,6-tri-*O*-benzyl-2-deoxy-D-glucopyranosyl-(1 → 6)-1,3,4,5-tetra-*O*-benzyl-2-palmityl-D-*myo*-inositol (29).** To a solution of **49** (2 mg, 2 μmol) and TBAI (0.6 mg, 2 μmol) in dry THF (0.1 mL) was added NaH (60 % dispersion in mineral oil, 0.2 mg, 4 μmol, 2 equiv)**.** Hydrogen gas was evolved in the form of bubbles. The solution was allowed to stir for 20 min (note: reaction mixture should be cooled to 0 °C if reaction is done on large scale) after which pure 1-bromohexadecane (2 μL) was transferred into the reaction mixture using a syringe. The reaction mixture was then refluxed at about 60 °C under an argon atmosphere until TLC (6% EtOAc in benzene) showed almost 80% conversion of the starting material, approximately 24 h. THF was evaporated and the crude reaction mixture was purified by PTLC (7% EtOAc in benzene) yielding pure **29** (1.7 mg, 71%). $R_f$ = 0.73 (6% EtOAc in benzene). $^1$H NMR (400 MHz, $CDCl_3$) δ 0.77-0.98 (m, 8H, $CH_2CH_2(CH_2)_{12}\mathbf{CH_3}$ (3H)), 1.12-1.42 (m, 41H, $CH_2CH_2(\mathbf{CH_2})_{\mathbf{12}}CH_3$ (24H)), 1.44-1.75 (m, 35H, $H_2O$), 3.12 (dd, J = 2.0, 11.0 Hz, 1H, GluN-**H**-6a), 3.19 (dd, J = 2.0, 11.3 Hz, 1H, GluN-**H**-6b), 3.21 (dd, J = 3.7, 10.4 Hz, 1H, GluN-**H**-2), 3.35 (dd, J = 2.3, 9.9 Hz, 1H, Ino-**H**-1), 3.39 (Ψt, J = 9.2, 9.4 Hz, 1H, Ino-**H**-5), 3.42 (dd, J = 2.2, 9.6 Hz, 1H, Ino-**H**-3), 3.59-3.73 (m, 3H, GluN-**H**-4, GluN-**H**-5), 3.83-3.88 (m, 1H, Ino-**H**-2), 3.94 (Ψt, J = 9.1, 10.3 Hz, 1H, GluN-**H**-3), 3.98-4.07 (m, 2H, Ino-**H**-4, Ino-**H**-6), 4.15 (d, J = 9.6 Hz, 1H, Ph$\mathbf{CH_2}$O), 4.20 (d, J = 11.9 Hz, 1H, Ph$\mathbf{CH_2}$O), 4.35 (d, J = 11.5 Hz, 1H, Ph$\mathbf{CH_2}$O), 4.52 (d, J = 11.9 Hz, 1H, Ph$\mathbf{CH_2}$O), 4.58-

4.67 (m, 5H, Ph**CH$_2$**O (4H)), 4.69 (d, J = 11.2 Hz, 1H, Ph**CH$_2$**O), 4.79 (d, J = 10.8 Hz, 1H, Ph**CH$_2$**O), 4.82-4.89 (m, 2H, Ph**CH$_2$**O), 4.94 (d, J = 10.4 Hz, 1H, Ph**CH$_2$**O), 5.00 (d, J = 10.8 Hz, 1H, Ph**CH$_2$**O), 5.69 (d, J =4.2 Hz, 1H, GluN-**H**-1), 6.92-7.48 (m, 55H, **Ph**$CH_2O$ (42H) + C**H**$Cl_3$). HRMS (ESI): m/z calcd for $C_{77}H_{95}O_{10}N_3$: 1222.7090. Found: 1222.7084.

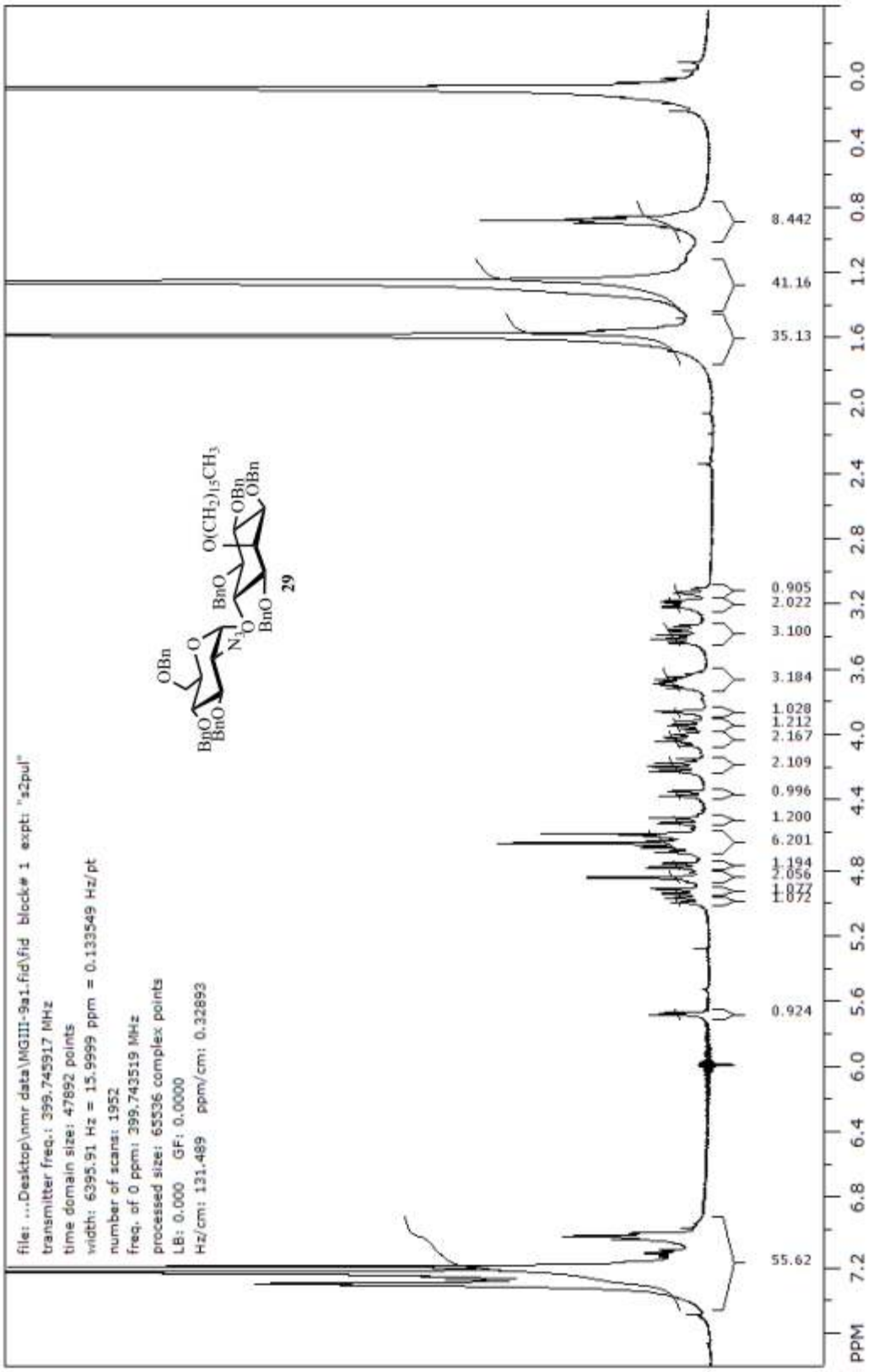
file: ...Desktop\nmr data\MGIII-9a1.fid\fid block# 1 expt: "s2pul"
transmitter freq.: 399.745917 MHz
time domain size: 47892 points
width: 6395.91 Hz = 15.9999 ppm = 0.133549 Hz/pt
number of scans: 1952
freq. of 0 ppm: 399.743519 MHz
processed size: 65536 complex points
LB: 0.000 GF: 0.0000
Hz/cm: 131.489 ppm/cm: 0.32893
OBn
BnO
BnO
O
N3
BnO
BnO
OBn
OBn
O(CH2)15CH3
29
8.442
41.16
35.13
0.905
2.022
3.100
3.184
1.028
1.212
2.167
2.109
0.996
1.200
6.201
1.194
2.056
1.077
1.072
0.924
55.62
PPM
7.2
6.8
6.4
6.0
5.6
5.2
4.8
4.4
4.0
3.6
3.2
2.8
2.4
2.0
1.6
1.2
0.8
0.4
0.0

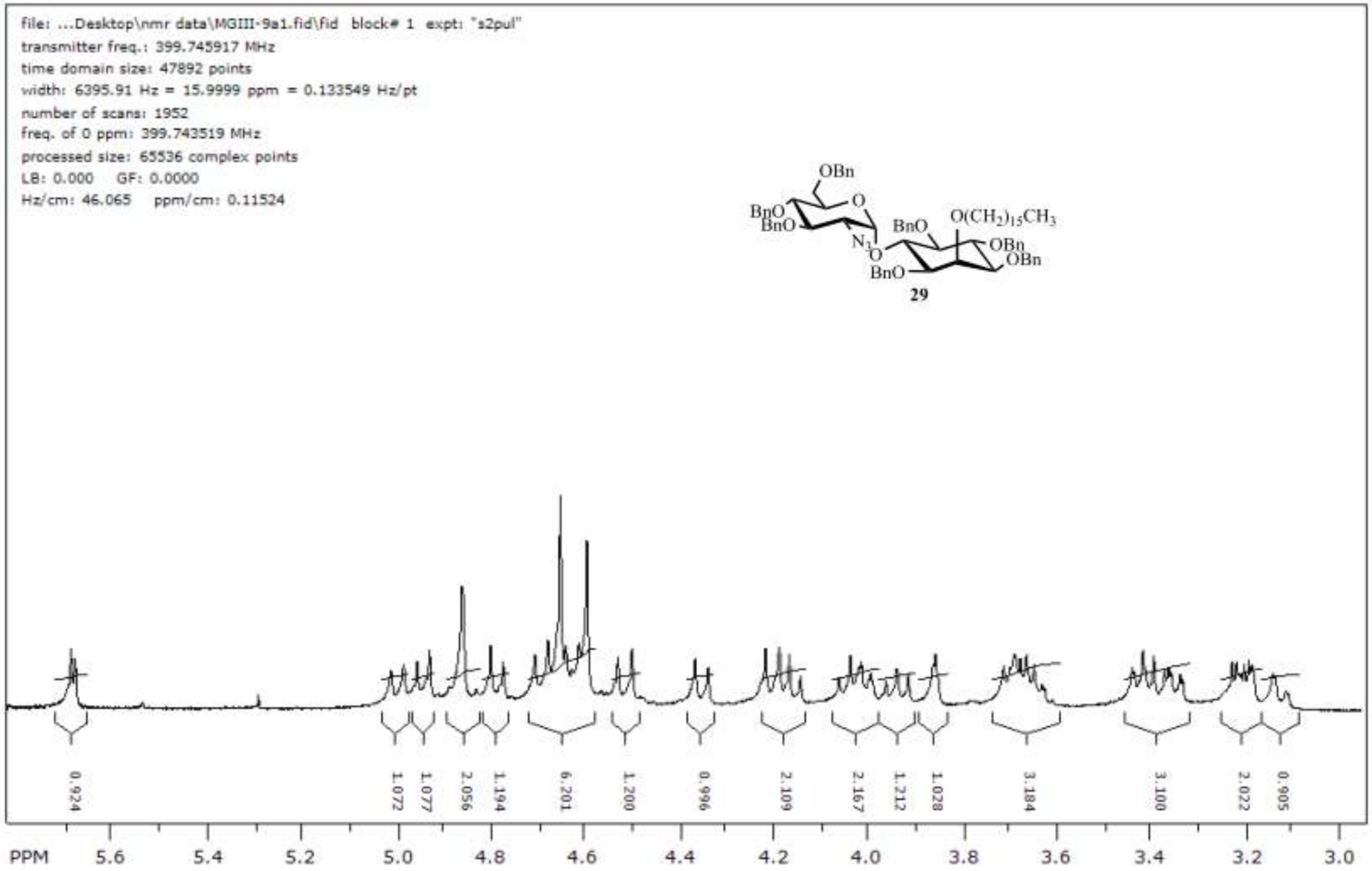
file: ...Desktop\nmr data\MGIII-9a1.fid\fid block# 1 expt: "s2pul"
transmitter freq.: 399.745917 MHz
time domain size: 47892 points
width: 6395.91 Hz = 15.9999 ppm = 0.133549 Hz/pt
number of scans: 1952
freq. of 0 ppm: 399.743519 MHz
processed size: 65536 complex points
LB: 0.000 GF: 0.0000
Hz/cm: 46.065 ppm/cm: 0.11524
OBn
BnO
BnO
O
N3
O
BnO
O(CH2)15CH3
OBn
OBn
BnO
29
0.924
1.072
1.077
2.056
1.194
6.201
1.200
0.996
2.109
2.167
1.212
1.028
3.184
3.100
2.022
0.905
PPM
5.6
5.4
5.2
5.0
4.8
4.6
4.4
4.2
4.0
3.8
3.6
3.4
3.2
3.0

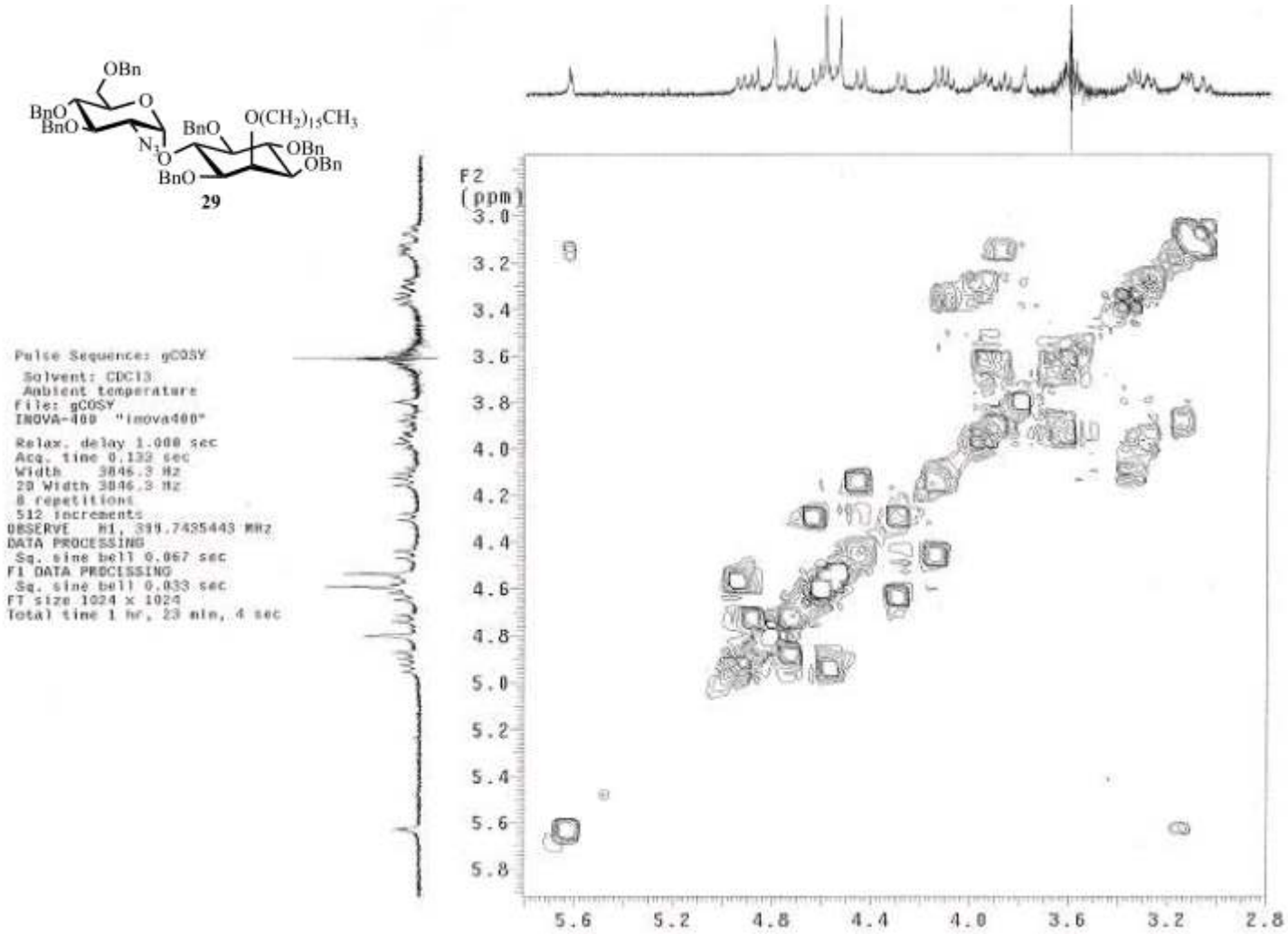
OBn
BnO
BnO
O
N3
O
BnO
O(CH2)15CH3
OBn
OBn
BnO
29
Pulse Sequence: gCOSY
Solvent: CDCl3
Ambient temperature
File: gCOSY
INOVA-400 "inova400"
Relax. delay 1.000 sec
Acq. time 0.132 sec
Width 3846.3 Hz
2D Width 3846.3 Hz
8 repetitions
512 increments
OBSERVE H1, 399.7435443 MHz
DATA PROCESSING
Sq. sine bell 0.067 sec
F1 DATA PROCESSING
Sq. sine bell 0.033 sec
FT size 1024 x 1024
Total time 1 hr, 23 min, 4 sec
F2 (ppm)
3.0
3.2
3.4
3.6
3.8
4.0
4.2
4.4
4.6
4.8
5.0
5.2
5.4
5.6
5.8
5.6
5.2
4.8
4.4
4.0
3.6
3.2
2.8

**REFERENCES:**


(1) Ferguson, M. A. J.; Homans, S. W.; Dwek, R. A.; Rademacher, T. W. *Science* 1988, *239*, 753-759.
(2) Low, M. G. *Biochemical Journal* 1987, *244*, 1-13.
(3) McConville, M. J.; Ferguson, M. A. J. *Biochemical Journal* 1993, *294*, 305-324.
(4) Stevens, V. L. *Biochemical Journal* 1995, *310*, 361-370.
(5) Guo, Z. W.; Bishop, L. *European Journal of Organic Chemistry* 2004, 3585-3596.
(6) Low, M. G. *Faseb Journal* 1989, *3*, 1600-1608.
(7) Jones, D. R.; Varela-Nieto, I. *International Journal of Biochemistry & Cell Biology* 1998, *30*, 313-326.
(8) Schofield, L.; Tachado, S. D. *Immunology and Cell Biology* 1996, *74*, 555-563.
(9) Mayer, T. G.; Kratzer, B.; Schmidt, R. R. *Angewandte Chemie-International Edition in English* 1994, *33*, 2177-2181.
(10) Campbell, A. S.; Fraserreid, B. *Journal of the American Chemical Society* 1995, *117*, 10387-10388.
(11) Pekari, K.; Tailler, D.; Weingart, R.; Schmidt, R. R. *Journal of Organic Chemistry* 2001, *66*, 7432-7442.
(12) Ferguson, M. A. J. 1997, p 1295-1302.
(13) Ferguson, M. A. J. *Journal of Cell Science* 1999, *112*, 2799-2809.
(14) Saltiel, A. R. *Journal of Bioenergetics and Biomembranes* 1991, *23*, 29-41.
(15) Saltiel, A. R.; Cuatrecasas, P. *Proceedings of the National Academy of Sciences of the United States of America* 1986, *83*, 5793-5797.
(16) Treumann, A.; Lifely, M. R.; Schneider, P.; Ferguson, M. A. J. *Journal of Biological Chemistry* 1995, *270*, 6088-6099.
(17) Roberts, W. L.; Myher, J. J.; Kuksis, A.; Low, M. G.; Rosenberry, T. L. *Journal of Biological Chemistry* 1988, *263*, 18766-18775.
(18) Davitz, M. A.; Hereld, D.; Shak, S.; Krakow, J.; Englund, P. T.; Nussenzweig, V. *Science* 1987, *238*, 81-84.
(19) Jones, D. R.; Avila, M. A.; Sanz, C.; VarelaNieto, I. *Biochemical and Biophysical Research Communications* 1997, *233*, 432-437.
(20) Misek, D. E.; Saltiel, A. R. *Journal of Biological Chemistry* 1992, *267*, 16266-16273.
(21) Misek, D. E.; Saltiel, A. R. *Endocrinology* 1994, *135*, 1869-1876.
(22) Mato, J. M.; Kelly, K. L.; Abler, A.; Jarett, L. *Journal of Biological Chemistry* 1987, *262*, 2131-2137.
(23) Larner, J.; Huang, L. C.; Schwartz, C. F. W.; Oswald, A. S.; Shen, T. Y.; Kinter, M.; Tang, G.; Zeller, K. *Biochemical and Biophysical Research Communications* 1988, *151*, 1416-1426.
(24) Huang, L. C.; Fonteles, M. C.; Houston, D. B.; Zhang, C. G.; Larner, J.

*Endocrinology* 1993, *132*, 652-657.
(25) Larner, J. *Journal of Cyclic Nucleotide Research* 1982, *8*, 289-296.
(26) Low, M. G.; Saltiel, A. R. *Science* 1988, *239*, 268-275.
(27) Deeg, M. A.; Humphrey, D. R.; Yang, S. H.; Ferguson, T. R.; Reinhold, V. N.; Rosenberry, T. L. *Journal of Biological Chemistry* 1992, *267*, 18573-18580.
(28) VarelaNieto, I.; Leon, Y.; Caro, H. N. *Comparative Biochemistry and Physiology B-Biochemistry & Molecular Biology* 1996, *115*, 223-241.
(29) Larner, J.; Price, J. D.; Heimark, D.; Smith, L.; Rule, G.; Piccariello, T.; Fonteles, M. C.; Pontes, C.; Vale, D.; Huang, L. *Journal of Medicinal Chemistry* 2003, *46*, 3283-3291.
(30) Saltiel, A. R. *Endocrinology* 1987, *120*, 967-972.
(31) Romero, G.; Gamez, G.; Huang, L. C.; Lilley, K.; Luttrell, L. *Proceedings of the National Academy of Sciences of the United States of America* 1990, *87*, 1476-1480.
(32) Alvarez, J. F.; Cabello, M. A.; Kelly, K. L.; Mato, J. M.; Feliu, J. E. *Diabetologia* 1987, *30*, A493-A493.
(33) Myers, M. G.; White, M. F. *Annual Review of Pharmacology and Toxicology* 1996, *36*, 615-658.
(34) Saltiel, A. R. *Cell* 2001, *104*, 517-529.
(35) Azev, V. N. Ph.D, Tufts University, 2007.
(36) Hresko, R. C.; Mueckler, M. *Journal of Biological Chemistry* 2005, *280*, 40406-40416.
(37) Lizcano, J. M.; Alessi, D. R. *Current Biology* 2002, *12*, R236-R238.
(38) Muller, G. *FEBS Lett.* 2002, *531*, 81-87.
(39) Kitamura, T.; Kitamura, Y.; Kuroda, S.; Hino, Y.; Ando, M.; Kotani, K.; Konishi, H.; Matsuzaki, H.; Kikkawa, U.; Ogawa, W.; Kasuga, M. *Molecular and Cellular Biology* 1999, *19*, 6286-6296.
(40) Pilkis, S. J.; Granner, D. K. *Annual Review of Physiology* 1992, *54*, 885-909.
(41) Alvarez, J. F.; Sanchezarias, J. A.; Guadano, A.; Estevez, F.; Varela, I.; Feliu, J. E.; Mato, J. M. *Biochemical Journal* 1991, *274*, 369-374.
(42) Turner, D. I.; Chakraborty, N.; d'Alarcao, M. *Bioorganic & Medicinal Chemistry Letters* 2005, *15*, 2023-2025.
(43) Larner, J.; Huang, L. C.; Suzuki, S.; Tang, G.; Zhang, C.; Schwartz, C. F. W.; Romero, G.; Luttrell, L.; Kennington, A. S. *Annals of the New York Academy of Sciences* 1989, *573*, 297-305.
(44) Muller, G.; Wied, S.; Frick, W. *Molecular and Cellular Biology* 2000, *20*, 4708-4723.
(45) Muller, G.; Jung, C.; Frick, W.; Bandlow, W.; Kramer, W. *Archives of Biochemistry and Biophysics* 2002, *408*, 7-16.
(46) Muller, G.; Hanekop, N.; Kramer, W.; Bandlow, W.; Frick, W. *Archives of Biochemistry and Biophysics* 2002, *408*, 17-32.
(47) Smart, E. J.; Graf, G. A.; McNiven, M. A.; Sessa, W. C.; Engelman, J. A.;

Scherer, P. E.; Okamoto, T.; Lisanti, M. P. *Molecular and Cellular Biology* 1999, *19*, 7289-7304.
(48) Muller, G.; Frick, W. *Cellular and Molecular Life Sciences* 1999, *56*, 945-970.
(49) Plourde, R.; Dalarcao, M.; Saltiel, A. R. *Journal of Organic Chemistry* 1992, *57*, 2606-2610.
(50) Cobb, J. E.; Johnson, M. R. *Tetrahedron* 1991, *47*, 21-30.
(51) Ley, S. V.; Yeung, L. L. *Synlett* 1992, 997-998.
(52) Frick, W.; Bauer, A.; Bauer, J.; Wied, S.; Muller, G. *Biochemistry* 1998, *37*, 13421-13436.
(53) Kornienko, A.; Turner, D. I.; Jaworek, C. H.; d'Alarcao, M. *Tetrahedron-Asymmetry* 1998, *9*, 2783-2786.
(54) Kornienko, A.; d'Alarcao, M. *Tetrahedron-Asymmetry* 1999, *10*, 827-829.
(55) Jaworek, C. H.; Iacobucci, S.; Calias, P.; d'Alarcao, M. *Carbohydrate Research* 2001, *331*, 375-391.
(56) Chakraborty, N.; d'Alarcao, M. *Bioorganic & Medicinal Chemistry* 2005, *13*, 6732-6741.
(57) McLean, P.; Kunjara, S.; Greenbaum, A. L.; Gumaa, K.; Lopez-Prados, J.; Martin-Lomas, M.; Rademacher, T. W. *Journal of Biological Chemistry* 2008, *283*, 33428-33436.
(58) Goel, M.; Azev, V. N.; dâ€™Alarcao, M. *Future Medicinal Chemistry* 2009, *1*, 95-118.
(59) Reddy, K. K.; Falck, J. R.; Capdevila, J. *Tetrahedron Letters* 1993, *34*, 7869-7872.
(60) Jones, D. R.; Varela-Nieto, I. *Molecular Medicine* 1999, *5*, 505-514.
(61) Bevan, P. *Journal of Cell Science* 2001, *114*, 1429-+.
(62) Saltiel, A. R.; Kahn, C. R. *Nature* 2001, *414*, 799-806.
(63) Wagman, A. S.; Nuss, J. M. *Current Pharmaceutical Design* 2001, *7*, 417-450.
(64) d'Alarcao, N. C. M.
(65) Gottschalk, W. K.; Jarett, L. *Archives of Biochemistry and Biophysics* 1988, *261*, 175-185.
(66) Pelicano, H.; Martin, D. S.; Xu, R. H.; Huang, P. *Oncogene* 2006, *25*, 4633-4646.
(67) Gatenby, R. A.; Gillies, R. J. *Nature Reviews Cancer* 2004, *4*, 891-899.
(68) King, A.; Selak, M. A.; Gottlieb, E. *Oncogene* 2006, *25*, 4675-4682.
(69) Warburg, O. *Science* 1956, *123*, 309-314.
(70) Gambhir, S. S. *Nature Reviews Cancer* 2002, *2*, 683-693.
(71) Kroemer, G. *Oncogene* 2006, *25*, 4630-4632.
(72) Carew, J. S., Huang, P. *Molecular Cancer* 2002, 1-9.
(73) Robey, R. B.; Hay, N. *Oncogene* 2006, *25*, 4683-4696.
(74) Elstrom, R. L.; Bauer, D. E.; Buzzai, M.; Karnauskas, R.; Harris, M. H.; Plas, D. R.; Zhuang, H. M.; Cinalli, R. M.; Alavi, A.; Rudin, C. M.; Thompson, C. B. *Cancer Research* 2004, *64*, 3892-3899.

(75) Rempel, A.; Mathupala, S. P.; Griffin, C. A.; Hawkins, A. L.; Pedersen, P. L. *Cancer Research* 1996, *56*, 2468-2471.
(76) Debatin, K. M.; Poncet, D.; Kroemer, G. *Oncogene* 2002, *21*, 8786-8803.
(77) Gatenby, R. A.; Gillies, R. J. *International Journal of Biochemistry & Cell Biology* 2007, *39*, 1358-1366.
(78) Smith, T. K.; Sharma, D. K.; Crossman, A.; Brimacombe, J. S.; Ferguson, M. A. J. *Embo Journal* 1999, *18*, 5922-5930.
(79) Khan, N.; Afaq, F.; Mukhtar, H. *Carcinogenesis* 2007, *28*, 233-239.
(80) Mitsunobu, O. *Synthesis-Stuttgart* 1981, 1-28.
(81) Parker, R. E.; Isaacs, N. S. *Chemical Reviews* 2002, *59*, 737-799.
(82) Luchetti, G.; Ding, K. J.; d'Alarcao, M.; Kornienko, A. *Synthesis-Stuttgart* 2008a, 3142-3147.
(83) David, S.; Hanessian, S. *Tetrahedron* 1985, *41*, 643-663.
(84) Goncalves, A. G.; Noseda, M. D.; Duarte, M. E. R.; Grindley, T. B. *Carbohydrate Research* 2005, *340*, 2245-2250.
(85) Kolb, H. C.; Vannieuwenhze, M. S.; Sharpless, K. B. *Chemical Reviews* 1994, *94*, 2483-2547.
(86) Martin-Lomas, M.; Flores-Mosquera, M.; Chiara, J. L. *European Journal of Organic Chemistry* 2000, 1547-1562.
(87) Dietrich, H.; Espinosa, J. F.; Chiara, J. L.; Jimenez-Barbero, J.; Leon, Y.; Varela-Nieto, I.; Mato, J. M.; Cano, F. H.; Foces-Foces, C.; Martin-Lomas, M. *Chemistry-a European Journal* 1999, *5*, 320-336.
(88) Nashed, M. A.; Anderson, L. *Tetrahedron Letters* 1976, 3503-3506.
(89) Simas, A. B. C.; Pais, K. C.; da Silva, A. A. T. *Journal of Organic Chemistry* 2003, *68*, 5426-5428.
(90) Srinivasan, K.; Michaud, P.; Kochi, J. K. *Journal of the American Chemical Society* 1986, *108*, 2309-2320.
(91) Palucki, M.; Pospisil, P. J.; Zhang, W.; Jacobsen, E. N. *Journal of the American Chemical Society* 1994, *116*, 9333-9334.
(92) Jacobsen, E. N.; Zhang, W.; Muci, A. R.; Ecker, J. R.; Deng, L. *Journal of the American Chemical Society* 1991, *113*, 7063-7064.
(93) Adam, W.; Bialas, J.; Hadjiarapoglou, L. *Chemische Berichte* 1991, *124*, 2377-2377.
(94) Murray, R. W.; Jeyaraman, R. *Journal of Organic Chemistry* 1985, *50*, 2847-2853.
(95) Freccero, M.; Gandolfi, R.; Sarzi-Amadè, M.; Rastelli, A. *Tetrahedron* 1998, *54*, 6123-6134.
(96) Tsuda, T.; Nakamura, S.; Hashimoto, S. *Tetrahedron* 2004, *60*, 10711-10737.
(97) Wang, D. P.; Wang, M.; Zhang, R.; Wang, X. N.; Gao, A. P.; Ma, J.; Sun, L. C. *Applied Catalysis a-General* 2006, *315*, 120-127.
(98) Dueno, E. E.; Chu, F.; Kim, S.-I.; Jung, K. W. *Tetrahedron Letters* 1999, *40*, 1843-1846.
(99) Dijkstra, G.; Kruizinga, W. H.; Kellogg, R. M. *Journal of Organic*

*Chemistry* 1987, *52*, 4230-4234.
(100) Salvatore, R. N.; Nagle, A. S.; Schmidt, S. E.; Jung, K. W. *Organic Letters* 1999, *1*, 1893-1896.
(101) Yan, R. B.; Yang, F.; Wu, Y. F.; Zhang, L. H.; Ye, X. S. *Tetrahedron Letters* 2005, *46*, 8993-8995.
(102) Orgueira, H. A.; Bartolozzi, A.; Schell, P.; Litjens, R.; Palmacci, E. R.; Seeberger, P. H. *Chemistry-a European Journal* 2003, *9*, 140-169.
(103) Cottaz, S.; Brimacombe, J. S.; Ferguson, M. A. J. *Carbohydrate Research* 1995, *270*, 85-91.
(104) Luchetti, G.; Ding, K. J.; Kornienko, A.; d'Alarcao, M. *Synthesis-Stuttgart* 2008, 3148-3154.